Development and applications of electrically driven separation methods.

BENKE, Peter I.

Fines are charged at 50p per hour

REFERENCE

Development and Application of Electrically Driven Separation Methods

Peter I. Benke

A thesis submitted in partial fulfillment of the requirements of Sheffield Hallam University for the degree of Doctor of Philosophy

October 2004

Abstract

Capillary Electrochromatography (CEC) is one of the newest separation techniques. It is a hybrid technique of high performance liquid chromatography (HPLC) and capillary zone electrophoresis (CZE). It combines the simplest capillary electrophoresis mode where separations are based on the differences in the electrophoretic migration of charged analytes under the influence of a high electric field with separation based on analyte partitioning between the mobile phase and stationery phase from liquid chromatography.

Mass spectrometry (MS), which requires ionized analytes in order to be detected, is an ideal detection technique for CZE. It is also a sensitive, selective and universal detector. However, CZE-MS interfacing is difficult. It is crucial to maintain a stable electrical contact throughout the CE capillary and ion-source as well as adequate grounding of the high voltage applied in CE. The main practical problem is the great mismatch in flow rates through the CE capillary and the solvent flow required for the general LC-MS ion-sources, such as electrospray. Thus, the evaluation of the interfacing is also reported.

The CEC work presented in this thesis details the examination of effects of physicochemical properties of different silica based C_{18} stationary phases on their chromatographic performance in CEC separations for a series of different acidic, neutral and basic type of analytes.

In the other half of this thesis, the application of a fast electrophoretic separation to improve previous HPLC separation and mass spectrometric detection of surfactants with great importance in oil recovery is reported. The surfactants, commercial nonylphenol ethoxysulphates (NEPOSp) and sulphonates (NEPOS), have been separated by reversed type CZE and the surfactants were also analysed then by mass spectrometric detection on a triple quadruple mass spectrometer using home-built co-axial sheath flow electrospray interfaces.

The obtained data indicates that reverse mode CZE provided faster separation with the same ethoxymer resolution than HPLC, while the calculated average number of ethoxymer units in the surfactants formulations (6.46 for NPEOS and 6.45 for NPEOSp) were in good agreement with previous data obtained in our group by different methods.

Acknowledgment

I would like to express my sincere thanks to:

My supervisors, Malcolm Clench and Vikki Carolan, for their help, guidance and full support throughout the course of this study.

My late supervisor, Lee Tetler for his supervision in the beginning of this research.

Boris Duerner and Edward Baidoo for their friendship and help over the years, who stood by me during the difficulties.

My colleagues and staff, especially for Joan Hague, in the Biomedical Research Centre and in the Material Research Institute of the Sheffield Hallam University, both for their advice and making my time in the department more enjoyable.

Finally, I would like to thank my family for their love and support.

Declaration

A thesis submitted to Sheffield Hallam University for the degree of Doctor of Philosophy.

All the results and data (otherwise stated) presented in this thesis were obtained by me. No portion of the work referred to in the thesis has been submitted in support of an application for another degree or qualification of this or any other university or other institute of learning.

Signed JLI **Date**

CONTENTS

Acronyms

ACN	Acetonitrile
CAPS	3-(cyclohexylamino)-1-propane-sulphonic acid
CE	Capillary electrophoresis
CEC	Capillary electrochromatography
CTAB	Cetyl trimethyl ammonium bromide
CZE	Capillary zone electrophoresis
DMSO	Dimethylsulphoxide
EOF	Electroosmotic flow
ESI	Electrospray ionisation
GC	Gas chromatography
HEPES	N-2-hydroxyethylpiperazine-N'-2-ethanesulphonic acid
HDB	Hexadimethrine bromide
HPLC	High performance/pressure liquid chromatography
MES	2-[N-morpholino]-ethanesulphonic acid
MS	Mass spectrometry
NPEOS	Nonylphenol ethoxylate sulphonates sulphates
NPEOSp	Nonylphenol ethoxylate sulphates
ODS	Octadecyl silane
PVA	Polyvinyl alcohol
QSSR	Quantitative structure-retention relationships
TRIS	Tris(hydroxymethyl)-amino-methane
SAX	Strong anion exchange
SCF	Supercritical fluid chromatography
SCX	Stron cation exchange
SDS	Sodium dodecylsulphate
SEM	Scanning electron microscope
SIMS	Secondary ion mass spectrometry
XPS	X-ray photoelectron spectroscope

Symbols and Units

N	Bonded phase coverage	[μmol m^{-2}]
σ	Charge density at the surface of the shear	[C cm^{-2}]
e	Charge per unit surface area	[C cm^{-2}]
c	Concentration (of solution)	[g or mol L^{-1}]
K	Conductance	[Ω^{-1}]
I	Current	[A]
d (ρ)	Density	[g cm^{-3}]
d_p	Diameter of particles	[μm]
ε_r	Dielectric constant of the mobile phase	[C^2 J^{-1} m^{-1}]
D	Diffusion Coefficient	[cm^2 s^{-1}]
l_{eff}	Effective capillary length	[cm]
N	Efficiency (theoretical plate number)	-
E	Electric field strength	[V cm^{-1}]
μ_{ep}	Electrophoretic mobility	[cm^2 V^{-1} s^{-1}]
ν_{ep}	Electrophoretic velocity	[mm s^{-1}]
ν_{EOF}	Electroosmotic velocity	[cm s^{-1}]
F	Faraday *constant*	[*9.648x10^4* C mol^{-1}]
R	Gas *constant*	[*8.314* J K^{-1} mol^{-1}]
G	Gravitational *constant*	[*6.67x10^-11* m^3 s^{-2} kg^{-1}]
I	Intensity of light	[W m^{-2}]
μ_{EOF}	Mobility of electroosmotic flow	[cm^2 V^{-1} s^{-1}]
M	Molecular weight	[g mol^{-1}]
ε	Molar absorptivity	[L mol^{-1} cm^{-1}]
Λ	Molar conductance	[Ω^{-1} m^2 mol^{-1}]
q	Number of charges (on an ion)	[C]
ε_0	Permittivity of vacuum	[*8.85x10^-12* C^2 N^{-1} μ^{-2}]
H	Plate height	[μm]
R	Resistance	[Ω]
ϕ_0	Surface Potential	[mV]
P	Pressure	[mbar]
r	Radius(capillary, particle etc.)	[μm]
S	Surface area	[m^2 g^{-1}]
T	Temperature	[K]
δ	Thickness of the double layer	[nm]
L	Total length of column	[cm]
η	(dynamic) Viscosity of solution	[g cm^{-1} s^{-1}]
V	Voltage	[V]
W	Watts	[J s^{-1}]
ξ	Zeta potential	[mV]

The units and/or dimensions are shown in the most commonly used form in CE practice, which are generally not SI base units.

CHAPTER 1

Capillary Electrophoresis

Introduction

Classical electrophoresis is one of the oldest separation techniques. It was developed by Tiselius [1] in 1937 who was later awarded a Nobel prize for his work in separation science. Separation efficiency in free solution, as used by Tiselius, was limited by the thermal diffusion caused by Joule heating and convection. For this reason, classical electrophoresis is traditionally performed in an anti-convective support media such as gels [3]. This form of electrophoresis is still used for separation of biological macromolecules, despite the efficiency and sensitivity problems and long analysis times observed.

The use of narrow tubes allowed open tube electrophoresis of free solutions to be studied, but many problems were encountered. Kolin developed rotating tube electrophoresis in 1954 [2] to reduce unwanted convection. Initial work in open tube electrophoresis, firstly using capillaries, with the minimum 1mm internal diameter available that time, was described by Hjérten in 1967 [3]. He also used rotation (along the longitudinal axis of the capillaries) to reduce convection effects. In the 70`s Virtanen [5] and then Mikkers [4] used smaller (ID=~200μm) glass and Teflon capillaries to demonstrate the advantage of capillaries over narrow bore columns in electrophoresis.

Historically, Isotachophoresis (ITP) is very important in the development of modern CE. It was used as early as in 1970 by Everaerts and his group [6] to separate organic acids. ITP was the most widely used CE technique prior the 80's and the principles and practicalities learned were used later in Capillary Zone Electrophoresis (CZE).

The breakthrough in the modern application of the capillary electrophoretic techniques started in the 80`s after Lukacs and Jorgenson clarified the theory and demonstrated the potential of the technique [7,8],

using 75μm fused silica capillaries. Several new techniques, utilising electrophoretic effects in capillaries were developed at that time:

- Micellar electrokinetic chromatography (MEKC) a technique for the separation of non-ionic species, which do not migrate in an electric field, was developed in 1984 Terabe *et al.* [9,10];
- Isoelectric focusing (CIEF) [11,12] by Hjérten in 1985
- Gel electrophoresis (CEG) for the size-based separation of macromolecules by Cohen and Karger in 1987 [13,14]
- Column-transient Isotachophoresis (CITP) by Karger and Foret in 1992 [15,16].

The last CE technique (of which first application can be traced back ironically to the time of birth of the CE technique itself, when Strain applied electric field across in an absorption column in 1939 [17]) to be developed, is the combination of HPLC and CE, Capillary Electrochromatography (CEC). The potential of this technique was first demonstrated by Jorgenson and Lukacs in 1981 [7,8], using fused silica capillaries similar to those employed in GC, but it took another 10 years when Knox and Grant confirmed their theoretical work in 1991 [18,19], before the resurrection of the CEC technique and it's worldwide application really started. In the last decade, several groups have made contributions [20,25] to the development of CEC, and this is a process, which is ongoing.

Instruments for CE have been commercially available since 1988. At the beginning the precision of these instruments was too poor for quantitative analyses. The worldwide spread of the application of CE started after 1993 when precision reached 1-2% RSD for peak areas and heights for the available instruments [26] and the experience of validation of the CE methods and instruments had grown [27].

1 Theory

1.1 Electrophoretic mobility

Electrophoresis is the movement of electrically charged species towards the oppositely charged electrodes in a conductive media (electrolyte) under the influence of an electric field. In capillary zone electrophoresis, separation is based on an ion's electrophoretic mobility (μ_e). The rates and directions of migrations of a spherical ion are the function of the charge-to-size ratio of the ions and the signs of their charges [28,29].

$$\mu_e = \frac{q}{6\pi\eta r} \tag{1.1}$$

q = Number of charges on an ion; η = Buffer viscosity; r = Ion radius

The electrophoretic velocity of an ion (v_e) is directly proportional to the electric field (E) across the system

$$v_e = \mu_e E \tag{1.2}$$

$$E = \frac{V}{L} \tag{1.3}$$

V = Voltage, L = Total length of the capillary.

Thus, the smaller and/or multivalent ions are moving faster than the big and/or monovalent ions, while the neutral molecules are not influenced by the electric field and they only move together with the conductive media, therefore they cannot be separated from each other.

1.2 Electroosmosis

In a CE system the conductive media, the so called running buffer is also experiencing a movement through the capillary by the effect of the electric

field due to the electroosmosis, which is the basis of the possibility of separation between positive and negative ions.

When an electrolyte solution is placed into a fused silica, an electric double layer is created at the interface between solid and liquid phases [30-32]. The inner wall of fused-silica capillary is negatively charged due to the presence

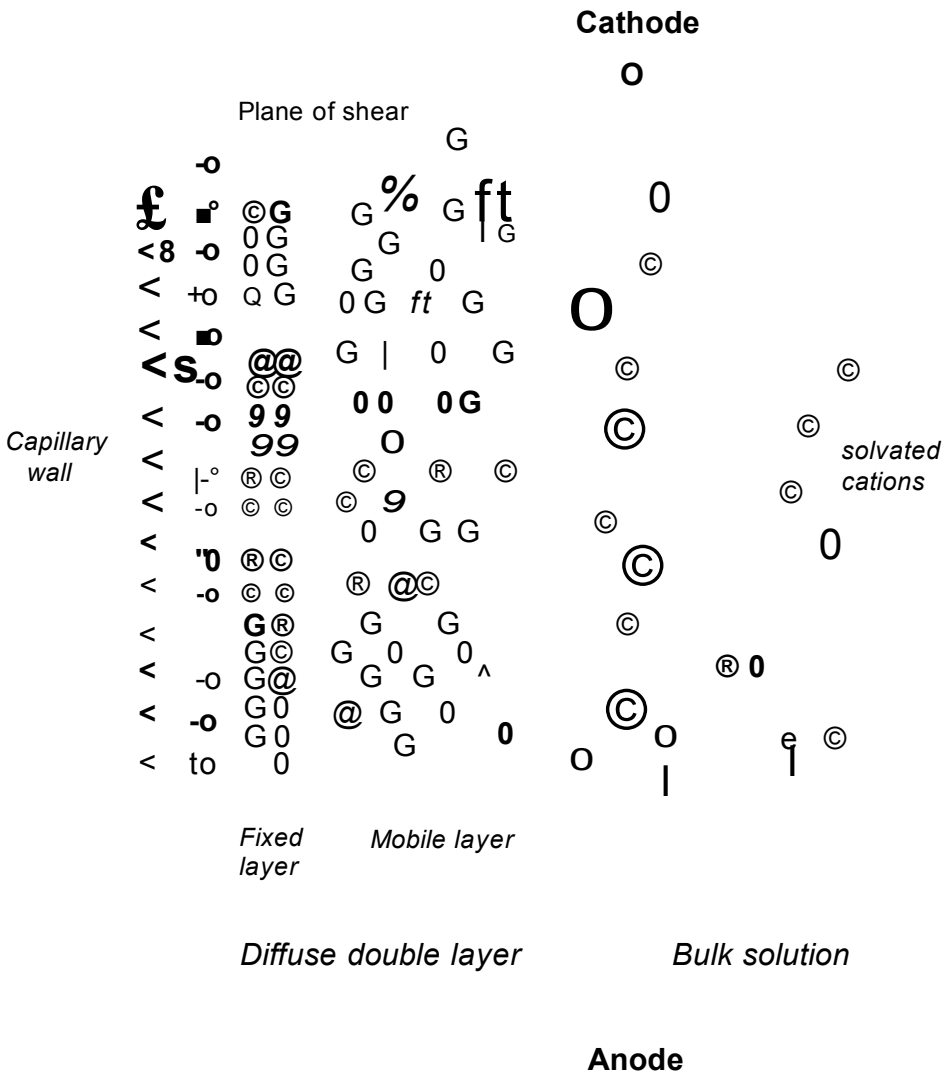

Figure 1.1 Representation of electric double layer at the fused silica surface of the capillary.

of weakly acidic silanol groups (pKg 2.2) which dissociate to silanolate groups (=Si-CT) above pH=2. Positive ions in solution gather near the capillary

surface to balance this negative charge, giving rise to an electric double layer (Figure 1.1).

The electric double layer contains a compact ion-binding region, the Stern or fixed layer, and a diffuse layer, or Gouy-Chapman layer [33,34]. The reason for the formation of the diffuse layer is that the fixed layer is not able to neutralise the surface's negative charge, due to steric hindrance. The excess cations that are firmly held in the Stern layer, close to the capillary surface are believed to be less hydrated than those in the diffuse region [35]. The cations in the Gouy-Chapman layer are more diffuse, hence the name, and able to move into the bulk solution and back. The plane where the diffuse layer begins is called the outer Helmholtz plane, and the edge for the compact region of bound cations is called the inner Helmholtz plane [33].

The potential at the fused-silica capillary wall is proportional to the charge density resulting from the dissociation of the silanol groups. The potential decreases linearly from the wall potential (ϕ_0) to the Stern potential (ϕ_ζ) in the Stern layer, and then exponentially from ϕ_ζ to zero in the diffuse layer (Figure 1.2).

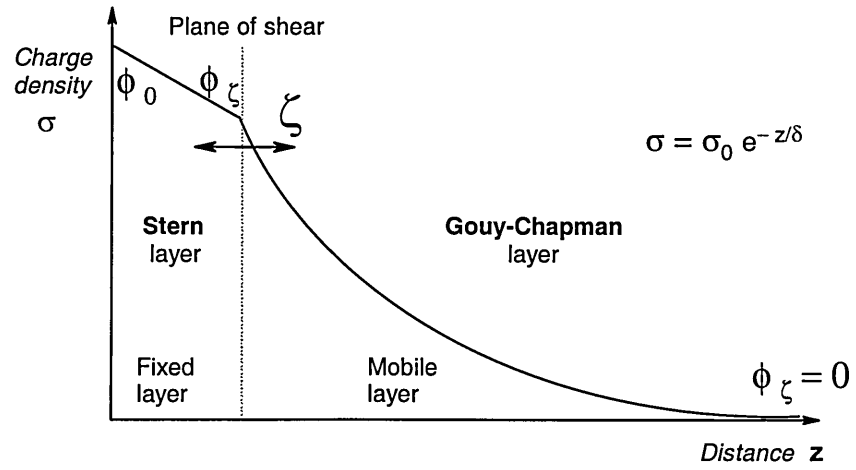

Figure 1.2 Diagram of charge density in the electric double layer.

The potential difference at the surface between the Stern layer and the diffuse layer is the zeta potential (ζ) [34-36].

The zeta potential is influenced by the dissociation of the silanol groups at the fused-silica capillary wall, the charge density in the Stern layer and the thickness of the diffuse layer. Each of these parameters depends on several variables, such as pH, specific adsorption of ions in the Stern layer and ionic strength of the electrolyte solution. The dielectric constant, viscosity and nature of the solvent also all have an effect on the zeta potential [36].

$$\zeta = \frac{4\pi\delta e}{\varepsilon} \tag{1.4}$$

δ = Thickness of diffuse double layer; ε = Dielectric constant of the buffer; e = Charge per unit surface area.

The thickness of the double layer is inversely proportional to buffer concentration.

$$\delta = \sqrt{\frac{\varepsilon_0 \varepsilon_r RT}{2cF^2}} \tag{1.5}$$

ε_0 = Permittivity of a vacuum; ε_r = Relative dielectric constant of the buffer solution; R = Gas constant; T= Temperature; c = Concentration of the electrolyte; F= Faraday constant.

For binary electrolytes in aqueous solution, the double layer thickness of electrolytes with concentrations of 10^{-6} to 10^{-2} M ranges from 3 to 300 nm [37]. A 10 mM buffer producing an approximately 1 nm thick double layer [38]. Under an electric field, the thickness of the diffuse layer is indirectly proportional to the square root of the ionic strength of the electrolyte solution [32,35]

The pH of the solution has a major effect on the zeta potential. An increase in solution pH directly influences the charge density on the capillary wall [34,39] due to increasing deprotonation of the surface silanol groups. Zeta potentials of a silica surface in a typical aqueous CE media are in the range of 1-100 mV [40,41]

1.3 Electroosmotic Flow

If an electric field is applied across the fused-silica capillary the cations in the fixed layer stay tightly held, but the cations in the diffuse layer can migrate towards the cathode, dragging their solvation spheres with them. Since the water molecules associated with the cations are in direct contact with the bulk solution, all the electrolyte solution moves towards the cathode. This flow is called the electroosmotic flow (EOF).

The magnitude and direction of the EOF are controlled by the zeta potential, and can be described by the Helmholtz and Smoluchowski equation [28,29]

$$\mu_{EOF} = \frac{\varepsilon\zeta}{4\pi\eta} \tag{1.6}$$

μ_{EOF} = Electroosmotic mobility; ε = Dielectric constant of the solution; ζ = the zeta potential and η = Viscosity of the solution.

The electroosmotic mobility is analogous to electrophoretic mobility, both have the same units, [$cm^2/V{\cdot}s$]. The same applies to electroosmotic velocity, which can be calculated on the same basis as Eq. 1.2. The observed velocity, v_{obs}, of an ion is influenced by its electroosmotic velocity and mobility and the velocity and mobility of the running buffer (EOF)

$$v_{obs} = v_{EOF} + v_e \tag{1.7}$$

from Equation 1.2

$$v_{obs} = (\mu_e + \mu_{EOF})E \tag{1.8}$$

The observed velocity of the EOF can be easily calculated using a neutral analyte, the so called neutral marker, which moves together with the EOF, by measuring migration time (or retention time), t_{marker}:

$$v_{obs} = \frac{l_{eff}}{t_{marker}} \tag{1.9}$$

l_{eff} = Effective capillary length (from the point of injection to the point of detection).

The migration time for an ion can be obtained from:

$$t_m = \frac{l_{eff} L}{(\mu_e + \mu_{EOF})V} \tag{1.10}$$

The calculation of the electrophoretic velocity of an ion is possible from its migration time, t_m, by rearranging Eq. 1.7 and substituting into Eq. 1.9 to give:

$$v_e = \frac{l_{eff}}{t_m} - \frac{l_{eff}}{t_{marker}} \tag{1.11}$$

The electrophoretic velocity can be calculated from experimental parameters (rearranging Eq. 1.8 after substitution of eqs. 1.3, 1.7 and 1.9) using:

$$\mu_e = \left(\frac{l_{eff} L}{t_m V}\right) - \left(\frac{l_{eff} L}{t_{marker} V}\right)_{EOF} \tag{1.12}$$

As can be seen from the above equations, the separation of differently charged and neutral species (but not between the neutral species) is possible.

Under normal conditions of CE (when the negatively charged electrode is at the same side as the detector, and the EOF move towards the outlet vial) the migration order, from equation 1.8, will be as follows:

- Cations migrate first, before the EOF as their electrophoretic mobilities add to the mobility of the EOF.
- Neutral species migrate at the same rate as the EOF as the electric field has no effect on them.
- Despite the opposite direction of the electrophoretic migration of the anions, the EOF of the buffer solutions (μ_{EOF}) is usually greater than their electrophoretic mobility. Thus, anions are carried along behind the EOF and they migrate last.

The migration order of ions with the same charge is based on their charge-to-size ratio, as described in Section 1.1.

1.4 Analytical parameters in CE

The quality of a separation method is described by efficiency, resolution and analysis (migration/retention) time. Further parameters such as peak asymmetry and selectivity also give useful information about the analytical performance of the techniques. The main advantage of capillary electrophoresis is that much higher efficiencies can be obtained in analyses, as will be explained.

1.4.1 Standard deviation

In chromatography moving solutes disperse into a diffuse band and this is detected as a Gaussian peak with standard deviation (σ) due to differences in the analyte velocity within the solute zone. The resultant peak width at the baseline (w) can be expressed as

$$w = 4\sigma \tag{1.13}$$

If the dispersion arises only from diffusion (which is the main cause of broadening), the standard deviation of a solute zone is

$$\sigma = \sqrt{2Dt} \tag{1.14}$$

D = Diffusion coefficient of the analyte; t = migration time

Under ideal conditions in CE, the only diffusion is longitudinal as radial diffusion is negligible due to the flat flow profile.

The amount of dispersion of a zone over t time caused by diffusion is described by the square of the standard deviation, which is called the spatial

variance (σ^2). Eq. 1.14 can be written after substituting migration time (Eq. 1.10) as

$$\sigma^2 = \frac{2Dl_{eff}L}{(\mu_e + \mu_{EOF})V} \tag{1.15}$$

1.4.2 Efficiency

Efficiency (N) relates the analyte zone (peak) width to the distance it travelled during the separation in the system and is expressed as the number of theoretical plates (the name originates from distillation procedure theory, firstly presented by *Martin and Synge* (1941) and *Glueckauf* (1949))

$$N = 16 \times \left(\frac{t_r}{w}\right)^2 \tag{1.16}$$

t_R = Migration time; w = peak width at the baseline

The number of theoretical plates can be related to the variance as

$$N = \left(\frac{L}{\sigma}\right)^2 = \frac{L}{H} \tag{1.17}$$

H = Height equivalent to a theoretical plate; L = Length of column

The maximum separation efficiency of a CE system in ideal conditions, where only longitudinal diffusion contributes to brand broadening, can be derived from 1.14 and 1.10

$$N = \frac{\mu_{app}V}{2D} \tag{1.18}$$

As diffusion is the most important factor causing brand broadening the shorter the separation time the higher the efficiency as the analytes spend less time in the capillary and therefore they have less chance to diffuse. Thus equation 1.18 illustrates one very important aspect of CE that efficiency is not based on the length of the capillary used and therefore short capillaries can be used, which means faster separations. This is in contradiction to

liquid and gas chromatography, where longer columns give higher efficiencies.

In CE high efficiency can be achieved by the application of a higher voltage (see Section 1.5.1.1-1.5.1.2), which leads to higher EOF.

1.4.3 Resolution

The most important separation parameter, the resolution (R) between two adjacent peaks is defined as the difference in migration times (t) related to the peak width:

$$R = \frac{\Delta t}{\overline{w}} = 2\frac{(t_2 - t_1)}{w_1 + w_2} \tag{1.19}$$

$\overline{w}$ = average peak width at the baseline; Δt = separation time difference

Baseline separation is achieved for two peaks with the same area when the resolution is 1.5. When resolution is 1.0 the overlap is 2.3% and the separation time difference between the peak tops is 4σ [42]. Resolution can be related to efficiency [28] as

$$R = \frac{1}{4}\sqrt{N}\frac{\Delta v}{\overline{v}} \tag{1.20}$$

Δv = velocity difference between two peaks; v = average velocity of the two analytes

It can be also expressed with electrophoretic parameters as

$$R = 0.177\frac{(\mu_2 - \mu_1)\sqrt{N}}{(\overline{\mu} + \mu_{EOF})\sqrt{D}} \tag{1.21}$$

$\overline{\mu}$ = average electrophoretic mobility of the two analyte species.

As can be seen, increasing the efficiency will result in less improvement in resolution than increasing the difference in the electrophoretic mobility of the analytes. Maximum resolution can be obtained when the average electrophoretic mobility of the analytes is equal to the EOF but in opposite direction. Although, the migration time is at maximum in this case due to Eq. 1.10.

Optimising the mobility difference between the analytes (*e.g.* controlling the pH, application of proper running buffer and/or organic solvents) is the main approach for achieving good resolution.

1.4.4 Peak Capacity

The separation capabilities of different techniques can be compared by the peak capacity (C_p or P). This gives information about the "ideal", maximum number of peaks that can be resolved in a given system and specified time, when the resolution between consecutive peaks is 1.0.

$$C_P = 1 + \frac{\sqrt{N}}{4} \ln \frac{t_r}{t_{nm}} = 1 + \frac{\sqrt{N}}{4} \ln(1 + k) \tag{1.22}$$

t_r = Migration (retention) time of the analyte; t_{nm} = Migration (retention) time of a neutral marker or an unretained sample; k= retention factor.

The lower limit of peak capacity is the dead time of the system - the time of the mobile phase passes through the system - which is equivalent with t_{nm}. The practical maximum limit – due to the finite peak width as defined by the plate number - is when t_r/t_{nm} is 10 in most LC and 50 in many GC separations. Giddings *et al.* have shown [43] that, relative to the peak capacity for closely spaced peaks, a chromatogram will never contain more than about 37% of its potential peaks and 18 % of its potential single-component peaks as component peaks are generally spaced randomly on complex chromatograms, thus many components occupying the same space.

1.4.5 Selectivity

The selectivity (α) of a chromatographic system describes the separation level that can be achieved between two adjacent analytes based on their selective retention by the stationary phase (in CEC, for example). It is expressed as the distance at the peak apex between two consecutive analyte peaks:

$$\alpha = \frac{t_2 - t_{nm}}{t_1 - t_{nm}} \tag{1.23}$$

t_1 , t_2 = Migration times of the analytes; t_{nm} = Migration time of a neutral marker.

Substituting Eq. 1.2 and 1.11 into the selectivity equation, the selectivity can be related to electrophoretic mobility (μ) of the analytes

$$\alpha = \frac{\mu_2}{\mu_1} \times const \tag{1.24}$$

As can be seen, selectivity can be improved by changing the difference between the electrophoretic mobilities of the analytes (*e.g.* altering the pH, see 1.6.3)

In partition chromatography (*e.g.* LC, CEC) the selectivity can be described as a function of the retention of each component by the stationary phase

$$\alpha = \frac{k_2}{k_1} \tag{1.25}$$

Where k is the retention or formerly capacity factor. It describes the retention properties of the stationary phase, the ratio of the total number of molecules in the stationary and mobile phases. It can be calculated with regard to the migration times:

$$k = \frac{t_r - t_0}{t_0} \tag{1.26}$$

t_R = Migration (retention) time of the analyte; t_0 = The column/capillary dead time.

The dead time is the time for the mobile phase reaches to the detector throughout the system. In CE this can be related to the migration time of a neutral marker (t_{nm}), which moves at the same velocity as the running buffer in the capillary and is unretained on the stationary phase in the case of CEC.

1.4.6 Peak Asymmetry

Peak Asymmetry (A_S) and Peak Tailing Factor (PTF) describe the deviation of the resulting peak shape from a perfect Gaussian distribution. Peak asymmetry is calculated as shown in Figure 1.3, at one-tenth of the maximum peak height, while tailing factor is calculated at 5% of the maximum peak height [44]

$$A_S = \frac{b}{a} \tag{1.27}$$

$$PTF = \frac{a+b}{2a} \tag{1.28}$$

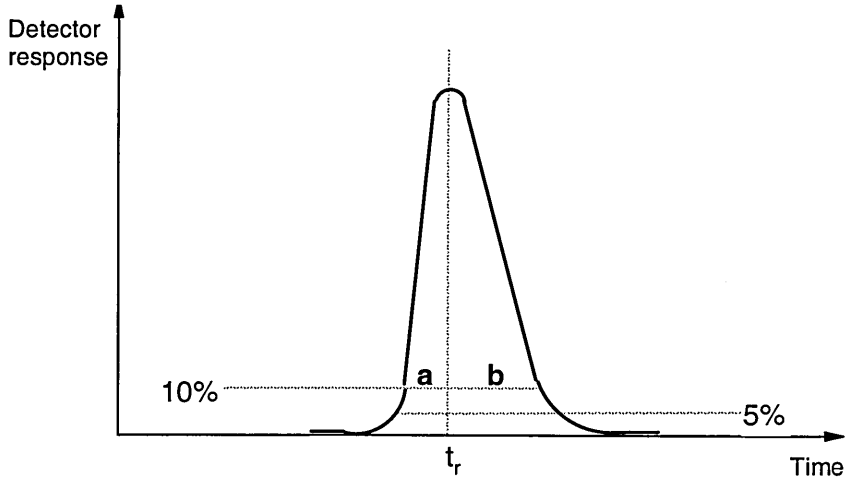

Figure 1.3 Determination of peak width fractions for peak asymmetry and tailing.

A peak asymmetry value of 1.0 indicates symmetrical peaks, whereas higher values indicate "tailing" peaks and lower values indicate "fronting" peaks.

These measurements of the peak shape are important indicator values of chromatographic problems such as

- analyte-capillary wall/stationary phase interactions (absorption) causing peak tailing
- sample overloading causing peak fronting
- mismatch in sample and running buffer conductivities (electrodispersion) causing tailing or fronting

It should be noted that strictly - as the plate theory is based on symmetrical Gaussian peaks – parameters such as efficiency become more complex if asymmetry occurs. An approximate calculation, the *Dorsey-Foley* equation, can be used for plate numbers in the case of asymmetric peaks [42]

$$N \approx \frac{41.7 \times \left(\frac{t_r}{a+b}\right)^2}{\left(\frac{b}{a}+1.25\right)} \qquad (1.29)$$

t_r = retention time; a and b = the peak width fractions at one-tenth-height as in Figure 1.3.

However, asymmetry values up to 1.25 are considered as indicating acceptable peak shapes in HPLC methods and the analytical parameters are calculated as normally.

1.5 Dispersion in CE

1.5.1 Flow profile

In an electrically driven CE system where the driving force is the ions in the diffuse double layer on the inner capillary wall, the EOF is uniformly distributed along the whole capillary. There is no pressure drop, and therefore practically the flow velocity difference across the capillary diameter, which causes substantial band broadening, is not present. Although the EOF

velocity is reduced directly at the capillary wall due to frictional forces, its effect is negligible compared to the total flow profile. The overall result is a relatively flat flow profile (Figure 1.4).

This is the opposite to pressure driven systems (such as LC, GC) which have a laminar (HPLC) or turbulent (GC) flow, with parabolic flow profile due to the frictional forces which creates different flow velocities across the column/capillary.

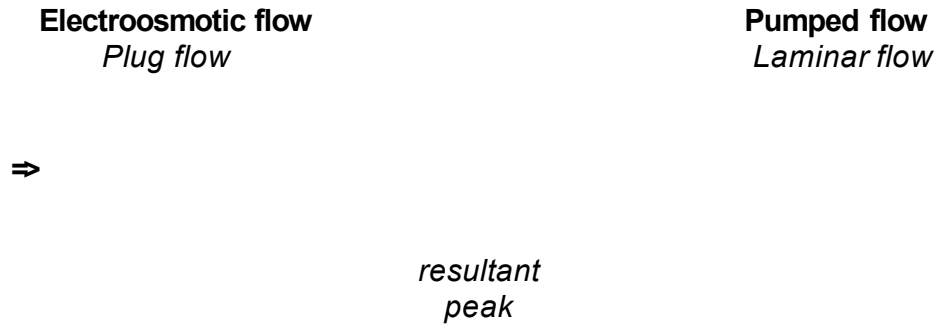

Figure 1.4 Comparison of electrically and hydrodynamically driven flow profiles and their resulted peaks

The flat flow profile of the electrically driven systems not only occurs in open tubes, but in packed capillaries as used in CEC as well (Figure 1.5). Although, the generation of the flow is mainly connected to the surface of the stationary phase particles in CEC (see Chapter 2.1), the generation of the EOF is the same.

Figure 1.5 Comparison of flow profiles through a stationary phase in CEC and HPLC.

Despite the several flow channels in the stationary phase among the particles, the EOF is uniformly distributed along the whole stationary phase, thus the same plug flow produced throughout each channel and the whole capillary, with an overall flat flow profile.

The result is that all analytes will move with the same velocity and hence peak broadening is minimal in CE systems. Therefore narrower peaks with very high efficiencies and better separations can be obtained compared to pressure driven systems (Table 1.1).

Technique	N [plates/m]
TLC	<5000
GC	3000
SCF	260 000
HPLC	100 000
CEC	250 000
CZE	4 000 000

Table 1.1 Comparison of the most common separation techniques [28]

1.5.2 Band broadening processes

The reachable efficiency in a practical application (measured by Eq. 1.16) is generally smaller than the theoretically calculated one (Eq. 1.18), due to the presence of several dispersive processes other than the longitudinal diffusion. The total dispersion in an analytical system can be described by accounting for all possible dispersive processes which contribute to the variance of the final band broadening:

$$\sigma^2_{observed} = \sum \sigma^2_{i.} = \sigma^2_{Diffusion} + \sigma^2_{Electrodipersion} + \sigma^2_{Injection} + \sigma^2_{Temperatue} + \sigma^2_{Adsoption} + \sigma^2_{Detection} + \ldots \quad (1.30)$$

The effects of these factors will be discussed in Section 1.6.

1.5.3 The Van Deemter model

To improve the separating performance of a chromatographic system, the original plate number theory is not adequate as it is not related to the real physical and chemical processes taking place in a practical column/capillary. It was van Deemter *et al.* [45] who described a general equation to describe the band broadening processes in practical chromatographic separations, relating the plate height (H) to the linear velocity (u) of the mobile phase through the column. Later several corrections were published to improve the van Deemter equation [46-47]

$$H = A + \frac{B}{u} + (C_S + C_M)u \tag{1.31}$$

A, B and C coefficients are constants for a particular analyte and experimental condition as the flow rate is varied. They describe different band broadening processes.

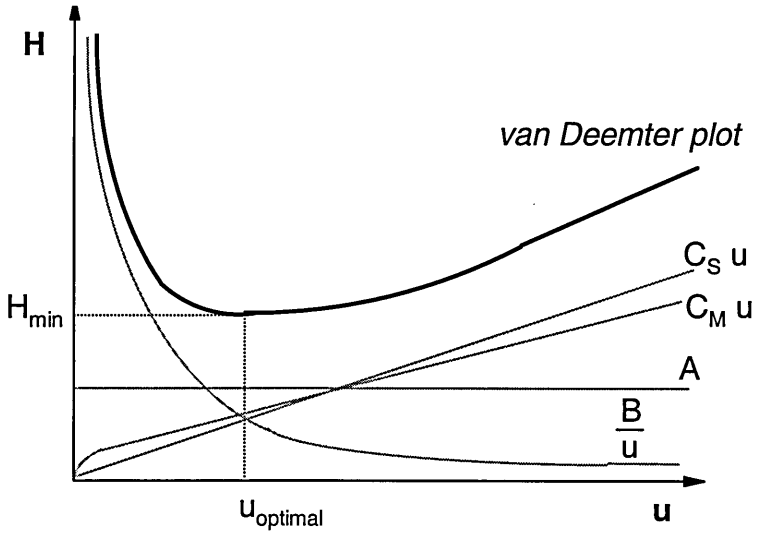

Figure 1.6 Hypothetical van Deemter plot showing the relative contribution of different components into the total plate height

The A term (Eddy diffusion) is related to the stationary phase, thus it is absent in capillary electrophoresis except in CEC. Eddy diffusion describes the band broadening caused by the various flow paths that the individual

solutes take during migration through a packed column. This results in different speeds for each solute as they migrate through different lengths of the packed bed during the separation. The A-term in CEC is generally less than in HPLC for any particular particle size as individual flow velocities in the different flow channels are the same due to EOF, as described in Section 1.5.1. The value of A can be reduced, thus less band broadening can be achieved by using smaller particles with a smaller size distribution. This generally improves the homogeneity of the packing. Unlike in HPLC, there is no pressure limit in electrochromatography, thus the use of much smaller particles are possible. The A term only depends on the packing geometry (density and homogeneity) of the stationary phase, and is independent of flow rate.

The B term (Molecular diffusion) is related to the concentration gradients between the sample plug and the surrounding mobile phase. This concentration gradient causes molecular diffusion in all directions independently from the flow direction. The longitudinal diffusion – along the axis of the column - will result an axial sample zone spreading. The diffusion rate is proportional to the component's diffusion coefficient and temperature (section 1.4.1). It is also depends on the time the solute spends in the column and is thus inversely proportional to the flow rate. Therefore the higher the velocity the less the diffusion occurs.

The EOF offers no advantage over pressure driven systems for the reduction of molecular diffusion. This is the main band-broadening factor in electrophoretical separations under ideal conditions.

The C term (Resistance to mass transfer) is related to the finite time required for the solutes to attain equilibrium between the mobile and stationary phase during the elution process. Thus it is also absent in electrophoresis other than CEC. As the equilibrium distribution of the analyte cannot be established between the two phases instantaneously some of the analyte for

example will stay in the stationary phase while others moved further, causing tailing.

The C term is often used in a combined form, but it can be described by two separate coefficients. The C_s term describes the diffusion in the stationary phase and C_M in the mobile phase. Both factors are dependent on the diffusion coefficient in the given phase. Further more C_S is related to the stationary phase film thickness, while C_M is related to the particle diameter and can be reduced by using smaller particles. The effect of C_S can be largely ignored as the mass transfer of the analyte onto and off of the stationary phase is a very rapid process.

The C term is directly proportional to the flow rate. The slower the flow, the more complete the equilibration can be, thus less band broadening occurs.

1.6 Effect of variables on electroosmotic flow and analytical parameters

To obtain a good separation by CE a stable and constant EOF is very important. In some techniques inhibition of the EOF is required (*i.e.* capillary isotachophoresis, isoelectric focusing and capillary gel electrophoresis).

It should be noted that the effect of the variables that will be described can be multi-fold (*e.g.* influencing the dispersion and other parameters as well) and that they can work in opposition for or support of other variables. Thus increasing or decreasing the effects of each other. Thus the optimisation of the system is very important.

The basis of EOF control, the effect of different variables will be described briefly.

1.6.1 Electric field

The electric field can be changed by the applied voltage or the total length of the capillary (Eq. 1.3).

1.6.1.1 Voltage

As shown by Eq. 1.2-1.3, increasing the voltage will increase the EOF. This results in shorter migration times, thus faster separation, and higher efficiencies. This suggests the use of the maximum voltage possible. The maximum available voltage is ±30kV in most commercial instruments. Unfortunately, higher voltages will result in higher current and the generation of Joule heat. The effects of the temperature will be described in Section 1.6.2.

The heat generated is proportional to the power, P,

$$P = VI \tag{1.32}$$

I = Current

The relationship between the current and voltage is described by Ohm's law

$$V = IR \tag{1.33}$$

R= the resistance of the system, which is related to the buffer electrolyte and the parameters of the capillary. This can be calculated as

$$R = \frac{4\Lambda LC}{\pi d^2} \tag{1.34}$$

Λ = Molar conductivity of the buffer; C= Concentration of the buffer; L=Total length of the capillary; d= Diameter of the capillary.

By combining Eqs. 1.32-1.34, the rate of heat generated can be expressed as

$$P = \frac{\pi d^2 V^2}{4\Lambda CL} \tag{1.35}$$

The optimal maximum voltage can be determined by plotting, E versus V (Ohm's plot). The relationship between the applied voltage and the generated current is linear until excessive heat is not generated. When this happens the resistance will rapidly decrease, causing a rapid increase in the current [27]. The maximum voltage that should be used is the voltage at the end of the linearity in the Ohm's plot.

The maximum voltage depends on the buffer's concentration, composition and pH, as well as the capillary length and diameter (as can be seen in Eqs. 1.34-1.35)

1.6.1.2 Capillary Length and Diameter

Reducing the capillary length, if the voltage is kept constant, will reduce the resistance of the system (Eq. 1.34) and consequently will increase the generated current and heat. That means that shorter capillaries have lower optimum maximum voltage.

Changes in the diameter have the opposite effect, due to the increased resistance in narrower capillaries. The maximum diameter for CE was reported to be 200μm, as above this it is not possible to effectively dissipate the heat [48].

In contrast to liquid chromatography, the length of the capillary is independent of the efficiency of the separation (see Section 1.5). Thus the application of short capillaries would be advantageous as they give faster separation with no decreased efficiency. The downside is that the Joule heat generated is higher and that the heat dissipation is more difficult due to the smaller total capillary surface. Thus the convective diffusion, which reduces the efficiency, is higher. Lukacs and Jorgensson found [49] that there is a minimum length at which the efficiency remained constant, as the capillary has enough surface (directly proportional to the length) to dissipate the

produced heat. The resolution, on the other hand, is better for longer capillaries, but the analysis time is also longer. As can be seen, just from this section, CE optimisation can be difficult as the variable parameters and their effects are all connected.

1.6.2 Temperature

Temperature has various problematic effects in a CE system. Some of them have been explained in the previous section.

The effect of the temperature on EOF is complicated as it is influenced by two factors, the viscosity and dielectric constant of the buffer, which work against each other. These have an opposite effect on the EOF as can be seen in Eq. 1.6. The final effect of the temperature depends on the composition of the buffer and its ε/η ratio. Table 1.2 (at 25°C unless otherwise indicated).

Solvents	Dielectric Constant [ε]	Viscosity [η]	ε/η
Acetonitrile	36.6	0.38	96.3
Water	80.1	1.00	80.1
Acetone	21.01 (20°C)	0.33 (20°C)	63.5
Methanol	32.7	0.54	60.6
DMF	36.7	0.80	45.9
DMSO	46.7	1.96	23.8
Ethanol	24.55	1.10	22.3
Dichloromethane	8.93	0.44 (20°C)	20.3
Tetrahydrofuran	7.52 (22°C)	0.47	15.8
i-Propanol	19.92	2.40 (20°C)	8.3

Table 1.2 Dielectric constant and viscosity values of common solvents used in CE

Increasing the temperature will decrease the value of both of these constants. A 1 degree Celsius change in temperature can result in a 2–3% change of viscosity (water: 2.4%), and consequently the same change in mobility [50]. The same change results in less change in the dielectric constant of water (0.5%) [27]. Therefore the overall effect for water will be an increase in EOF.

The main problem that can be caused by the generation of excess heat is when the temperature is high enough in the buffer or solute zone for boiling. This results in bubble formation. Sample decomposition or denaturation may occur as well. Such bubbles not only produce separation and detection problems (*e.g.* false peaks), but they can stop the EOF. Since air bubbles are not conductive, the electrical contact through out the system is broken and therefore there is no electrical field. If the method used is not open-tubular, the bubbles can damage the packed media in the capillary. This is a major problem, especially in CEC, where the formation of a good packed capillary is still a major difficulty. If bubble formation occurs, the system must be flushed out with the running buffer. This can be done easily in CZE, but not in CEC.

The heat generated can result in temperature and density gradients and subsequent convection. These temperature gradients can damage the separation, due to zone broadening and unreproducible migration times (section 1.5) [51]. The temperature in the centre of the capillary is higher than that at the edges, producing a parabolic flow profile within the capillary. Joule heating can be controlled by operating at a voltage where the heat can be effectively dispersed [51]. However, theoretical calculations have suggested that, a 1.5°C centre-to-wall temperature difference in aqueous electrolyte will not cause a serious decrease in the plate numbers of the system for thermostated capillaries with an inner radius ≤ 50 μm [52].

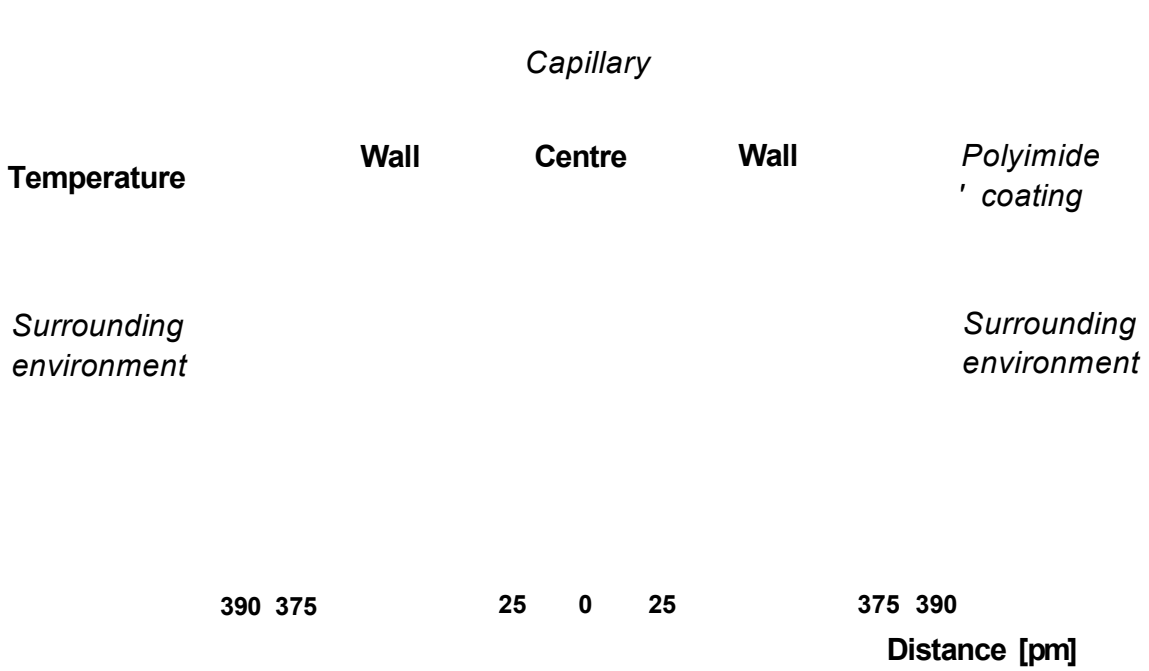

Figure 1.7 Schematic of temperature gradients in a CE capillary and around it.

Dissipation of heat through the walls, causing a thermal gradient between the capillary centre and the surrounding environment is shown schematically in Figure 1.7 [53].

The application of longer capillaries with narrower inner radius and larger outer diameter is advantageous due to the better heat dissipation to the

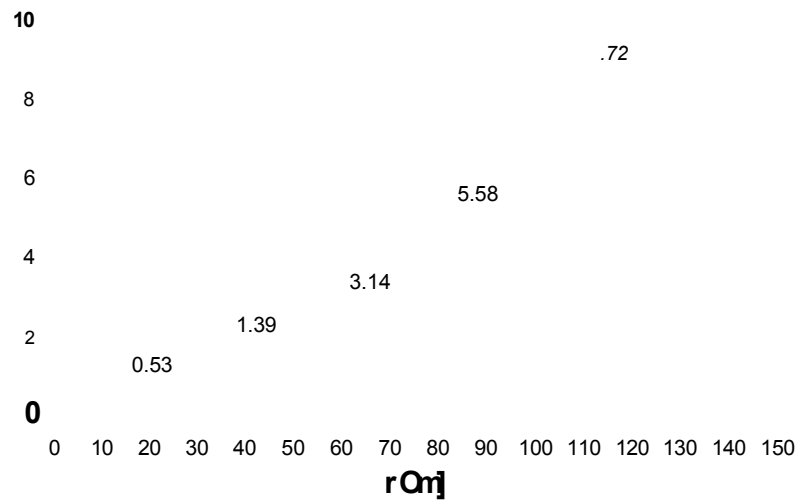

Figure 1.8 Graphical example of the calculated centre-to-wall temperature difference for capillaries with different radius (based on [52])

surrounding environment as the insulating effects of the polyimide coating is reduced.

However, the analysis time can be reduced at higher temperature and in some cases enhanced resolution can be obtained or can be used to affect protein conformation [54,55].

Despite these positive effects, the problems caused by the excess heat are generally much greater. Therefore temperature is usually not an operational variable in method development and CE systems are generally thermostated with high velocity airflow, to reduce the generated heat and maintain a constant temperature (± 0.1°C) through the analyses.

1.6.3 pH of the running buffer

The pH is the most crucial parameter in CE. It has a significant effect on the generation of EOF, since it changes the zeta potential through its influence on the deprotonation of the inner surface of the capillary. The pH dependence of the EOF for different capillary materials has been discussed by Lukacs and Jorgenson [49].

The pH also influences the analytes' electrophoretic mobility due to the changes in the degree of ionisation.

The effective mobility, μ_{eff}, of a monovalent weak acid or base is determined by

$$\mu_{eff} = \mu_e \alpha \tag{1.36}$$

α = the degree of dissociation, given for a monovalent acid by

$$\alpha = \frac{1}{(1+10^{pKa-pH})} \tag{1.37}$$

and for a monovalent base by

$$\alpha = \frac{1}{(1+10^{pH-pKa})} \tag{1.38}$$

pK_a =the acid constant.

The charge and, thus, the electrophoretic mobility of an ion are affected by the pH of the electrolyte solution [38]. Thus, altering the pH a general step in method development.

1.6.4. Concentration and Ionic strength of the Running Buffer

The EOF is reduced at constant temperature, if the ionic strength or concentration of the buffer is increased. The reason is the reduced zeta potential since the increased ionic strength compresses the diffuse double layer, and decreases its thickness (Eq. 1.5).

Reducing the buffer concentration too much, to obtain a high EOF, can cause asymmetric peaks and band broadening. The conductivity can be different in the running buffer and the sample plug and this can cause distortion in the electric field. (The ionic strength of inorganic buffers is usually higher than that of the organic buffers at the same concentration. Therefore, this must be take account when choosing a buffer for a given pH range).

1.6.5 Injection plug length

During injection it is important to minimise the sample plug length as the resolution and efficiency is diminished if it is longer than the dispersion caused by diffusion (see 1.5).

$$\sigma^2{}_{Inj} = \frac{w_{nj}^2}{12} \tag{1.39}$$

σ^2 = spatial variance; w_{inj} = injection plug length.

To minimise the injection contributions to the loss in efficiency, the injected plug length should be as short as possible. It is recommended that it should be less than 1-2% of the total capillary length [51,56]. This is equivalent to less than a few tens of nanolitre of sample [6-70nl] or 3-16mm plug length for generally used capillaries (L=30-80cm, I.D.=50 and 75 μm)

1.6.6 Conductivity of the sample (Electrodispersion)

The conductivity of the sample and the running buffer should be similar to avoid peak distortions caused by electrodispersion. Since the conductivity is inversely proportional to electric field strength, the electric field will be lower outside the sample zone if the running buffer has a higher conductivity than the sample. Thus, when an analyte diffuses into the buffer from the back of the sample zone it meets a lower electric field and its velocity is reduced. As the sample zone moves away, peak tailing also occurs. If the analyte diffuses into the buffer from the sample zone front, its velocity will also be reduced. But as the zone reaches this slower analyte it can diffuse back into the sample zone. This keeps the sample front sharp. The overall result will be a skewed, triangular shape peak, which can lead to loss of resolution.

To minimise band broadening the conductivity of the sample should match with the running buffer or the sample concentration should be much less (approximately one hundred times) than the concentration of the running buffer.

1.7 Capillary wall modification (Coatings and Surface modifiers)

Separation efficiency in CE can be reduced by the presence of an irreproducible EOF and by the adsorption of analytes to the capillary wall. In particular, positively charged analytes have a tendency to interact with the negative silanoate groups, resulting in peak broadening and peak distortion. These decrease separation efficiency and sensitivity. In addition, the

magnitude of the EOF becomes unpredictable leading to poor repeatability of mobilities of analytes.

In particular proteins have the unfortunate property of sticking to the capillary wall due to multi-modal interactions, such as hydrophobic, hydrophilic, electrostatic, hydrogen bonding and van der Waals interactions [59]. The adsorption of the analytes reduces the separation performance due to peak broadening and tailing resulting in decreased efficiency or even the analytes total retention on the inner surface.

Capillary conditioning (pre-treatment and regeneration of the inner surface) for fused-silica is commonly used to overcome this problem. Before the application of a new silica capillary, it is generally washed through with alkaline solution - typically 1M Sodium hydroxide solution - then with water and finally with the running buffer. This procedure will ensure the full deprotonation, and uniform charge of the inner capillary wall. The regeneration of the charged capillary surface is often required between sample runs, to overcome the problem of analyte-wall interaction, or migration instability. The regeneration step applies the same procedure, but with less concentrated alkaline media (0.1M) as the silica surface can be damaged by strong alkalis, since the silica is soluble in strong bases. At pH greater than 11, dissolution of the silica capillary material becomes on issue.

Simple rinsing between the runs, with the running buffer, was also reported to help reproducibility [57]. It must be noted that capillary reconditioning with alkalines cannot be used with most of the coated capillaries and with packed CEC capillaries, as it may damage the modified inner surface or the stationary phase particles.

Besides the above mentioned capillary conditioning, there are two general strategies to modify the capillary wall: permanent coatings (bonded and altered phases) and dynamic coatings (continuous modification with additives

in the running buffer) [58,59]. Both modification methods have advantages and disadvantages.

The use of extreme pH can make capillary wall derivatisation unnecessary, although in the case of protein analysis care should be taken using such pH. Outside of their physiological conditions protein structure may be irreversibly altered, aggregation and/or unfolding may occur and biological activity may become very different.

1.7.1 Permanent Coatings

The EOF can be suppressed or controlled at a certain pH, and analyte-wall interactions can be reduced or eliminated, by coating the active sites on the inner surface of the fused-silica capillary. The active sites contain unreactive siloxane bridges, hydrogen bonding sites and ionisable vicinal, geminal and isolated silanol groups [35,44]. The structure of the silica surface will be more fully discussed in Chapter 4.

Several approaches have been tried for the preparation of permanent coatings. These can be divided into two types: (1) coatings that are covalently attached to the capillary surface; (2) coatings that are adsorbed to the surface by physical or ionic forces, which however, unlike dynamic coating are not dissolved in the running buffer during the separation [53,58,59].

The most widely used method for covalent bonding includes three main steps: capillary pre-treatment including etching and leaching, introduction of double bonds to the capillary wall by silylation, and finally deactivation by binding of a polymer to this reactive layer to form a stable, both (chemically and mechanically) capillary surface (Si-O-Si-R) [58]. However the siloxane bond still has only a limited stability to pH (range between pH=4-7) and to hydrolysis, and hence the coatings have limited stability as well [61,62].

This can be overcome by direct Si-C-R coupling. The direct Si-C bond can be formed by the use of a Grignard reagent. These coatings were reported to be stable between pH=2-10 [63]. However, these processes are difficult and time-consuming and the coating may not be reproducible as a result [64].

Single step procedures were described by Zhao *et al.* [65]. First a static coating (using Poly(ethylene glycol), PEG) is formed on the surface, then after the evaporation of the volatile solution, the permanent coating is formed by heating.

To achieve a homogeneous coating surface, the capillary wall must be cleaned and activated prior to the coating process in a similar way to capillary conditioning. This rinsing procedure includes etching with sodium hydroxide to remove impurities from the fused-silica capillary surface, and leaching with hydrochloric acid to remove trace metals. [58]

The adsorbed coatings are prepared by flushing the capillary through with the reagent in a suitable electrolyte solution. The hydroxylic polymers usually require thermal fixation (to cross-link between the polymer chains) to become stable. Before the analysis, the unbonded reagent is flushed out of the capillary [60].

The adsorbed compounds in the coating are hydrophilic, and include mainly two types of compounds: polycationic (amines) and neutral (hydroxylic) polymers. Aminated compounds (*e.g.* polyethyleneimine, polyamine) create a stable positively charged coating surface [66] and are useful over a wide pH range of 2-11. Hydroxylic polymers (*e.g.* polyvinyl alcohol and polyethylene oxide) create a neutral coating surface by weak interactions such as hydrogen bonds. Because these compounds are not charged, the coating is stable over almost the entire pH range [59].

Depending on the deactivation, the EOF can be [53] :

- Accelerated or - *e.g.* polymethylsiloxane
- Decreased - *e.g.* polyethylene glycol
- Reversibly modified by the pH - *e.g.* amphoteric species (*e.g.* proteins)
- Eliminated - *e.g.* polyvinyl alcohol
- Reversed - *e.g.* polyethylenimine

1.7.2 Dynamic Coatings

Addition of surface modifiers to the running buffer, and in-situ deactivation of the capillary wall is a simpler alternative approach. As the modifiers continuously (re)generate the coatings in each run, the stability of these are better than that of permanent coatings. The application of these additives are simple as they can be prepared by simply dissolving them in the running buffer. Dynamic coatings can be not only easily formed, but removed as well, by flushing the capillary. The additives used in dynamic coatings can interact strongly with the capillary wall by Ionic/Coulombic forces (amines, ionic additives), hydrogen bonding (neutral polymer additives) and van der Waals forces (surfactants). Dynamic coatings alter the charge and/or hydrophobicity of the capillary wall and can modify, block or reverse the EOF.

The polymers used in adsorbed coatings can be applied as additives for dynamic coatings as well (Table 3). The applied concentrations should be very low compared to permanent coatings in order not to alter the viscosity of the running buffer significantly. For example, the effect of polyvinyl alcohol (PVA) modification as permanent and dynamic coatings on protein separation and EOF has been studied [69].

Permanently coated, thermal immobilised PVA gave better efficiency and EOF suppression at higher pH (above pH=9) due to the more efficient shielding of the cross-linked multimolecular polymer layer at the surface and thus the reduced analyte-wall interactions.

Type	Effects, comments
1, Hydrophilic polymers • Polyvinyl alcohol • Polyacrylamide • Alkyl Celluloses • Dextrans	• Shield wall charge and reduce EOF • Increase Viscosity
2, Surfactants • Anionic (SDS) • Cationic (CTAB, TTAB) • Zwitter ionic (CHAPS, CHAPSO) • Non-ionic (BRIS, Triton X)	• Can decrease or reverse EOF • Easy to use, wide variety of surfactants • May denaturate proteins
3, Quaternary amines • DETA, Hexadimethrine bromide • Polymers (Polybrene, Praestol)	• Can decrease or reverse EOF • Also act as ion-pairing reagents
4, Adsorbed polymers • Cellulose • Poly(ethylene glycol) • Polyvinyl alcohol	• Poor long term stability • pH=2 - 4 range • Relatively hydrophobic
5, Adsorbed cross-linked polymers • Polyethyleneimine	• Reverses EOF • Stable at physiological PH

Table 1.3 Common additives in dynamic coatings (1-3), and adhered phases (4-5) in permanent coatings [53].

Detection can be problematic when additives are used, especially post-column detection using CE/MS coupling *i.e.* addition of surfactants can result in the ion current being dominated by the surfactant, difficulties can also arise in spraying due to foaming *etc.* [59,92]

Dynamic and permanent coatings of the fused-silica capillary inner surface have been studied extensively, especially in the field of protein separations. Characterisations of the properties of the coated capillaries are commonly

performed by measuring the EOF and investigating its dependence on the pH of the electrolyte solution [40]. It was also found that the effectiveness of the dynamic coatings in protein separations is not always sufficient.

1.8 Instrumental Considerations

A schematic of a general capillary electrophoresis system is shown in Figure 1.9. The overall typical instrumentation is very simple and similar for all CE instruments. These include a high-voltage power supply (30kV), electrodes, a source (inlet) and destination (outlet) buffer and sample vials, fused silica capillary and a detector linked to an integrator or PC.

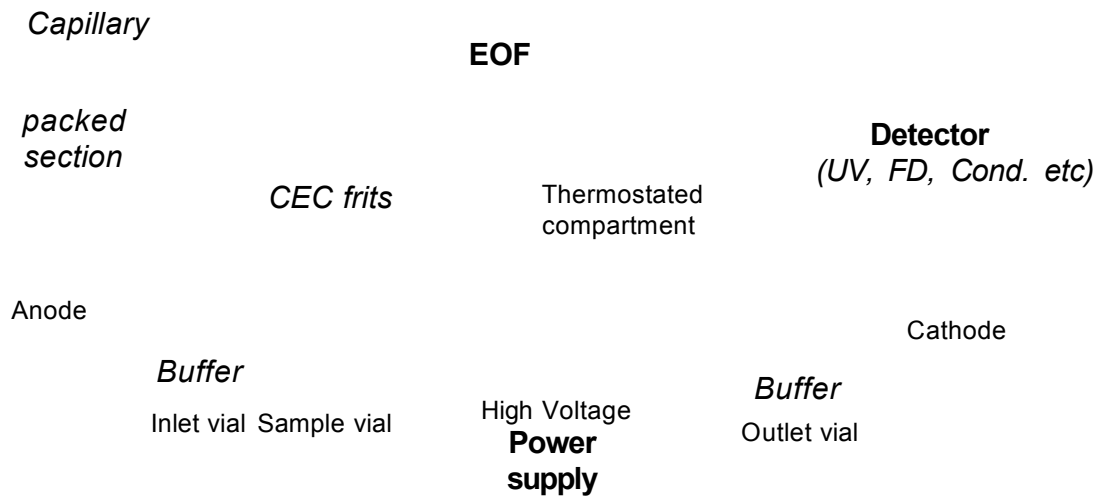

Figure 1.9 Diagram of a general CE and CEC instrumentation.

The purpose of the power supply is to provide the electric field (voltage, current) needed for electrophoresis. Modern instruments can operate in constant voltage and constant current mode and supply up to 30 kV. Beyond this voltage corona discharge and high current, causing high Joule heating, occurs. The maximum currents of 300 are generally available. The polarity of the voltage is generally reversible. In "normal mode" injection occurs at the anode and the EOF is towards the cathode. Most instruments contain a thermostated compartment to control the capillary temperature for

dissipation of the undesirable Ohmic heating and a small pressurisation system for capillary wash and sample injection.

1.8.1 Sample Injection

One of the advantages of CE is that only a very small amount of sample is required, usually just a few nanolitres are introduced into the capillary. Conversely, these minute sample volumes raise serious sensitivity and detection difficulties for diluted samples (see 1.8.2.).

Although several injection techniques - to be precise, sample introduction techniques - have been reported (*i.e.* microinjection [70], rotary type injection [71] *etc.*), basically only two different methods are used to deliver the sample into the capillary: electrokinetic and hydrodynamic injection. In either case, the loaded sample quantity is generally not known, but can be calculated.

1.8.1.1 Hydrodynamic Injection

The most widely used hydrodynamic injection method is based on the pressure difference across the capillary between the inlet and outlet sample vials. This can be accomplished by several techniques such as adding pressure or vacuum to the inlet or outlet sample vial or lifting the inlet vial relative to the outlet (siphoning).

The injected sample volume (V_{inj}) can be easily calculated by using the Hagen-Poiseuille equation:

$$V_{inj} = \frac{\Delta P r^4 \pi t}{8 \eta L} \tag{1.40}$$

ΔP = Pressure difference across capillary; r = Capillary radius; π = Pi; t = Injection time; η = Viscosity; L = Total length of capillary.

The volume injected by siphoning can be calculated from equation. 1.40 after replacing ΔP as

$$\Delta P = \rho g \Delta h \tag{1.41}$$

ρ = Density of the buffer (0.9972 g/ml for water at 20°C); g = Gravitational constant (6.67×10^{-11} Nm^2 kg^{-2}); Δh = Height difference between the vials.

After combining 1.40 and 1.41, a more practical equation (1.42) can be used for calculation of injected volume:

$$Vinj = \frac{1.775 \times 10^{-9} \Delta h r^4 t}{L} \tag{1.42}$$

Δh = Height difference between the vials; r = Capillary radius; t = Injection time; L = Total length of capillary.

The main advantage of hydrodynamic injection is that the injected sample quantity is nearly independent of the sample matrix and analyte electrophoretic mobility. In general, hydrodynamic injection has good reproducibility (if the temperature of the sample is kept constant the only sample variable, the viscosity will be constant as well) and good control over the injected amount of sample. However, providing a stable and accurate pressure is rather complicated and requires extra instrumentation and is not or hardly applicable with capillaries that are filled with gels or packed with solid stationary phases.

1.8.1.2 Electrokinetic injection

Instrumentally, electrokinetic injection is the simplest sample introduction technique since it uses no extra parts. The inlet of the capillary is placed into the sample vial with the electrode while the outlet is placed into a separation buffer vial and high voltage is applied for a given period of time. Analyte ions enter into the capillary due to the combination of electroosmotic flow of the

sample solution and the electrophoretic migration of the ions. After the injection the inlet is placed back into the separation buffer vial.

The injected sample quantity, Q (gram or mole) can be calculated by

$$Q = \frac{(\mu_E + \mu_{EOF})V\pi r^2 Ct}{L} \tag{1.43}$$

μ_E = Electrophoretic mobility; μ_{EOF} = Electrophoretic mobility of the buffer; V = Voltage; r = Capillary radius; C = Analyte concentration; L = Total length of capillary.

As can be seen from Eq. 1.43 the injected quantity is dependent on the individual electrophoretic mobility of the analyte molecules. If the molecules are charged, discrimination occurs amongst them, as they migrate into the capillary by different amounts. The more mobile ions are loaded to a greater extent than those that are less mobile [72]. This sample bias or sample preconcentration is explained in Figure 1.10

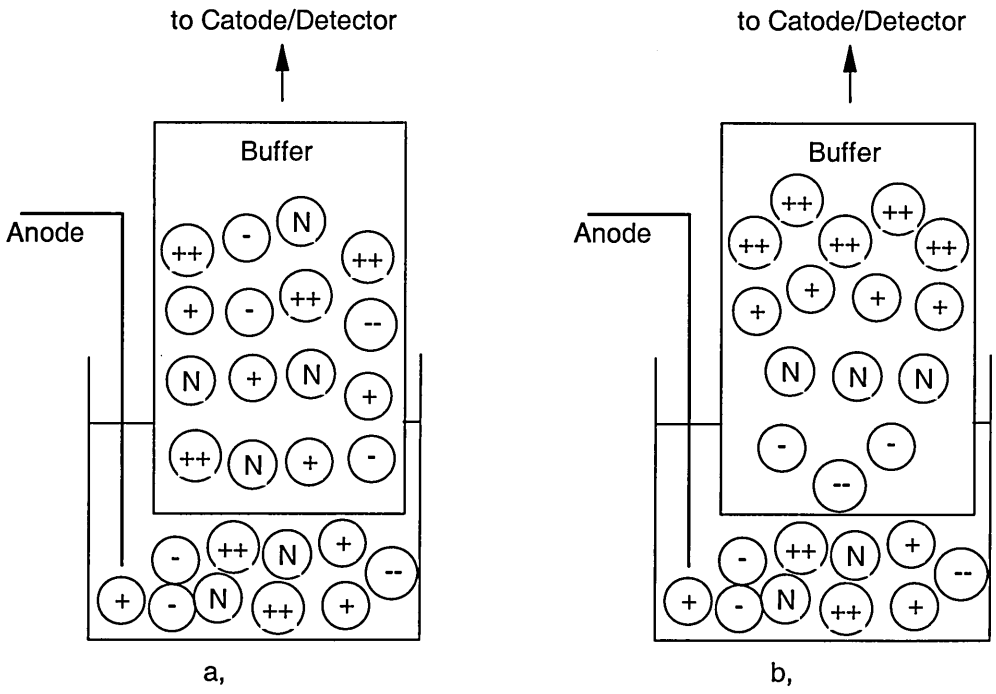

Figure 1.10 Representation of solute distribution and sample bias in hydrodynamic (a,) and electrokinetic (b,) injection during injection.

Variations in conductivity and/or resistance (*i.e.* ionic strength, solution composition and pH) of the sample will influence the amount loaded. This effect was first described by Huang *et al.* [73] who plotted the peak areas vs. resistance of the sample solutions using various buffer concentrations with both electrokinetic and hydrodynamic injection. Lower buffer concentrations resulted in a higher resistance, and the EOF and the electrophoretic mobilities of the solutes increased (see section 1.3), so the quantities of the of the injected solutes increased.

Another effect of sample bias is sample depletion. If the sample is injected from the same source the concentration of the high-mobility solute will continuously decrease as a larger amount of it is loaded into the capillary with every injection than of the low-mobility solute. This results in a decrease in the ionic strength of the sample, which will cause further variation in the injected sample quantity.

It was also found by Boer and Ensing [74] that the positions of the electrodes and the volume in the sample vial also can influence the injected amount of the analyte. They found that this effect is reduced if the capillary is positioned inside the electrode, like in the Hewlett-Packard ^{3D}CE system. In the more conventional set-up, where the electrode needle is parallel to the end of the capillary, the system causes more friction, which leads to a change in the alignment. The sample volume in the vial was found to be proportional to the peak area. This effect is explained by the fact that the electric field over the samples during the injection is decreased with the volume of sample solution, which leads to a reduced sample amount in the capillary. They also found that a lower injection voltage with longer injection time (10kV and 9seconds) produced more reproducible peak areas than a shorter injection applying higher voltage (30kV and 3 seconds).

Several studies have been carried out to correct these quantitative errors [75] or to develop non-discriminating electrokinetic injection, such as on-

column fracture injection [76] but they are complicated, inaccurate and not fully discrimination free [77].

Despite the sample bias, sample depletion and quantitative limitations, electrokinetic injection is very simple and requires no extra instrumentation. It is the sole injection technique used for gel electrophoresis and electrochromatography, where hydrodynamic injection cannot be used due to the fact that hydrodynamic flow is hampered or suppressed by the high back pressure of the packed capillary or due to the danger of pushing the gel or CEC stationary phase out of the filled/packed capillary.

1.8.2 Detection

Detection in CE is a challenge due to the very small dimensions of the capillaries, the extremely low zone volumes of the solutes, high peak efficiencies and limited detection time available.
Despite these difficulties a large number of detection methods have been used and demonstrated in CE. Most of these detection techniques are based on light and have been previously employed for HPLC as similarly to CE the separated solutes elute from a tube in a liquid.

These techniques include:

1 Optical detectors (UV/Vis; Fluorescence [78-79]; Laser-induced-fluorescence [80-81], Raman [82-83], Refractive index [84-85] and Laser-Light Scattering [86] *etc.*),
2 Electrochemical detectors (Amperometry [87-88], Potentiometry [89] and Conductivity [90-91]).
3 Spectrometric detectors (Mass spectrometry [92-93] and NMR [94-95])
4 Radiometric detectors [96-97].

Table 1.4 lists many of these methods with their features and approximate detection limits.

Detector	Approximate Detection Limits		Features	
	Moles	Molarity*	Selective	Universal
Laser-induced Fluorescence	10^{-18}-10^{-20}	10^{-13}-10^{-16}	Yes	
Amperometric	10^{-18}-10^{-19}	10^{-7} -10^{-10}	Yes	
Radiometric	10^{-17}-10^{-19}	10^{-10}-10^{-12}	Yes	
Mass Spectrometry #	10^{-16}-10^{-17}	10^{-8} -10^{-10}	Yes	Yes
Fluorescence	10^{-15}-10^{-17}	10^{-7} -10^{-9}	Yes	Yes
Conductivity	10^{-15}-10^{-16}	10^{-7} -10^{-9}		Yes
Indirect Fluorescence	10^{-14}-10^{-16}	10^{-6} -10^{-8}		Yes
Refractive index	10^{-14}-10^{-16}	10^{-6} -10^{-8}		Yes
UV/Vis absorbance (DAD) #	10^{-13}-10^{-16}	10^{-5} -10^{-7}	Yes	
Indirect absorbance	10^{-12}-10^{-15}	10^{-4} -10^{-6}		Yes

* Depends upon injected sample volume (10nl assumed). # Qualitative information possible.

Table 1.4 Generally available capillary electrophoresis detectors. Their approximate detection limits and features [27,36]

1.8.2.1 Ultraviolet/Visible detection

UV/Vis absorbance detection is the most widely used (as in HPLC) method due to its almost universal detection nature, ease of use, great simplicity and relatively low cost. And most of all, UV/Vis absorbance detection is compatible with all of the modes used in CE. On-column detection can be carried out with externally and internally coated fused silica capillaries. UV transparent polyimide coatings are also available, although at higher price than the conventional coatings. Thus the detection window formation is not required, which makes the system more resistant towards physical interactions, such as bending, moving *etc*. On-column detection can be used

even with packed capillaries [98,99] when the stationary phase, which is in contact with the mobile phase, is translucent to UV light (which is the case with the most widely used silica phases and usual liquid mobile phases).
UV/Vis absorbance (A) detection is based on the Beer-Lambert's law:

$$A = \log \frac{I}{I_0} = \varepsilon bc \tag{1.44}$$

I_0 = Intensity of the initial light; I = Intensity of the transmitted light after the detector cell; ε = Molar absorptivity; b = Optical path-length and c = Concentration of the analyte.

As equation 1.44 shows, the sensitivity of UV/Vis detection of a solute of a certain concentration depends on the optical path-length and the analyte's molar absorptivity. The latter parameter further depends on the molecular structure (presence of chromophores), the wavelength of the light and the composition and pH of the mobile phase (buffer).

The application of capillaries with larger internal diameter - although an obvious choice to improve the path-length – is not advisable due to the generation of higher current and subsequent Joule heating in the system. A two-fold increase in the internal diameter (and in sensitivity) would increase the current four-fold, which would degrade the separation efficiency and resolution (see section 1.6.1.2) .

A further problem is that due to the capillaries' curvature the actual optical path-length is less than the internal diameter (d) by a factor of $\pi d/4$ [100]. As only a fraction of the total light is able to pass through the capillary centre not only is the sensitivity reduced but the linear detection range is as well. The observed absorbance can be calculated from equation 1.45:

$$A = \log \frac{I + I_S}{I_0 + I_S} \tag{1.45}$$

I_S = Intensity of stray light through the capillary wall.

This problem from stray light (the light which reaching the detector directly, without passing through the solute, *i.e.* through the silica capillary wall) increases with narrower capillaries. Its effect can be reduced by the optimisation of the optics (slit size, positioning *etc.).*

Several approaches have been made to increase the optical path-length in the detector cell without increasing the overall capillary diameter as well. The main developments are the Z-cell [101], rectangular-cell [102], bubble-cell [103] and multi reflection-cell [104,105].

b,

d, e,

Figure 1.11 Different detection cells developed to increase path-length detection sensitivity: (a) Conventional capillary with removed polyimide coating, (b) Rectangular cell, (c) Bubble-cell, (d) Z-cell and (e) Multi reflection-cell.

Optimisation of the molar absorptivity is mainly by the choice of the optimum wavelength (where ε is maximum), although the pH buffer composition, and degree of ionisation of the analyte can also influence the optimum wavelength and the value of ε. Therefore it may be necessary to optimise these parameters as well.

In the short wavelength UV light range (≤200nm), most analytes have some absorbance, and molecules without chromophores that cannot be derivatised can be detected. Carbohydrates, (oligo)saccharides are general examples, the detection of sweeteners at 192nm [106] and oligosaccharide alditols at 185nm [107] have been reported.

The main drawback of short wavelength detection is the available running buffers, solvents and additives; as most absorb in this UV region. Aqueous phosphate and borate buffer solutions are adequate for these analyses, while Tris, Hepes, Mes organic buffers *etc.* are appropriate only above 220nm. Table 1.5.

Buffer (conc. 10 mM)	Minimum Wavelength
Borate	185 nm
Phosphate	195 nm
Triethylamine	<200 nm
Ammonium Hydroxide	200 nm
Formic acid	210 nm
Acetate	220 nm
Tris	220 nm
MES	230 nm
HEPES	230 nm
Citrate	260 nm

Table 1.5 Minimum useful wavelengths of common pH buffers in UV detection [108].

Except for acetonitrile, most organic solvents absorb above 205nm (Table 1.6) thus their usage is limited in the far-UV. Buffer components (especially those that contain carboxylates) that have a high absorbance below 200 nm must be avoided as well *e.g.* as glycols, EDTA [109].

In addition to the sample and buffers, oxygen also absorbs UV light. Oxygen can be removed by purging with nitrogen.

Solvents	UV Cut-off [nm]*
Acetonitrile	185
i-Propanol	205
Methanol	205
Ethanol	210
Dichlomethane	233
Ethyl Acetate	256
Dimethyl Sulphoxide	268

*The wavelength at which the solvent absorbance in a 1cm pathlength cuvette is equal to 1 absorbance unit [AU] using water as the reference.

Table 1.6 UV cut-off wavelengths of common CE solvents and buffer additives [110].

Absorptivity can be modified by derivatisation of the analyte, but this requires an extra reaction stage between the analyte and a molecule with chromophore, which is not always possible or desirable.

For analytes without a UV/Vis absorbing chromophore (for example certain aliphatic carboxylic acids, carbohydrates, and inorganic ions) and where there is no available derivatisation possibility, then indirect detection can be used.

In this method the running buffer (*i.e.* 4-aminopyridine, phthalate) and/or additive (*i.e.* chromate or small amines such as imidazole, benzylamine) with high chromophoric properties can provide the means of visualisation. Since they have high UV absorption analytes are detected as negative peaks due to the decrease in the background signal. Beside the high absorptivity, the mobility of the buffer and/or additives should match that of the analytes to prevent asymmetrical peaks (See 1.6.6). The useful concentration range of the buffers and/or additives is rather limited, generally in the 2-20mM range. Higher concentrations affect the linearity of the detection and give a high background noise level, while lower concentrations increase peak broadening.

The noise level in indirect detection is often much higher than expected compared to direct detection [111,112]. This noise does not arise from the detector rather it is related to disturbances connected to a thermal node and heat dissipation problems in the whole the system (capillary, injection port, detector) [113,114]. Thus uniform cooling is very important in indirect detection.

References

1. Tiselius A.; *Trans. Faraday Soc.* 33 (1937) 524
2. Kolin A.; *J. Appl. Phys.* 25 (1954) 1442
3. Hjérten S.; *Chrom. Reviews* 9 (1967) 122
4. Mikkers F.E.P.; Everaerts F.M. and Verheggen Th.P.E.M.; *J. Chrom.* 169 (1979) 11
5. Virtenen P.; *Acta Polytech. Scand.* 123 (1974) 1
6. Everaerts F.M., Beckers J.L. and Verheggen T.P.E.M.; *Isotachophoresis: Theory, Instrumentation and Application.* Elsevier, Amsterdam 1976
7. Jorgenson J.W. and Lukacs K.D.; *Anal. Chem.* 53 (1981) 1298
8. Jorgenson J.W. and Lukacs K.D.; *J. Chrom. 218* (1981) 209
9. Terabe S., Otsuka K., Ichikawa K., Tsuchiya A. and Ando T.; *Anal. Chem.* 56 (1984) 111
10. Terabe S., Ozaki H., Otsuka K. and Ando T.; *J. Chrom.* 332 (1985) 211
11. Hjérten S. and Zhu M.D.; *J. Chrom.* 346 (1985) 265
12. Hjérten S.; *J. Chrom.* 347 (1985) 191
13. Cohen A.S. and Karger B.L; *J. Chrom.* 397 (1987) 409
14. Cohen A.S. Paulus A. and Karger B.L; *Chromatographia* 24 (1987) 14
15. Foret F.; Szoko E.; Karger B.L.; *J. Chrom.* 608 (1992) 3
16. Thompson T.J.; Foret F.; Vouros P. and Karger B.L.; *Anal. Chem.* 65 (1993) 900
17. Strain H.; *J. Am. Chem. Soc.* 61 (1939) 1292
18. Knox J.H. and Grant I. H.; *Chromatographia* 24 (1987) 135
19. Knox J.H. and Grant I. H.; *Chromatographia* 32 (1991) 317
20. Behnke B., Bayer E.; *J. Chrom.* A 680 (1994) 93
21. Smith N.W. and Evans M.B.; *Chromatographia* 38 (1994) 649
22. Tsuda T.; *LC-GC Int.* Vol 5 No.9 (1992) 26

23. Dittmann M.M., Wienand K., Bek F. and Rozing G.P.; *LC-GC* 13 (1995) 800
24. Rathore A.S. and Horvath Cs.; *J. Chrom. A 781* (1997) 185
25. Bartle K.D. and Myers P.; *J. Chrom. A 916* (2001) 3
26. Watzig H; Dette C and Fresenius J.; *Anal. Chem.* 345 (1993) 403
27. Kunkel A; Degenhart M; Schirm B and Watzig H.; *J. Chrom.* 768 (1997) 17
28. Baker D.R.; *Capillary Electrophoresis.* John Wiley & Sons, Inc. 1995
29. Melanson J. E., Baryla N. E. and Lucy C. A.; *TrAC.* 20 (2001) 365
30. Salomon K., Burgi D.S. and Helmer J.C.; *J. Chrom.* 559 (1991) 69
31. Foret F. and Bocek P.; *Adv. Electrophoresis* 3 (1990) 272
32. Schwer C. and Kenndler E.; *Anal. Chem.* 63 (1991) 1801
33. Huang T.L., Tsai P., Wu C.T. and Lee C. S.; *Anal. Chem.* 65 (1993) 2887
34. Corradini D., Rhomberg A. and Corradini C.*; J. Chrom. A.* 661 (1994) 305
35. Corradini D.; *J. Chrom. B.* 699 (1997) 221
36. Tsuda T., Nomura K. and Nagakawa G.; *J. Chrom.* 248 (1982) 241
37. Ewing A.G., Wallingford R. A. and Olefirowicz T. M. *Anal. Chem.* 61 (1989) 292A
38. Knox J.H.; *J. Chrom. A.* 680 (1994) 3
39. Lambert W. J. and Middleton D. L.; *Anal. Chem.* 62 (1990) 1585
40. Kohr J. and Engelhardt H.; *J. Chrom. A.* 652 (1993) 309
41. Kosmulski M., Hartikainen J., Maczka E., Janusz W. and Rosenholm J.B.; *Anal. Chem.* 74 (2002) 253
42. Harris D.; *Quantitative Chemical Analysis,* W.H.Freman and Co. 4th Ed. 1995
43. Davis M. and Giddings J.C; *Anal. Chem.* 55 (1983) 418
44. Snyder L.R, Kirkland J.J and Glajch J.L; *Practical HPLC Method Development*, Wiley 2nd Ed. 1997
45. Van Deemter J.J, Zuiderweg F.J. and Klinkenberg A.; *Chem. Eng. Sci.* 5 (1956) 271

46. Kennedy G.J. and Knox J.H; *J. Chrom. Sci.;* 10 (1972) 549
47. Knox J.H.; *J. Chrom. A.* 960 (2002) 7
48. Knox J.H.; *Chromatographia* 26 (1988) 329
49. Lukacs K.D. and Jorgenson J.W.; *J. High Res. Chrom.* 8 (1985) 407
50. Lee T.T and Yeung E.S.; *Anal Chem.* 64 (1992) 1226
51. Ward V. L. and Khaledi M. G.; *J. Chrom. A* 859 (1999) 203
52. Gruska E., McCormick R.M. and Kirkland J.J.; *Anal. Chem.* 61 (1989) 241
53. Heiger D.; *An Introduction, High Performance Capillary Electrophoresis*; Agilent Technologies 2000
54. Guttman A. Horvath J. and Cooke N.; *Anal. Chem. 65* (1993) 199
55. Rush R.S., Cohen A.S. and Karger B.L.; *Anal. Chem. 63* (1991) 1346
56. Albin M., Grossman P.D. and Moring S.E.; *Anal. Chem. 65* (1993) 489A
57. Khaledi M.G., Smith S.C. and Strasters J.K.; *Anal. Chem. 63* (1991) 1820
58. Horvath, J. and Dolník, V.; *Electrophoresis* 22 (2001) 644
59. Khaledi M.G. *High Performance Capillary Electrophoresis*, Wiley and Sons. 1998
60. Rodriquez, I. and Li, S. F. Y. *Anal. Chim. Acta* 383 (1999) 1
61. Melanson, J. E., Baryla, N. E. and Lucy, C. A.; *TrAC.* 20 (2001) 36
62. Nakatani, M., Shibukawa, A. and Nakagawa, T.; *Electrophoresis* 16 (1995) 1451
63. Cobb K. A., Dolnik V. and Novotny M.; *Anal. Chem.* 62 (1990) 2478
64. Cifuentes, A., Canalejas, P., Ortega, A. and Díez-Masa, J. C.; *J. Chrom. A* 823 (1998) 561
65. Zhao Z., Malik A. and Lee M.L.; *Anal. Chem.* 65 (1993) 2747
66. Erim, F. B., Cifuentes, A., Poppe, H. and Kraak, J. C.; *J. Chrom. A* 708 (1995) 356
67. Lux J.A., Yin H. and Schomburg G.; *J. High Res. Chrom.* 13 (1990) 145

68. Maa Y.F., Hyver K.J. and Swedberg S.A.; *J. High Res. Chrom.* 14 (1991) 65
69. Gilges M., Kleemiss M.H. and Schomburg G.; *Anal. Chem.* 66 (1994) 2038
70. Wallingford R.A. and Ewing A.G.; *Anal Chem.* 60 (1988) 1972
71. Tsuda A., Nomura K. and Nakagawa G.; *J. Chrom.* 264 (1983) 385
72. Albin M. Grossman P.D. and Moring S.E.; *Anal. Chem.* 65 (1993) 489A
73. Huang X, Gordon D.L. and Zare R.N; *Anal. Chem.* 60 (1988) 375-377
74. De Boer Th. and Ensing K.; *J. Chrom. A.* 788 (1997) 212
75. Qi S., Huang A. and Sun Y.; *Anal. Chem.* 68 (1996) 1342
76. Linhares M.C. and Kissinger P.T.; *Anal Chem.* 63 (1991) 2076
77. Wei H., Ang K.Ch. and Li S.F.Y.; *Anal. Chem.* 70 (1998) 2248
78. Hemnel G. and Blaschke G.; *J. Chrom. B.* 675 (1996) 131
79. Lee T.T., Lillard S.J. and Yeung E.S.; *Electrophoresis.* 14 (1993) 429
80. Cherkaoui S., Faupel M. and Francolte E.; *J. Chrom. A.* 715 (1995) 159
81. Shaole Wu and Dovichi N.J.; *J. Chrom. A.* 480 (1989) 141
82. Walker P.A., Kowalchyk W.K. And Morris M.D.; *Anal. Chem.* 67 (1995) 4255
83. Chen C-Y. and Morris M.D.; *J. Chrom.* 540 (1991) 355
84. Chen C-Y., Demana T., Huang S.D. and Morris M.D.; *Anal. Chem.* 61 (1989) 1590
85. Bruno A.E., Kratigger B., Maystre F. and Widmer H.M.; *Anal. Chem.* 63 (1991) 2689
86. Watt P.J.; *Anal.Chim. Acta* 272 (1993) 1
87. Ewing A.G., Mesaros J.M. and Gavin P.F.; *Anal. Chem.* 66 (1994) 527A
88. Wallingford R.A. and Ewing A.G.; *J. Chrom.* 441 (1988) 229
89. Virtaen R. *Acta Polytech. Scand.* 123, 1 (1974)
90. Huang X., Pang TK., Gordon M.J., and Zare R.N.; *Anal. Chem.* 59 (1987) 2747

91. O'Shea T.J., Greenhagen R.D., Lunte S.M., Lunte C.E., Smyth M.R., Radzik D.M. and Watanabe N.; *J. Chrom. A.* 593 (1992) 305
92. Tomer K.B., Moseley M.A., Deterting L.J. and Parker C.E.; *Mass Spec. Reviews* 13 (1994) 431
93. Cai J. and Henion J.; *J. Chrom. A.* 703 (1995) 667
94. Pusecker K., Schewitz J., Gfrorer P., Tseng L-H., Albert K. and Bayer E.; *Anal. Chem.* 70 (1998) 3280
95. Jayawickrama D.A. and Sweedler J.V.; *J. Chrom. A.* 1000 (2003) 819
96. Rentoney S.L., Zare R.N. and Quint J.F.; *Anal. Chem.* 61 (1989) 1642
97. Tracht S., Toma V. and Sweedler J.V.; *Anal Chem.* 66 (1994) 2382
98. Smith N.W. and Evans M.B.; *J. Parm. and Biomed. Anal.* 12 (1994) 579
99. Chen H. and Horvath Cs.; *Anal. Meth. and Instr.* 2 (1995) 122
100. Bruin G.J.M., Stegeman G., Van Asten A.C., Xu X., Kraak J.C. and Poppe H.; *J. Chrom.* 559 (1991) 163
101. Moring S.E., Reel R.T. and van Soest R.E.J.; *Anal. Chem.* 65 (1993) 3454
102. Tsuda T., Sweedler JV. and Zare RN.; *Anal. Chem.* 62 (1990) 2149
103. Heiger D.N., Kaltenbach P., and Sievert H.J.P.; *Electrophoresis* 15 (1994) 1234
104. Taylor J.A. and Yeung E.S.; *J. Chrom.* 550 (1991) 831
105. Wang T., Aiken J.H., Huie C.W. and Hartwick R.A.; *Anal. Chem.* 63 (1991) 1372
106. Ross. G.; *Appl. of HP CE System*, Hewlett Packard (1995) pp 54
107. Kakehi K., Susami A., Taga A., Suzuki S. and Honda S.; *J. Chrom.* 680 (1994) 209
108. Landers J.P. *Handbook of Capillary Electrophoresis.* CRC Press, Boca Raton 1997
109. Hows M.E.P., Alfazema L.N. and Perrett D.; *LC-GC International*, 10 (1997) 656
110. *Burdick & Jackson solvents catalogue*, Honeywell
111. Wang T. and Hartwick R.; *J. Chrom.* 607 (1992) 119

112. Xu X., Kok W.T., Kraak J.C. and Poppe H.; *J. Chrom. B.* 661 (1994) 34

113. Xu X., Kok W.T. and Poppe H.; *J. Chrom.* A. 716 (1995) 231

114. Xu X., Kok W.T. and Poppe H.; *J. Chrom.* A. 786 (1997) 333

CHAPTER 2

Capillary Electrochromatography

2 Capillary Electrochromatography

2.1 Introduction

Capillary electrochromatography (CEC) is a hybrid technique of electrophoresis (CE) and liquid chromatography (LC). It provides the advantages of both techniques: the high efficiency, resolution and minimal solvent consumption of CE and the universality, versatility and selectivity of LC. The separation of the analytes is based on chromatographic partitioning between the stationary phase (packing material) and the mobile phase (running buffer) and by their electrophoretic mobility. Hence, it can separate neutral species, which is not possible by CZE.

The potential of CEC is clearly visible from a comparison to other chromatographic techniques [1,2,3,4].

	Typical Column Length [cm] Typical Particle size [μm]	Number of Theoretical Plates	Peak capacity
HP TLC	50 (6.0μm)	22 200	<90
SFC	25 (5.0μm)	100-200 000	190-260
HPLC	25 (5.0μm)	25 000	90
GC	5 000	200 000	260
CEC	25 (3.0μm)	60 000	140
	50 (5.0μm)	115 000	190
	50 (3.0μm)	120-170 000	>200
	50 (1.5μm)	200-250 000	>260

Table 1. Comparison of available efficiencies and peak capacities in different chromatographic techniques (based on equation 1.22).

2.2 History of CEC

The development of CEC can be traced back to the time of birth of the CE technique itself, when Strain [5] applied an electric field across, and a small pressure gradient to, an absorption column in 1939. Then there was a very long gap in the development of this technique, until Pretorius *et al.* [6] demonstrated electrochromatography in 1974 on a 1mm ID capillary packed with 75-125μm bare silica. No further developments were reported for seven years. Then the potential of this technique was demonstrated by Jorgenson and Lukacs [7] using a non-aqueous system on 10μm Partisil ODS-2 in glass capillaries with 170μm ID. In 1982, Tsuda *et al.* [8] reported the first open tubular electro-chromatography application, using capillaries internally coated with the stationary phase. The effect of different stationary phase particle sizes (10-, 50-, and 100μm) was studied by Stevens and Cortes [9] in the following year. They reported that the efficiency of electrochromatography is smaller than expected below 50 μm particle diameter, due to double layer overlapping disrupting the EOF. Later their results were shown to be incorrect by Knox and Grant's theoretical study [10], and this was confirmed practically in 1991 [11]. They found that the minimum particle size would be 0.4μm with 1-10mM electrolyte before double layer overlap occurs. This was the time of the resurrection of the CEC technique and when its worldwide application really started. It was also Knox in 1994, who suggested [12] – although the name was first used by Tsuda [13] – that capillary electrochromatography, CEC, should be the accepted name of this technique, as prior to this it was known under several names [14]. The first publication showing the potential of CEC in pharmaceutical analysis was reported by Smith and Evans [15] in 1994. Since then, several groups have made contributions to the development of CEC as will be reviewed in this chapter. This is a process, which is ongoing.

2.3 Theory

2.3.1 Electroosmotic flow

The generation of electroosmotic flow (EOF) in CEC is based on the same principles described for electrophoresis in Chapter 1. However, the presence of the packing particles crucially influences the overall EOF generation process. As can be seen in Figure 2.1, the surface of the packing material also contributes to the EOF generation.

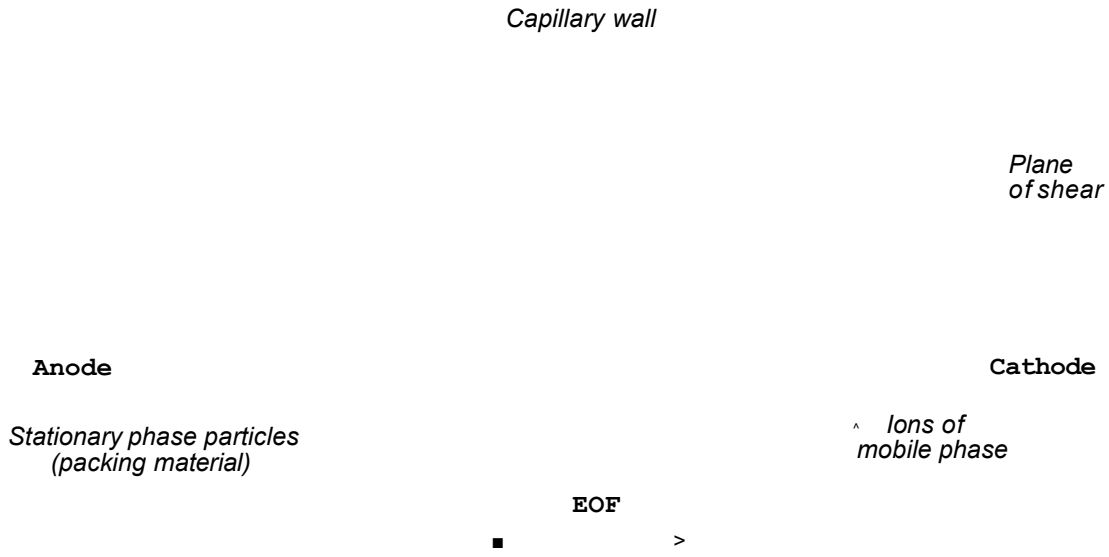

Figure 2.1 The generation of EOF in CEC

Although, here the number of free silanol groups is less than on the capillary wall, and there is also a covering of substituted alkyl chains *(e.g.* Cis) the overall surface of the packing material is far greater than the surface of the inner capillary wall. Consequently, most publications suggest that the packing material is responsible for the generation of EOF with little or no contribution from the capillary wall [16, 17, 18]. However, there is no credible principal theory and others have stated that a substantial contribution to the EOF from the capillary wall is also observed [1].

Thus, in CEC the EOF is not only highly dependent on pH, buffer composition and concentration [19 and Chapter 1.2] but on the type of the stationary phase as well. This is reflected in several publications on the study of different stationary phases for CEC separations [20, 21].

The generation of EOF is also influenced by the physical characteristics of the stationary phase such as particle diameter and pore size [10,22]. This is related to the thickness of the electrical double layer. Overlapping of the double layer reduces the EOF and degrades the flow profile from flat to parabolic. As long as the inter-particle channels are wider than the double layer, the velocity of the EOF is independent of particle size (see the Smoluchowski equation in Chapter 1.3). The average inter-particle channel width has been estimated to be a quarter to a fifth of the particle diameter for spherical particles [23], and the double layer thickness was calculated [10] to be 10nm in a 1mM, and 1nm in a 100mM aqueous electrolyte. From theoretical calculations Knox suggested [10] that the channel size between the packed particles needs to be greater than twenty times the thickness of the double layer that is formed around each particle to avoid destruction of the EOF. These calculations mean that with typical 1-10mM CEC mobile phases, particles with a size of 0.4μm could be used. Theoretical calculations showed that this particle size would yield the possibility of $N \geq 870000$ plates/metre, which is well beyond the obtainable efficiencies with HPLC. Particle sizes of 1.5μm or below are not feasible in HPLC, as these would generate extreme column backpressure. For example, in HPLC an 18cm column, packed with 1.5μm particles and operated at a flow velocity of 2mm/s would generate a backpressure of 1200bar [2]. This is beyond the capability of commercial HPLC instruments. Such conditions are however easily achievable with CEC. Columns packed with 1.5 and 1.8μm stationary phases were found to enable far better separations (both in efficiency and speed) [24,25] than could be achieved by HPLC. This particle size is in fact much smaller than that typically used *i.e.* 3μm for CEC applications. Thus further improvement in applications can be expected, although column

fabrication with particles of this size was found to be extremely difficult, with the available methods, due to the extreme back pressures generated (see also 2.4, packing). However, not many results have been published on sub-micron CEC [26, 119] since Lüdtke *et al.* [27] reported a separation of five n-alkylbenzenes on 0.5μm n-octyl bonded silica in a 8.5cm packed (100mm I.D.) column in less than a minute. However, their system was not optimised and the efficiencies obtained (288,800) were less than expected.

The double layer thickness of 10nm is greater than the typical 6-8nm pore size in conventional 3μm to 5μm HPLC stationary phase materials, thus an EOF generated through the particles, called the perfusive EOF, is not present. Remcho *et al.* [22,28] studied this intra-particle EOF and they found that macroporous particles (above 200 nm) can generate the perfusive EOF and better efficiency. Materials with pore size of 30nm gave improvements with buffers with high ionic strength [29], while Wei *et al.* [30] supported the results of Remcho *et al.* showing that an increase in pore size gives better chromatographic performances using macro-pores. The effects of pore sizes were also extensively studied by Stol *et al.* [31,32]. They found that high efficiencies can be obtained with a perfusive flow, due to the reduced and/or eliminated plate height contributions (see Chapter 1.5.3) from stationary phase mass-transfer resistance (C_s term) and flow inhomogeneity (A term) over the column. Better flow homogeneity was more easily obtained with pore sizes above 400nm [31]. Stol *et al.* [32] stated that the pore size distribution of the particles is also important as different combinations of particles with the same average pore size could give highly different perfusive EOF. The described porosity effects in electrically driven chromatography are in contrast with pressure driven chromatography, where porous particles give lower efficiencies.

As CEC capillaries are generally not fully packed, the packed and open sections both influence the observed EOF velocity due to their different conductivities. This leads to different voltage gradients and consequently

different electric fields in each segment, since the current is conserved across the whole capillary length. The result is a sudden change in their values at the interface [33]. However, this was observed at very low or high pH, while at neutral pH very little difference was found [34]. Horváth *et al.* [35,36] found from modelling, that by varying the length of the packed or open segments, the selectivity and speed can be improved for separations that were dependent on chromatographic and electrophoretic contributions (*i.e.* samples containing both neutral and charged analytes). Thus, the length of the packed part can be an important variable in optimising the chromatographic and electrophoretic effects of the CEC capillary and therefore the overall chromatographic performance. However, there is still no adequate theory that explains the contribution of the different segments to EOF and hence overall chromatographic performance.

The interface between the packed and open segments is a source of discontinuities in the electric field strength and flow velocity as well as bubble formation. This is also the case for the frits, which are also sources of these discontinuities due to the changes in the packing material or in the properties of the material (see sintering at Chapter 2.5.1).

2.3.2. Separation

The separation in CEC is based on the combined selective interactions of the analytes with the stationary phase and the differences in the electrophoretic mobility of the analytes. Therefore, calculation of separation parameter is more complex than in HPLC or in GC, which explains the fact that there are several formulas used in CEC for calculating retention factor.

In HPLC, the partitioning is represented by the retention (formerly capacity) factor (k'), which can be defined as the ratio of the amount of the analyte in the stationary and mobile phase or consequently as the ratio of the time that the analyte spent in the stationary ($t_{st.ph}$) and mobile phases ($t_{m.ph}$)

$$k' = \frac{t_{st.ph}}{t_{m.ph}} = \frac{t_r - t_0}{t_0} \quad (2.1)$$

t_r = total time of the analyte spent in the chromatographic system, the retention or elution time; t_0 = the column dead time, which is the time taken for a fully unretained analyte to move through the system.

In an electrophoretic system, equation 2.1 can be expressed as the k_{EO} electrophoretic velocity factor [18]

$$k'_{EO} = \frac{t_{EO} - t_m}{t_m} \quad (2.2)$$

t_{EO} = the retention time of an analyte moved only by EOF (*e.g.* a neutral marker); t_m = the migration time.

As CEC is the simultaneous combination of these two separation procedures, the retention factor for CEC can be defined [37] as

$$k_{CEC} = k' + k'k_{EO} + k_{EO} \quad (2.3)$$

As can be seen, for neutral species (when k_{EO}=0) the CEC separation operates as in HPLC, while for a fully unretained and charged species (k'=0) the separation process is like in CZE. However, when the analyte is charged the separation process is more complicated and the elution depends on the direction and rate of electrophoretic migration of the analyte with respect to the EOF (Chapter 1.3).

A further definition, the actual chromatographic factor (k_C), is also used in the literature for characterizing the chromatographic process if charged solutes are present [118]:

$$k_C = \frac{\left(1 + \frac{\mu_{EP}}{\mu_{EO}}\right) t_m - t_0}{t_0} \quad (2.4)$$

μ_{ep} and μ_{EO} = the electroosmotic and electrophoretic mobility of the ionised solute.

2.4 Instrumentation

A schematic of a general capillary electrophoresis system is shown in Figure 1.9 (Chapter 1.8). CEC does not requires any specific or major instrumentation and it can be run on CE instruments [38]. The overall typical instrumentation is very simple and similar for all CE instruments. However, to gain the full potential of electrochromatography, CEC would need especially dedicated instruments with the possibility of p-CEC and μ-LC set up, rather than modified CE instruments [39]. There are several practical considerations to be considered. A major problem arises from the CEC column fabrication itself. For fused silica capillaries, no end fittings with retaining sieves are available, that would fit together with the electrodes into the buffer vials of most commercial CE instruments. The generally used sintering technique provides the required frit inside the packed column, but it also makes the capillary fragile at the frit. The protection of this section (usually by inserting it into PEEK tube), as well as the design of cooling systems, can have the effect of limiting the insertion of the capillary into the system and thus the minimum and/or maximum packing length of instrument compatible CEC columns.

A second problem arises from the stability of the polyimide coatings on the fused silica capillaries. When the polyimide is removed (*e.g.* at the detection window and frits) the silica column is brittle and extremely fragile. Also, unfortunately, the chemical stability of the polyimide is not very good in acetonitrile which is the most common organic modifier in the mobile phase (section 2.5.1.5). Long-term contact with this and other organic solvents [40] soften the coating, which eventually will swell. This leads to reduced chromatographic performances and limited capillary lifetime due to breakages and clogging. Based on GC experiences, Bauelm and Welsch [41] reported that heat treatment of the capillary at 300°C for 200 hrs improved the resistance of polyimide coated capillaries against swelling caused by acetonitrile and extended the lifetime of the capillary.

The third major problem arises from bubble formation. Although, with appropriate column and mobile phase preparations bubble formation can be avoided [42] it is a serious problem in CEC. Unlike in CE, this cannot be solved easily in the instruments with a simple flush of the capillary after bubble formation occurs. As in HPLC columns, the backpressure of the packed capillaries are very high and the available pressurisation (usually 2 bar) for earlier common CE instruments is too low to allow easy and rapid flush out of a CEC system. However, pressurisation of the column has become general in recent years to prevent bubble formation. The best approach in CEC is that of applying the same small pressure to both the inlet and outlet vials [15,17,38,43]. Thus, the plug flow profile of the EOF is not disturbed. Another approach is to apply high pressure to the inlet vial to generate additional flow and thus was used in the early years of CEC development [13,44]. This mixed mode hydrodynamic and EOF driven separation is called pressure assisted or pseudo-electrochromatography (p-CEC). Despite the fact that p-CEC provides theoretically less efficiency than CEC, due to band broadening from the laminar flow profile, it has several advantages; such as increased stability, by preventing bubble formation, and faster separations, especially at low pH-s where EOF is restricted [38]. Different groups reported universal or modified commercial pressurised CEC systems which can be used in CEC, p-CEC or μ-HPLC mode without dismantling the instrument [45,46,47] but such systems are still not commercially available.

A further desirability in CEC instruments is to have the facility of gradient elution, which can considerably improve the separations, as in HPLC. The simplest methods, however require no additional instrumentation, as they use a series of inlet vials containing the required compositions of the mobile phase for the separation. The main disadvantage of this method is that the separation is interrupted by changing these vials, although Ding *et al.* [48] reported reproducible separation, without extra band broadening, of isomeric polycyclic aromatic hydrocarbon-deoxyribonucleoside adducts.

A simple continuous gradient elution method was developed by Zhang *et al.* [46] and Wu *et al.* [49] by mixing solvents in the inlet vial with continuous addition of solvent by a HPLC pump and syringe. A further development on p-CEC was published by Behnke and Bayer [50], who were the first to connect the inlet vial to a gradient LC system and provide the solvent gradient without additional mixing. The effectiveness of their approach was later demonstrated by several groups [45,47,51,52] who employed gradient-CEC-MS to study drug mixtures, using this method..

Lister *et al.* [53] studied a gradient system using a flow injection analysis interface. It was found simple and reliable but it was not fully evaluated and peak broadening was observed. This was connected to the capillary positioning and to the injection system.

Carter-Finch *et al.* [54] presented a similar HPLC pump generated gradient elution system using a by-pass capillary between the Tee and micro cross unions at the ends of the packed capillary. This was applied to the separation of an insecticide mixture of 11 pirimicarb and related compounds although the chromatogram from isocratic elution was not presented to enable critical comparison.

A way of carrying out gradient-CEC without the need for an HPLC pump was suggested by Yan *et al.* [55]. They used two separate power supplies and independent inlet vials to generate a gradient solvent mixing in a T-piece by the EOF itself. The advantage of this, so called electroosmotic pumping system, was the instant supply of an gradient to the separation capillary, which is not the case in some pressure pumping CEC system, where (*e.g.* [51]) there are a several minutes time gap for the gradient to reach the separation capillary. The disadvantages of the electroosmotic pumping systems, is that the velocity of the running buffer is continuously changing with the solvent composition (see Chapter 1.3) and the actual eluent

composition, connected to the applied voltage, cannot be known without prior calibration [38].

Recently Kahle *et al.* [56] demonstrated a microprocessor controlled gradient elution system with very good reproducibility of retention times (RSD<0.1%). This automated system contained a liquid distribution system with the connection capillary to the CEC column via a grounded splitter. The solvent gradient was developed by turbulent mixing of weak and strong mobile phase at the needle of the injection syringe in the liquid distribution block.

2.5 CEC Columns

Three different kind of CEC column exists: micro-particle packed, open-tubular and monolithic (also known as sol-gel or continuous bed) capillaries [20,21,57]. Each column has its advantage and disadvantage in their fabrication, reliability and chromatographic performances as will be discussed in this section.

2.5.1 Packed columns

Packed columns were the obvious choice in CEC as it is the simplest way to utilise the wide range of available HPLC stationary phases. Due to their general HPLC usage, most CEC applications started with 5μm reverse phase C_{18} particles, but as smaller particles became more available the particle size of the packing materials reduced, and also stationary phases specially designed for CEC (*e.g.* CEC Hypersil C_{18}) had appeared. Packed columns require retaining frits to restrain the stationary phase inside the column. Not only against the EOF but against the migration of the stationary phase particles towards the electrode, as these particles contain charged surfaces under electrophoretic condition.

2.5.1.1 Frits and Restrictors

Frits play an important role in column fabrication, stability and performance. Their main role is to retain the micro-sized packing material inside the column. Due to general packing methods this means they should be mechanically stable, holding pressures up to 800bar, but they should also be porous enough to the allow a continuous mobile phase flow during analysis.

Currently there are four frit fabrication procedures reported [57,58]:

Despite its disadvantages [57,59], the most common procedure is sintering the actual packing material inside the column at high temperature (>550 °C) using a micro-torch or electrically heated filament [60]. The main advantages of this procedure are that it is simple, fast and can be fabricated at any point in the capillary. The sintering must take place while the packed capillary is flushed with water and thus kept under high pressure otherwise the supplied heat would form air bubbles during the sintering which would remove the particles from position. In such a situation no compact or in fact any frit at all would be generated. Further practical considerations will be described under Column Packing (Section 2.5.1.2).

The main disadvantage of this procedure is that different stationary phase particles have different optimum sintering conditions, such as sintering time, due to their physical and chemical properties (*i.e.* Sodium or potassium content, size and size distribution *etc.*) as well as column ID. [61].

Heating the stationary phase can lead to the destruction of the alkylated silica [62] and/or the uniformity of the packed bed around the frit. Each of these degrades the chromatographic performance of the column. The altered structure of the packing material (*i.e.* the lower porosity) in the frits also leads to velocity changes in the EOF (which are connected to bubble formation [63]), and absorption of polar analytes [64]. It was also shown

using unpacked capillaries containing two frits, that the frits themselves reduce the EOF by 35 % [65]. Whilst over heating the silica particles by either sintering time or temperature, gives amorphous and non-permeable frits.

The sintering process generally makes the capillary more fragile as it removes the protecting polyimide coating from the fused silica capillary. Although this can be overcome easily by fitting the capillary into other PTFE or PEEK tubing, using this simple way is often limited by the instrumental design of the CE instrument or the CE-MS interface, thus restricting the applicable packed length.

Achieving reproducibility is generally a problematic part of good frit fabrication. However, since the work of Bougthflower *et al.* [60] and Smith *et al.* [15,66] on the production of purpose build electrical burners, more reliable commercial instruments are available, but it is still difficult to achieve good reproducibility in consecutive column fabrication.

The source of bubble formation, the main practical problem in CEC, was originally thought to be connected to the Joule heating [11] (as in CZE, although the common mobile phases used in CEC have much lower ionic strength and thus generate lower current [58]) but is now commonly thought to be related to the sintered end-frits. First Rebsch and Pyrell [62] demonstrated that bubble formation started at the frit. Measuring chromatographic performance, they concluded that band broadening is caused by the frits, due to the flow inhomogeneities within them. Carney *et al.* [63] studied the effect of Joule heating, and variation of the EOF velocity at the packed and unpacked section on bubble formation. They found that the bubble formation was a function of frit length and applied voltage. They also found that recoating the frit with C_{18} material reduced bubble formation, even with long frits and high voltages.

Further frit formation techniques include:

- Polymerisation with potassium silicate solution in formamide [67]. Usually a small amount of this solution drawn is into the capillary, where it completely hardens after 1h at 120°C [68].
- Wetting silica gel with aqueous sodium silicate or potassium silicate and heating it above 250°C to form a wall supported porous silica gel.

These techniques are usually carried out by tapping the capillary end into the solution/paste, thus they are not suitable for the formation of frits in the middle of the capillary only at the capillary end.

A comparison study of the different frits was carried out by Behnke *et al.* [64]. They found that sintered frits provided the best baseline and current stability under CEC conditions, and gave good mechanical stability. However, these were drastically reduced for wider columns (150μm). Frits made by polymerisation with formamide gave the best mechanical stability but unstable baseline and current were observed. Frits made with wetted silicate gave little improvement in baseline stability but less than a quarter of the mechanical stability.

Frits are the most common way to retain the packing particles inside the columns but, as shown, they have several disadvantages. This makes them the most problematic part of column fabrication. This has led to several alternative approaches to retaining the stationary phase in CEC columns.

Tapers are a simple way to retain packing particles inside the capillary. They can be fabricated by drawing the capillary (externally tapered) or by melting the end of the capillary in a flame and than cautiously cutting it (internally tapered). Although, they have been used for CEC-MS by Lord *et al.* [69] and Horvath *et al.* [70], as is discussed in Chapter 3.5, tapers are not as common as frits due to their extreme fragility. It was also found that they cause extra

band broadening due to the dramatic changes in inner diameter influencing the flow [71].

2.5.1.2 Packing methods

Column packing quality is still the major draw back of the CEC technique. This has held up the widespread application and acceptance of this technique. The packing quality is influenced by several factors [72] and the whole process is highly skill dependent and based more on practical experience than on a clear and reliable scientific process [73].

Several packing procedures have been published such as liquid slurry [27,57,60,72,73,74,75], electrokinetic [76,77], centrifugal [78], gravitational [79] and supercritical fluid [80,81] packing. Although extra instrumentation and special fittings are required, the most common packing procedure is the slurry packing.

The general slurry packing procedure is a long process and includes several steps, as follows:

1. Pre-treatment of the capillary wall – *e.g.* rinsing with sodium hydroxide solution as in CZE - before packing is used by some groups (*e.g.* [73,75]), but is not a general step.
2. Formation of a temporary end frit, usually by tapping into wetted silica and sintering in a gas flame.
3. Producing a slurry solution (generally 10% [w/v]) of the required stationary phase in a suitable organic solvent.
4. Capillary packing with the slurry solution by addition of high pressure (200-1000bar) by HPLC or commercial air intensifier pumps. The slurry reservoir is usually sonicated in an ultrasonic bath to prevent the packing material from settling down before it is introduced into the capillary.

5. Flushing the packed capillary with water to remove the organic slurry solvent.
6. Producing the inlet and outlet frits at the desired length, generally by sintering the stationary phase under high pressure. Once the permanent outlet frit is produced, the temporary frit is cut out.
7. Washing out the excess packing material by pumping the mobile phase through the reversed capillary.
8. Formation of the detection window for UV detection.

As mentioned earlier, several factors influence the packing quality. The quality of the temporary frit plays an important role in the packing procedure. It should be strong enough to hold against the applied high pressure, but if it is not permeable enough, packing will not be possible due to the high backpressure. Thus, metal frits with finger-tight micro unions are also used [*e.g.* 81,82] to eliminate the need for the temporary frit.

Further problems can arise from the packing solvents used to make the slurry. Water is generally disregarded, as the packing materials are very hydrophobic and would aggregate. Since the backpressure is directly proportional to the solvent viscosity, the application of low viscosity solvents is beneficial. This also led to the development of packing using supercritical CO_2 [80], but this is not discussed here.

Organic solvents such as acetonitrile and acetone are the most common packing solvents described in the literature (Section 2.5.1.5). The disadvantage of the use of organic solvents is the need for the extra washing step in the packing procedure, as these solvents would degrade and carbonise under the high temperature used in frit making. Insufficient washing can also result in carbonisation of the organic solvent during sintering. This can block the capillary flow.

To prevent the stationary phase particles from settling down, the slurry reservoir, which is usually an empty HPLC guard column, and the capillary are sonicated. Sonication of the slurry for 5-15min before packing was found to be useful in breaking up aggregation and removing air from the pores. This helps to produce a more dense packing since the higher particle density, means that they move with higher kinetic energy in the column during packing [72].

The packing pressure is determined by the available pump. Most reported packing pressures are between 200 and 1000bar. Air assisted pressure systems provide higher pressure than HPLC pumps with the advantage of applying non-pulsing pressure. However, there are no studies reported on column performances based on the applied pressures. This indicates negligible effects, although extreme pressures can cause particle degradation in highly porous particles. On the other hand, depressurisation was found to be important. The applied pressure must be allowed to degrade very slowly (which can be more than 1hr) by the system during packing, otherwise sudden pressure changes disturb the packing bed. This leads to an inhomogeneous packed bed, which can lead to void formation during separation as the particles reorganise themselves. Any void in the packed capillary reduces column performance due to the parabolic flow profile.

2.5.1.3 Conditioning

A packed capillary should also be conditioned before use. Unlike in CZE, a sodium hydroxide flush cannot be applied as it can damage the stationary phase, but it can be used prior to the packing process [73]. In general, CEC conditioning is performed in a CE instrument by gradually applying voltage (from 2kV to 30kV) across the capillary until a stable current is observed. This could be a very long process and thus generally made overnight.

2.5.1.4 CEC Stationary Phases

As CEC is a hybrid technique of electrophoresis and liquid chromatography, and due to the widespread availability of HPLC stationary phases, their application in CEC predominates. Up to date, about 70% of CEC publications are based on the use of C_{18} bonded silica based materials [20]. As described in Section 2.3.1 the generated EOF in CEC is independent of the particle size until a theoretical limit is reached. This allows the application of smaller particles with greater efficiencies. At present, most publications are [21] based on 3μm particles. Studies on the application of smaller particles are minimal [21,22] compared to 3-5μm particles but further studies towards sub-micron particles are expected to grow due to the increase in efficiency that can be achieved. To date, the smallest investigated particle size for CEC is 0.2μm [26,119]. As described in Section 2.3.1 the generated EOF is influenced by the chemical properties of the stationary phase. Most studies have investigated the effects of different stationary phases on EOF and column performances using various test mixtures.

Most CEC work has been carried out with packed columns, however the difficulties arising from the frits and in the preparation of a reliable CEC columns has led to the development of other CEC columns such as monolithic (also knows as continuous bed) [83, 84] and open-tubular [85].

2.5.1.5 Mobile phases

One of the most significant differences between CEC and HPLC is the composition of the mobile phase, as it not only determines the retention of the solutes but also the observed electroosmotic mobility (see Chapter 1). It must contain enough ions to maintain conductivity through the column. The electrical connection between electrodes in CEC is supplied by the addition of salt or buffer ions to the mobile phase. However, the concentrations of these buffer salts is usually low (a few millimoles, generally below 10mM for

inorganic buffers) due to double layer overlap, Joule heating and solubility problems in the high volume of organic solvent. For the same reasons, biological buffers (*i.e.* TRIS, MES, HEPES) are more common than their inorganic counterparts as they produce much lower currents due to their lower ionic strength.

The CEC mobile phase is generally used between neutral and alkaline pH to ensure ionisation of silanol groups on the surface of the packing particles and the capillary wall. EOF drops to almost one third between pH=10 and pH=2 on ODS [19]. However, the application of mixed mode stationary phases has expanded the suitable pH range for CEC [86].

There are also differences between CEC and CZE mobile phases. In CEC, they generally contain organic solvents at higher percentage as the separation of solutes is based on their retention on the stationary phase. The most suitable organic modifier has been found to be acetonitrile [87] due to its higher ε/η ratio (Chapter 1.3 and Table 1.2) compared to other solvents or water. The generated EOF with various solvent mixtures was studied by several groups, and it was found, that mixtures showed a minimum around an organic solvent volume of 50-70% [1,88] or less [89]. However, the effect of ACN percentage is contradictory. Several groups reported both increasing [17,24,33,53,87] and decreasing [88,90,91] EOF with increasing ACN content. The reasons for these observations are still not clear, but experimental data suggest that the zeta-potential cannot be simply predicted from solvent properties. Other explanations are based on the flow differences in the packed and open section of the capillary [33,35,36,87], and on the microscopic structure of the several compositions of solvent mixtures [88].

2.5.2 Monolithic columns

Monolithic columns contain a single continuous stationary phase that is prepared inside the capillary. This eliminates all problems associated with the packing procedure and with frits, since no frit is required as the stationary

phase is bonded to the capillary wall. Monolithic columns used in CEC can be divided into two groups: porous silica or polymer based and fixed particle monoliths.

Silica based monoliths are the oldest continuous bed columns, although their application in CEC started only after 1996. They are prepared by a sol-gel method [92], which is a multi step, long process. This process involves hydrolytic polycondensation with alkyl siloxane (*e.g.* tetramethyl orthosilicate, tetraethoxy silane or methyltriethoxysilane [93]) in the presence of organic copolymer (*e.g.* polyethylene oxide or polyethylene glycol) in water with acid or base catalyst. Acids were reported to give linear or branched chains in the sol, while bases provide uniform particles [94]. The hydrogel was than heat treated, ammonium hydroxide washed and derivatised [92].
Due to the difficult preparation process, their lower stability towards pH extremes, and the difficulty in controlling the pore size and adjusting the column selectivity, silica sol-gels are less favourable than the organic polymer based monoliths [84]. Up to date, the polymer-based monoliths have been based on three different types of polymers. These columns in CEC have evolved from soft hydrophilic acrylamides to more efficient rigid methacrylates and then to more rigid polystyrenes.

The first application of polymer-based monoliths (*i.e.* polyacrylamide gel) was made by Hjertén *et al.* [95] and Fujimoto [96] in 1995. The soft continuous bed monoliths (including silica based) had a problem of the swelling and compressing of the gel on wetting and heat deformation, resulting in size changing in the gel which reduces chromatographic performance. This led to the search for more rigid columns.

Peters *et al.* [97,98,99] performed intensive studies on cross-linked poly-methacrylate. They demonstrated the formation of a rigid monolith without significant swelling in a simple one step reaction. This allowed the properties

of the columns, such as pore size and chromatographic performance to be easily controlled.

The more rigid polystyrene–divinylbenzene (PS-DVB) structures were proposed by Wand *et al.* [100] to over come the problem of swelling but these columns were used in CEC only later [84, 101]. Gusev *et al.* [84] presented successful peptide separations on N,N-dimethyloctylamine derivatised PS-DVB monoliths. PS-DVB based microparticles were also used recently in CEC as stationary phases due to their stability and favorable EOF in a strong acid buffer [102,103].

Particle fixed monoliths are made by thermal immobilisation (*e.g.* sintering) of silica particles. Thus, these columns also require a packing process, which explains why fewer applications compared to polymer-based monoliths have been reported. Particles can be fixed by one of three different methods:

A sintering process which is similar to frit making. Here the packed capillaries are washed with water and then heated to immobilize the particles [104]. Earlier methods including a $NaHCO_3$ and acetone wash [105] were found to be damaging the stationary phase which required deactivation and re-functionalising. In the "entrapping" process, the packed capillaries are flushed with a water-glass or silicate sol-gel solution to "glue" particles together during the following heat treatment [106,107]. In Particle loading [108] the capillaries are filled with a sol-gel matrix solution and particle suspension, which will embed the particles after drying. This type of column is usually very permeable.

Low sample loadability and concentration detectability is a common problem with microcapillaries due to their small diameter. Thus, the application of wider columns would be advantageous. However, Joule heating in electrically driven techniques is a main drawback above 200μm ID. The widest capillary used in electrochromatography so far was used with a monolithic column. Qu

et al. [109] recently published a successful semi-preparative separation with a 7cm monolithic column with 2.7mm inner diameter. Although, the applied voltage had to be only 1kV to prevent Joule heating, they presented a fast (less than 4min) separation for a simple benzaldehyde mixture, with an efficiency of 52000.

In summary, as the monolithic columns offers the same separation ability [110] as packed columns, with the advantage of no frits required, pH stability and surface versatility of polymer based columns there is great increase in applications of monolithic CEC columns in recent years. It is expected that the applications of packed columns will decrease [21] compared to monolithic columns in the future.

2.5.3 Open Tubular columns

The open tubular (OT) technique is well known and have been successfully applied in gas chromatography since the 60s providing the technique with the highest overall separation efficiencies among chromatographic techniques. However, this comes from the possibility of using extremely long columns due to the minimal backpressure. The application of OTs was reported as early as 1982 by Tsuda [8] and has been intensively studied by the group of Kraak and Poppe [111, 112, 113, 114].

OT columns are internally coated with the stationary phase, thus forming a very thin film layer. The main disadvantage of this technique is the much smaller stationary phase surface area than is obtained with packing materials. This is the reason for the low sample capacity and sample mass loadability of open tubulars.

There are three main approaches to over come this problem [115]. Increasing the inner surface area by etching [85] the capillary before forming the stationary phase layer or placing down a porous silica [116] or polymer

[117] layer on the surface followed by functionalisation. Other approaches include using cross-linked polymers [114] instead of a monolayer coating. However, these organic polymer coatings of the inner fused-silica capillary surface can slow down or stop the EOF by shielding the silanol groups of the inner capillary surface.

Unlike in packed columns, the analyte has to migrate much longer distances (in a molecular sense) inside the capillary to the separating stationary layer. Thus, OT columns are generally narrower (10-25μm) than packed or monolithic CEC columns to increase their lower solute diffusion. This enables higher voltage usage (as heat dissipation is faster), which results in a higher EOF. On the other hand, lower detection sensitivity is obtained with narrower capillaries with UV detection.

Despite its advantages, such as fritlessness and high efficiency, OT columns are the least important type of columns in CEC.

2.6 Conclusion

Interest in CEC separation technique has expanded in recent years as it combines the high efficiency of capillary electrophoresis with the versatility and selectivity of HPLC. It provides a high separation capability with economical and environmental advantages, as solvent consumption is negligible compared to HPLC.

However, despite the rapid increase in successful and highly efficient applications and the development of stationary phases specially designed for CEC, this technique is still in infancy. Although, intensive theoretical work has been carried out, there is still no general agreement on the capillary wall contribution to EOF generation and no consistent theory on the effect of the organic volume of the mobile phase on it. The same applies to separation theory. When the sample contains only neutral or charged components CEC

can be considered as an essentially chromatographic or an essentially electrophoretic process and the data can be processed according to the adequate theories of HPLC and CZE. However, when both types of solutes are present and both mechanisms take place, there is no consistent theory about the full CEC process.

It can be said that the situation in instrumentation and column fabrication is even worse. Several practical problems connected to the use of reproducible exact parameters for the packing process, for manufacture of the frits, and for the column fabrication still need to be addressed. It is still a question of skills and practices. Packing is still rather an art than a simple, fully understood process, which provides reliable, reproducible columns [73]. Most CEC applications are based on reverse phased packed columns but these problems have turned the attention towards fritless, macroporous monolithic columns.

This situation has many similarities to the story of supercritical fluid chromatography (both technique have/had great potential and almost similar problems). CEC requires further and intensive studies on its problems, otherwise, there is a possibility that it will suffer the same syndrome as SFC, which had similar rapidly growing interest in the 80s but since then this interest had dropped [4].

References

1 Bartle K.D. and Myers P.; *J. Chrom. A.* 916 (2001) 3

2 Dittmann M.M., Wienand K., Bek F. and Rozing G.P.; *LC-GC* Vol. 13 No. 10 (1995) 800

3 Poole C.F.; *J. Chrom.* A 1000 (2003) 963

4 Smith R.M.; *J. Chrom.* A 856 (1999) 83

5 Strain H.; *J. Am. Chem. Soc.* 61 (1939) 1292

6 Pretorius V, Hopkins B.J. and Schieke J.D.; *J. Chrom.* 99 (1974) 23

7 Jorgenson J.W. and Lukacs K.D.; *Anal. Chem. 53 (1981) 1298.*

8 Tsuda T., Nomura K. and Nakagawa G.; *J. Chrom.* 284 (1982) 241

9 Stevens T.S. and Cortes H.J.; *Anal. Chem.* 55 (1983) 1365

10 Knox J.H. and Grant I.H.; *Chromatographia* 24 (1987) 135

11 Knox J.H. and Grant I.H.; *Chromatographia* 32 (1991) 317

12 Knox J.H.; *J. Chrom.* A. 680 (1994) 3

13 Tsuda T.; *Anal. Chem.* 59 (1987) 521

14 Tsuda T.; *LC-GC Intl.* Vol 5 No.9 (1992) 26

15 Smith N.W. and Evans M.B.; *Chromatographia.* 38 (1994) 649

16 Cikalo M.G., Bartle K.D., Robson M.M., Myers P. and Euerby M.R.; *Analyst* 123 (1998) 87R

17 Dittmann M.M. and Rozing G.P.; *J. Micro Sep.* 9 (1997) 399.

18 Rathore A.S. and Horváth Cs.; *Anal. Chem.* 70 (1998) 3271

19 Cikalo M.G., Bartle K.D. and Myers P.; *J. Chrom. A* 836 (1999) 35

20 Pursch M. and Sandler L.C.; *J. Chrom.* A 887 (2000) 313

21 Jiskra J., Claessens H.A and Cramers C.A.; *J. Sep. Sci.* 26 (2003) 1305

22 Li D. and Remcho V. T.; *J. Microcol. Sep.* 9 (1997) 389

23 Stevens S.T. and Cortes H.; *Anal. Chem.* 55 (1983) 1365

24 Seifar R. M, Kok W. Th., Kraak J. C. and Poppe H.; *Chromatographia* 46 (1997) 131

25 Seifar R. M, Kraak J. C., Kok W. Th. and Poppe H.; *J. Chrom. A.* 808 (1998) 71

26 Adam T., Lüdtke S. and Unger K.K.; *Chromatographia* 49 (1999) S49

27 Lüdtke S., Adam T. and Unger K.K.; *J. Chrom. A.* 786 (1997) 229

28 Vallano P.T. and Remcho .T.; *Anal. Chem.* 72 (2000) 4255

29 Wen E. Asiaie R. and Horvath Cs.; *J. Chrom. A.* 855 (1999) 349

30 Wei Y., Fan L. M. and Chen L.R.; *Chromatographia* 46 (1997) 637

31 Stol R., Poppe H. and Kok W.Th.; *Anal. Chem.* 73 (2001) 3332

32 Stol R., Poppe H. and Kok W.Th.; *J. Chrom. A.* 887 (2000) 199

33 Choudhary G. and Horváth Cs.; *J. Chrom. A.* 781 (1997) 161

34 Cikalo M.G., Bartle K.D. and Myers P.; *J. Chrom. A* 836 (1999) 25

35 Rathore A.S. and Horváth Cs.; *Anal. Chem. 70* (1998) 3271

36 Rathore A.S. and Horváth Cs.; *Anal. Chem. 70* (1998) 3069

37 Rathore A.S. and Horváth Cs.; *J. Chrom.* 743 (1996) 231

38 Steiner F. and Scherer B.; *J. Chrom. A* 887 (2000) 55

39 Majors R.E.; *LC-GC* 16 (1998) 96

40 Walhagen K., Unger K.K., Olsson A.M. and Heam M.T.W.; *J. Chrom. A* 853 (1999) 263

41 Baeumel F. and Welsch T.; *J. Chrom. A* 961 (2002) 35

42 Van den Bosch S.E., Heemstra S., Kraak J.C. and Poppe H.; *J. Chrom. A* 755 (1996) 165

43 Paterson C. J., Boughtflower R. J., Higton D. and Palmer E.; *Chromatographia* 46 (1997) 599.

44 Verheij E.R., Tjaden U.R., Niessen W.M.A. and van der Greef J.; *J. Chrom.* 554 (1991) 339

45 Eimer T., Unger K. K. and Tsuda T.; *Fresen. J. Anal. Chem.* 352 (1995) 649

46 Zhang Y., Shi W., Zhang L. and Zou H.; *J. Chrom. A* 802 (1998) 59

47 Huber C. G., Choudhary G. and Horváth C.; *Anal. Chem.* 69 (1997) 4429.

48 Ding J., Szeliga J., Dipple A. and Vorous P.; *J. Chrom. A* 781 (1997) 327.

49 Wu J.T. , Huang P., Li M.X., Qian M.G. and Lubmann D.M.. *Anal. Chem.* 69 (1997) 320.

50 Behnke B. and Bayer E.; *J. Chrom. A* 680 (1994) 93

51 Taylor M.R. and Teale P.; *J. Chrom. A* 768 (1997) 89

52 Dittmann M.M, Rozing G.P., Ross G., Adam T. and Unger K.K..; *J. Cap. Electrophoresis* 4 (1997) 201

53 Lister A.S., Rimmer C.A. and Dorsey J.G.; *J. Chrom. A* 828 (1998) 105

54 Smith N.W. and Carter-Finch A.S.; *J. Chrom. A* 892 (2000) 219

55 Yan C., Dadoo R., Zare R.N., Rakestraw D.J. and Anex D.S.; *Anal. Chem.* 68 (1996) 2726

56 Kahle V., Vázlerová M. and Welsch T.; *J. Chrom. A* 990 (2003) 3

57 Tang Q. and Lee M.; *TrAC* 19 (2000) 648

58 Altria K.D., Smith N.W. and Turnbull C.H.; *Chromatographia* 46 (1997) 664

59 Rapp E. and Bayer E.; *J. Chrom. A* 887 (2000) 367

60 Boughtflower R.J., Underwood T. and Paterson C.J.; *Chromatographia* 40 (1995) 329

61 Mayer M., Rapp E., Marck C. and Bruin G.J.M.; *Electrophoresis* 20 (1999) 43

62 Rebscher H. and Pyell U.; *Chromatographia* 42 (1996) 171

63 Carney R.A., Robson M.M., Bartle K.D., Myers P. *J. High Res. Chrom.* 22 (1999) 29

64 Behnke B., Johansson J., Zang S., Bayer E. and Nilsson S.; *J. Chrom. A* 818 (1998) 257

65 Yang C. and Rassi E.; Elctrophoresis 20 (1999) 18

66 Smith N. W. and Evans M.B.; *Chromatographia* 41 (1995) 197.

67 Cortes H. J., Pfeiffer T. S., Prichter B. C. and Stevens T.S.; *J. High Res. Chrom.* 10 (1987) 446

68 Behnke B. Grom E. and Bayer E.; *J. Chrom. A* 716 (1995) 207

69 Lord G.A., Gordon D.B., Myers P. and King B.W.; *J. Chrom.* A 768 (1997) 9

70 Choudhary G., Horváth Cs. and Banks J.F.; *J. Chrom.* A 828 (1998) 469

71 Bartle K.D., Carney R.A., Cavazza A., Cikalo M.G., Myers P., Robson M.M., Roulin S.C.P. and Sealey K.; *J. Chrom. A* 892 (2000) 279

72 Angus P.D.A., Demarest C.W., Catalano T. and Stobaugh J.F.; *J. Chrom.* A 887 (2000) 347

73 Colón L.A., Maloney T.D. and Fermier A.M.; *J. Chrom.* A 887 (2000) 43

74 Gordon D.B., Lord G.A. and Jones D.S.; *Rapid Comm. Mass Spectrom.* 8 (1994) 544

75 Saevels J., Wuyts M., Van Schepdael A., Roets E. and Hoogmartens J.; *J. Pharm. and Biomed. Anal.* 20 (1999) 513

76 Dulay M.T., Yan C., Rakestraw D.J. and Zare R.N.; *J. Chrom.* A 725 (1996) 361

77 Stohl R., Mazereeuw M., Tjaden U.R. and van der Greef J.; *J. Chrom.* A 873 (2000) 293

78 Fermier A.M., Colón L.A.; *J. Microcol. Sep.* 10 (1998) 439

79 Reynolds K.J., Maloney T.D., Fermier A.M. and Colón L.A.; *Analyst* 123 (1998) 1493

80 Robson M.M., Roulin S., Shariff S.M., Raynor M.W., Bartle K.D., Cliford A.A., Myers P., Eurby M.R. and Johnson C.M.; *Chromatographia* 43 (1996) 313

81 Roulin S., Dmoch R., Carney R., Bartle K.D., Myers P., Eurby M.R. and Johnson C.M.; *J. Chrom.* A 887 (2000) 307

82 Zimina T.M., Smith R.M. and Myers P.; *J. Chrom.* A 758 (1997) 191

83 Svec F., Peters E.C., Sykora D. and Fréchet J.M.J.; *J. Chrom.* A 887 (2000) 3

84 Zou H., Huang X. Ye M. and Luo Q.; *J. Chrom.* A 954 (2002) 5

85 Pesek J.J. and Matyska M.T.; *J. Chrom.* A 887 (2000) 31

86 Smith N. and Evans M.B.; *J. Chrom.* A 832 (1999) 41

87 Banholczer A. and Pyell U.; *J. Chrom.* A 869 (2000) 363

88 Wright P.B, Lister A.S and Dorsey J.G.; *Anal. Chem.* 69 (1997) 3251

89 Gusev I., Huang X. and Horváth Cs.; *J. Chrom.* A 855 (1999) 273

90 Zhang S., Huang X., Zhang J. and Horváth Cs.; *J. Chrom.* A 887 (2000) 465

91 Abidi S.L. and Rennick K.A.; *J. Chrom.* A 913 (2001) 379

92 Siouffi A.M.; *J. Chrom.* A 1000 (2003) 801

93 Colon L .A., Guo Y., Fermier A.; *Anal. Chem.* 68 (1996) 2753

94 Minakuchi H., Nakanishi K., Soga N., Ishizuka N., Tanaka N.; *Anal. Chem.* 68 (1996) 3498

95 Hjertén S., Eaker D., Elenbring K., Ericson C., Kubo K., Liao J.L., Zeng C.M., Lindström P.A., Lindh C., Palm A., Srichiayo T., Valtcheva L., Zhang R.; *Jpn. J. Electroph.* 39 (1995) 105

96 Fujimoto C.; *Anal. Chem.* 67 (1995) 2050

97 Peters E.C., Petro M., Svec F. and Fréchet J.M.J.; *Anal. Chem.* 69 (1997) 3646

98 Peters E.C., Petro M., Svec F. and Fréchet J.M.J.; *Anal. Chem.* 70 (1998) 2288

99 Peters E.C., Petro M., Svec F. and Fréchet J.M.J.; *Anal. Chem.* 70 (1998) 2296

100 Wang Z., Svec F. and Frechet J.M.J.; *Anal. Chem.* 65 (1993) 2243

101 Xiong B., L. Zhang, Y. Zhang, Zou H. and Wang J.; J. High Res. Chrom. 23 (2000) 67

102 Liu Y. and Pietrzyk D.J.; *Anal. Chem.* 72 (2000) 5930

103 Liu Y. and Pietzryk D.J.; *J. Chrom.* A 920 (2001) 367

104 Adam T. Unger K.K., Dittmann M.M., Rozing G.P. *J. Chrom.* A 887 (2000) 327

105 Asiaie R., Huang X., Farnan D. and Horváth C.; *J. Chrom.* A 806 (1998) 251

106 Chirica G.T. and Remcho V.T.; *Electrophoresis* 20 (1999) 50

107 Chirica G.T. and Remcho V.T.; *Anal. Chem.* 72 (2000) 3605

108 Dulay M.T., Kulkami R.P. and Zare R.N.; *Anal. Chem.* 70 (1998) 5103

109 Qu Q-s., He Y-z., Gan W-e., Deng N. and Lin X-q.; *J. Chrom.* A 983 (2003) 255

110 Tanaka N., Kobayashi H., Ishizuka N. Minakuchi H., Nakanishi K., Hosoya K. and Ikegami T.; *J. Chrom.* A 965 (2002) 35

111 van Berkel O., Kraak J.C. and Poppe H.; *J. Chrom.* 449 (1987) 345

112 Tock P.P.H., Boshaven C., Poppe H. and Kraak. J.C.; *J. Chrom.* 477 (1989) 95

113 Tock P.P.H., Stegeman G.R., Peerboom R., Poppe H., Kraak J.C. and Unger K.K.; *Chromatographia* 24 (1987) 617

114 Swart R., Kraak J.C. and Poppe H.; *J. Chrom.* 670 (1994) 25

115 Crego A.L., González A. and Marina M.L.; *Crit. Rev. Anal. Chem.* 26 (1996) 261

116 Guo Y. and Colon L.A.; *Anal. Chem.* 67 (1995) 2511

117 Huang X., Zhang J. and Horváth Cs.; *J. Chrom.* A 858 (1999) 91

118 Liu Z., Otsuka K. and Terabe S.; *J. Chrom.* A 959 (2002) 241

119 Unger K.K., Kumar D., Grün M., Buchel G., Lüdtke S., Adam T., Schumacher K. and Renker S.; *J. Chrom.* A 892 (2000) 47

CHAPTER 3

Techniques for Coupling Capillary Electrophoresis to Mass Spectrometry

3 Capillary electrophoresis-Mass spectrometry

3.1 Introduction

Following the first demonstration of the use of mass spectrometry (MS) in combination with capillary electrophoresis (CE) by Olivares *et al.* in 1987 [1], the use of this hyphenated technique is slowly becoming more widespread in analytical chemistry [2,3,4]. This technique allows analyses in aqueous solutions that are complementary to HPLC/MS. However, CE-MS has advantages when analysing charged and polar compounds, since separation is based on the charge-to-size ratio of analytes. Although CE-MS is still not a routine technique it has been used for both quantitative and qualitative analysis of many chemically diverse compounds and is a useful analytical tool for the separation, quantitation and identification of several important classes of analytes, such as biologicals [5,6,7], therapeutics [8,9], environmental pollutants [10,11] and drugs [12,13,14] *etc.*

Although combinations with magnetic sector [15], ion trap [16], Fourier transform ion cyclotron resonance (FT) [17], time of flight (TOF) [7, 36] and even position and time-resolved ion counting (PATRIC) [18] MS analysers have been described, the most widely used mass spectrometers in combination with CE are based on quadrupole analysers. This is mainly due to their general availability and tandem MS capability.

The selectivity (that is, separation selectivity for co-eluting molecules of different nominal masses) and specificity that a MS can provide, more than compensates for variations in migration times of the analytes (which is a common occurrence in this separation technique) [1]. The coupling of MS with CE improves detection limits when compared to UV detection [Table 1.4, Chapter 1.8.2.], especially when considering the selected-ion-monitoring (SIM) mode of detection [3].

CE has been coupled to mass spectrometers employing atmospheric pressure chemical ionisation (APCI) [19], (continuous flow) fast atom bombardment (FAB) [20], laser vaporisation ionisation [21] and off-line matrix assisted laser desorption ionisation (MALDI) [22]. However only the widely used electrospray ionisation (ESI) technique will be discussed here.

In order to couple CE to MS an interface is required. ESI is generally considered the method of choice for interfacing CE to MS, since it allows even large biological and/or macromolecules to be transferred directly from the liquid phase to the gas phase (with the availability of forming multiple charged species) with high ionisation efficiency [1]. To date there are three types of interface (and their modifications) that can be used to couple CE with MS. These are:

- liquid-junction,
- coaxial sheath flow interfaces,
- sheathless or nanospray.

This review will mainly focusing on the most common coaxial sheath flow interface, which is relevant for the work reported in this thesis.

3.2 Liquid-junction Interface

The liquid-junction interface was first reported in the late 80's by Minard *et.al* for a CE-CFFAB/MS system [3] and by Henion *et al.* [23] for a CE-ESI(Ion spray)/MS system. The liquid junction interfaces for CFFAB and ESI are very similar with the exception of the absence FAB matrix in the sheath solution and/or nebuliser gas in the given ionisation technique. The liquid junction is constructed from a stainless steel T-piece to establish the electrical contact. The electrospray voltage is applied to the sheath liquid reservoir (or T-piece) and the electrical contact is formed through the sheath liquid filled narrow gap (typically 10 - 25 μm) between the CE and transfer capillary (Figure 3.1). The sheath reservoir not only provides the electrical contact but also

compensates for the difference between the flow rate generated in CE and that required for stable spray generation in ESI(ISP).

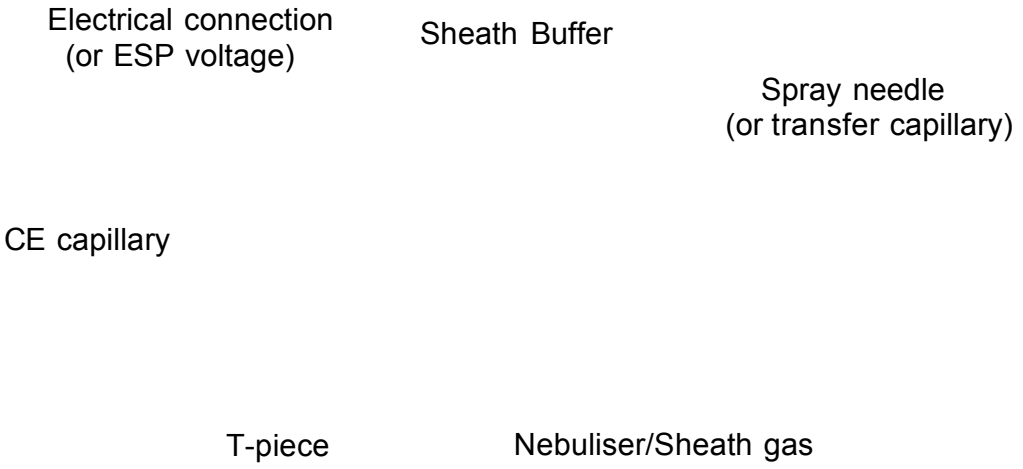

Figure 3.1 Schematic of a liquid-junction interface [23]

The main advantage of the liquid-junction interface is that it separates the CE capillary from the ESI emitter, thus preserving the capillary's lifetime (this is specially useful in CEC) and allows the independent optimisation of both the separation and the ESI spraying process.

Several modifications have been suggested to improve the liquid-junction coupling since its invention - such as controlling the sheath liquid flow rate by an infusion pump instead of the original gravity delivered set-up; application of fused-silica instead of stainless steel for the material of the spraying capillary, to reduce the adsorption of compounds on capillary walls; pressurisation of the CE capillary to avoid sheath liquid flow-back and a new design for improved alignment and set-up [24-25], but liquid-junction interfacing remains less used than the coaxial CE-MS coupling technique.

The main reason for this is the difficulty in the precise alignment and spacing between the CE and transfer/spray capillary. This could lead to a band broadening effect. Pleasance *et al,* have also reported [26] sheath liquid contamination problems and higher background noise level than with the

coaxial sheath liquid interface. Although, if optimum alignment is achieved the liquid-junction can provide better sensitivity and a lower dispersion factor [27] the benefits of the use of a coaxial sheath flow, such as its simpler fabrication, zero dead-volume, better stability, robustness and reproducibility [27] outweigh these benefits.

3.3 Co-axial interface

The sheath flow system is the most commonly used method for CE/ESI interfacing [4] and was developed in 1988 by Smith *et al* [28]. The coaxial sheath liquid interface (Figure 3.2) is constructed from three concentric, coaxial capillaries set at the interface of CE and MS. In this set-up [29-30]

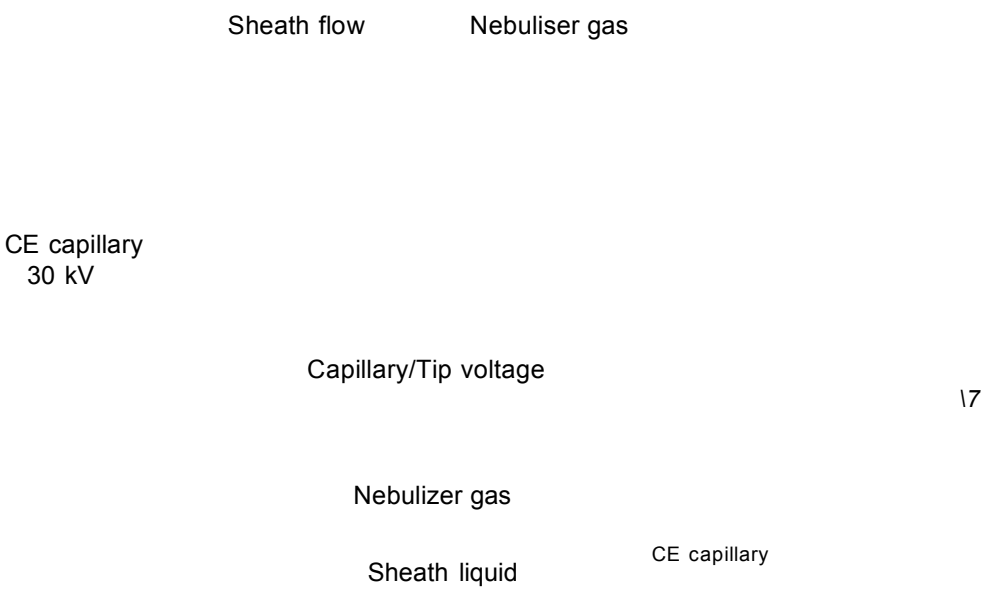

Figure 3.2. The schematic of a modified VG Quattro ESI ion-probe for Co-axial CE-MS interface used in thesis.

the innermost fused silica capillary is inserted into the atmospheric part of the ESI source through a narrow stainless steel capillary, which is responsible for the delivery of the sheath liquid to the outlet end of the fused silica capillary. The middle stainless steel capillary is inserted into another stainless

steel tube, in which a high velocity of an inert nebulising gas (usually nitrogen) flows. This assists the ion evaporation and spraying process in ESI.

The sheath liquid is generally delivered by a syringe driver, into the coaxial probe at 2-10 μL/min level, which is the optimum flow rate for ESI and CFFAB. The electrical connection between the stainless steel capillary tip and the separation capillary is provided by a liquid film that builds up on the outer surface of the tip of the fused silica capillary [31]. The outer polyimide protective coating, which has electrically insulating properties, is generally removed from the silica at the end of the separation capillary to help efficient electrical contact by the sheath liquid [32]. The typical ±(2-8) kV ESI voltage can be applied either to the spraying tip [29-30] or to the lens at the MS sampling entrance.

When coupling the CE system to the mass spectrometer, the capillary outlet is placed directly into the ESI interface via the coaxial probe. There is no requirement for the capillary outlet and cathode to be in a reservoir, since there is sufficient electrical contact with the run buffer flowing out of the fused silica capillary. The electrical contact is made via a sheath liquid, a large proportion of which is a volatile solvent to aid evaporation (such as methanol, acetonitrile *etc.*). The sheath liquid flows around the capillary, at 5-10 μL/ min. A voltage is applied to the stainless steel spray capillary to ensure the production of ions during electrospray. Thus upon the application of this voltage which is negative with respect to the anode (which is the fused silica capillary inlet of the CE system), which is in the CZE buffer in the high voltage region (30 kV), a potential difference is set up for CZE separation [38]. Solutes will then exit the capillary, through nebulisation, and are ionised in the electrospray source. Solute ions proceed through the MS system where they are separated according to their mass-to-charge (M/Z) ratios and are observed as generally protonated molecules $[M + H]^+$.

CE-ESI interfacing is further complicated by the need to complete electrical paths for both the CE and ESI systems [48]. This situation may be worsened,

since a constant voltage must be applied between the capillary outlet and the MS entrance, during ESI. Ideally the capillary outlet should be maintained at ground potential (where the electric field applied across the fused silica capillary is zero volts with respect to the out-let end), as is normally the case in CE/UV [48].

Although sensitivities in the femtomole to attomole range (amount injected) have been reported for CE-ESI/MS analysis of numerous analytes, especially peptides [31], it is generally known that CE-ESI/MS analysis gives poor detection limits. This is primarily due to the due to the high mismatch in the liquid flow rates between CE (which typically produces tens of nanolitres per minute) and traditional ESI flow rates (ranges 1 – 200 μL/min).

Achieving an optimal and reliable CE-ESI/MS system with maximum separation efficiency and detection sensitivity requires optimising the chemical parameters of the liquids used in spray formation and the adjusting of various physical (instrumentation and set-up) parameters.

3.3.1 Chemical parameters (Spraying Solvents)

Due to the large difference between the CE and sheath flow rates, the sheath liquid dominates the ESI process. The limitations and problems reported are related to its composition rather than that of the CE running buffer [48].

The ESI process itself is affected by various analyte properties (*e.g.* pKa, hydrophobicity, surface activity, ion solvation energy) which affect the ionisation. The nature of the solution affects the formation of gas-phase ions in multiple ways [33].

The advantage of the co-axial interface design is that the sheath liquid can be optimised independently of the separation buffer, thus enabling a variety

of buffers to be used. This is a crucial point in MS coupling since strong and stable ESI signals are generally obtained with volatile buffers with low salt content.

CE separations are however, primarily dependant on the running buffers, which usually posses high ionic strengths. That is, an increase in electrolyte concentration/ionic strength in the liquid to be sprayed leads to arcing and discharges with a decrease in ESI-MS performance [13]. But the introduction of a nebulising gas, at high velocity, assists the formation of the small droplets required for ESI, and hence the requirement for a low surface tension and low conductivity solution for the sheath liquid may be relaxed [48]. Furthermore, a lower ionic strength buffer, results in reduced separation efficiency.

Non-volatile buffers are seldom used since they encourage crystallisation on the metal surfaces of the instrument, and they can block the MS sample orifice. It is for this reason that ammonium acetate and formate buffers are generally recommended (even concentrations as high as 1M have been reported [34]), whilst phosphate and borate buffers are usually omitted from selection [13]. If acetate and formate give inadequate separation it is advisable to use a more volatile form of the "non ESI friendly" buffers (*i.e.* ammonium- instead of sodium salts of phosphate, carbonate *etc.*). Another solution for this problem is the application of a Z-spray ion source, which is more tolerant towards these buffers, as the spray is not employed directly towards the MS orifice.

The sheath liquid not only functions as the make-up flow for the required ESI flow rate, but as the outlet buffer reservoir, as well. This electrolyte background can interfere with the CE separation and resolution [35-36]. Due to the potential gradient across the CE capillary, it is possible for sheath liquid counter ions to enter into the fused silica capillary at the outlet end and alter the migration of the analytes [48]. When these counter ions are

different in the sheath and CE running buffer liquid the formation of a moving ionic boundary occurs inside the capillary [2]. This effect is mostly problematic in CE systems with low electroosmotic flow (EOF) [31]. Foret *et al.* concluded [35] that this effect can be minimized by the use of a common or a counter ion with similar pK_a and electrophoretic mobility in the CE buffer and sheath liquid; with application of high EOF and small additional pressure.

3.3.2 Physical parameters (Instrumentation)

Because of the difference in the physical size of commercially available CE instruments and mass spectrometers (*i.e.* the height of the CE in relation to the height of the ion source, from the ground or a bench), there is a limit to the smallest length of fused silica capillary that can be used [37]. This is important since the longer the fused silica capillary, the longer the analysis time (since there is a voltage drop per centimetre of capillary) and this may also decrease the separating power of CZE. In most cases a 1m capillary is used [38]. This often makes capillary thermostating impossible and thus Joule heating (causing bubble formation) can become an issue. Formation of a gas bubble in the spray capillary (stainless steel) and/or the fused silica capillary may lead to instability in the spray. The former may result in the isolation of the liquid solution from the metal high voltage contact halting the spraying process [39], the latter may lead to an unstable current within the capillary.

There should be no height difference between the liquid in the inlet CE vial and the spraying end (outlet the separation capillary) to prevent siphoning effects [40]. This is often helped by adding a low constant pressure to the CE capillary [37,43]. This few mbar additional pressure is often advantageous. For example, it can shorten analysis times, can avoid moving boundaries (as explained earlier) and - as electrospray has the potential to cause a vacuum on the column exit (which can lead to discontinuity in the liquid flow, as well as bubble formation) - can help maintain continuous spray. However, the

added pressure causes parabolic flow, which degrades separation efficiency and causes peak broadening, thus it must be kept minimal.

The dimensions of the capillaries, in particular the inner (i.d.) and outer (o.d.) diameters and wall thickness, have an influence on the spray formation. Tetler *et al.* [29] have shown that better operation and increased sensitivity can be achieved by reducing all dimensions of the sheath and CE capillaries. Thin-wall capillaries have improved wetability with sheath liquid and this can also be improved by the removal of the polyimide coating from the end of the fused-silica capillary [32]. This aids the stability of electrospray, but they are much more fragile. The durability of thin-wall capillaries, when used in conjunction with stainless steel sheath tubes, was found to be low due to "electrodrilling" [41], caused by an electrochemical processes. Siethoff *et al.* [42] successfully solved this problem by replacing the stainless steel sheath tube with a commercially available aluminium coated fused silica GC column. The aluminium coating also solved the problem of bubble formation which occurs at the steel surface when it comes to contact with liquids, especially at strongly acidic or basic pH [42].

Positioning of the capillary in relation to the MS orifice or counter electrode, and inside the coaxial probe is crucial for stable ESI operation. This position of the ion probe with respect to the orifice or counter electrode is instrument dependent and requires proper adjustment before analysis for optimum performance [37]. If the tip is located too close to the counter electrode electric discharge occurs at the tip, which causes instability in the ESI operation.

The distance between the fused silica capillary and the stainless steel capillary (see Figure 3.2) is also critical for a reliable CE-MS performance as it ensures the electrical contact. If the capillary is protruding too far out of the sheath tube unstable ESI current results due to insufficient electrical connection. If placed too far inside the tube, the dead volume, and

consequently sample mixing becomes high and the MS signal of the analyte is also reduced. Different groups have reported different optimum distances. The reported optimal range varying widely from the inside to outside position of the sheath tube.

The effect of the distance of the CE capillary end relative to sheath capillary and the nebulising gas flow on the obtained MS signal was studied by Banks [43] whilst optimising a peptide separation. His results demonstrated, that the signal optimises with the CE column extending out 0.3 mm from the sheath tube (Figure 3.3). This is in agreement with other suggestions for an optimum range of 0.2–1.0 mm [28, 44, 45]. However, different studies have reported different optimum positions. A Chinese group reported an optimum of 0.1– 0.4 mm, in the determination of alkaloids, and found the optimum at 0.05mm outside the sheath tube [46], while an optimum distance of 0.5 mm inside the sheath tube has been reported in the determination of derivatised carbohydrates [47].

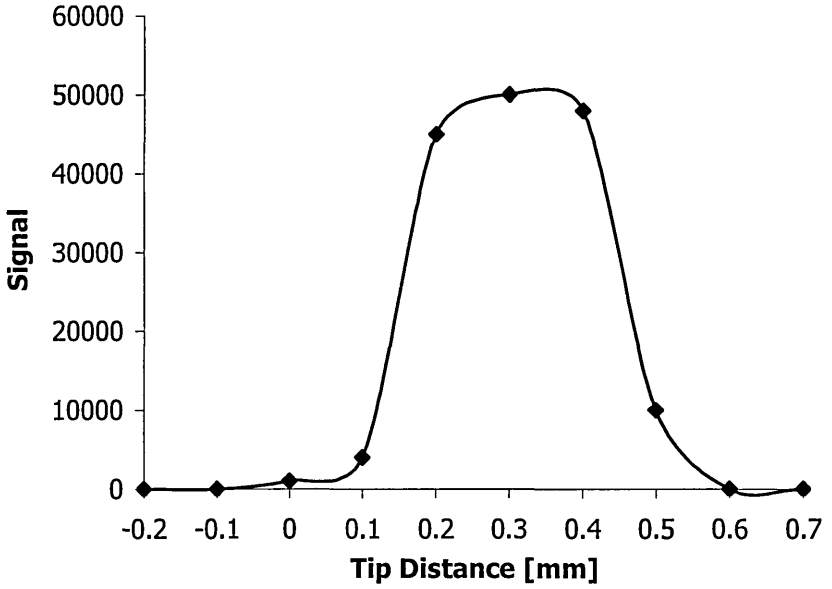

Figure 3.3 Effect of distance between CE column and sheath tube ends (reproduced from [43])

The only general rule appears to be that the capillary outlet distance from the sheath tube should be kept as small as possible, to ensure: optimal electrical contact (and hence good ESI current stability) and a small mixing

volume at the tip (to reduce band broadening caused by diffusion) [48]. Since CE-MS requires both an electrical contact and a stable electrospray at the capillary tip, it can benefit from improvements in interface durability and reproducibility [49].

The flow rate of both the sheath liquid and the nebuliser gas strongly influence the performance of any ESI/MS system. It has been reported by several groups that the flow rate of the nebulising gas influences the signal response [32] or even peak shapes [50] and CE flow [51] in fused-silica capillaries with inner diameter above 50μm.

3.4 Sheathless or Nanospray Interface

Nano(electro)spray was first suggested by Wilm and Mann [52]. Because of the low flow the application of nebuliser gas to assist fine droplets formation is not necessary. The spray is formed solely by the electrical voltage added to the tip. The required electrically conductive 1-10 μm spraying tip can be achieved by coating the drawn fused silica capillary or by using a metallised glass or a metal tip. Nanospray potentially offers an ideal interface for CE-MS as the supplied and required (around 20 nL/min) flow rates are similar, and as no sheath-flows are required, no dilution effects occurs, making nanospray a potentially more sensitive interface.

Currently there are four main nanospray CE-MS interfaces (Figure 3.4):

The most common construction includes a drawn fused-silica CE capillary with a conductive coating on it [53,54]. The second construction includes separate nanospray tips attached to the CE separation capillary via a low or zero-dead- volume unions with direct electrical connection [55]. The third constructions use make-up liquids (thus in strict sense it is not a sheathless application) across the outlet of the separating CE capillary. The electrical

Figure 3.4 Different Sheathless/Nanospray Interfaces:

(a) Gold coated and (b) conductive silver painted drawn fused silica capillaries, (c) ESI Nano/Pico tip with union, (d) sheath liquid assisted and (e) in-capillary electrode

connection is made by an external electrode inserted into this make-up liquid. The nanospray interface developed by Hsieh *et al.* [56] to analyse peptides used a 1 μl/min flow rate, which was reported not to interfere with the obtained 50 nl/min nanospray flow rate. In a recent publication [57] the nanotip was inserted into a liquid reservoir (microcentrifuge tube), which automatically provided the make-up liquid without any external flow system. This was used for low flow ESI applications in the separation of phenolic compounds by CZE-MS and triazines by MEKC-MS. The fourth construction uses capillaries with a conductive wire inserted inside. This is achieved by inserting the electrode wire from the end of the CE capillary [58], threaded through a small hole in the capillary near the CE end and sealed in place [59].

3.4.2 Physical parameters of the Nanotips

Reliable and efficient CE-Nano-ESI/MS analysis requires nanotips with stable conductive coatings. Up to date there have been several attempt to obtain stable coatings.

Painted tips - generally with conductive silver - are the easiest to manufacture and this can provide very robust coatings. The obtained surfaces are however rough without uniformity. This can lead to discharging from the edges on the surface. It has also been observed that these coatings produce silver adducts ions [60]. A very simple and cheap carbon coating was also reported [61] using a paint marker pen (containing an oil-based resin) to smear the capillary, followed by graphite coating using an ordinary soft pencil. Gold coatings are generally made by vapour deposition of gold dust under vacuum. These coatings with nm thickness were found to be very unstable as the gold layer rapidly sputter out of the silica surface under operation [60]. Several groups [62,63,64] have suggested derivatising methods for the nanotip or using additional adhesives to improve the life time and stability of the coating. Recent developments use conductive

polymers such as conductive polyaniline [65] or polypropylene [66] which have good mechanical stability and are resistant to discharges.

3.5 CEC-MS Interface Developments

The first real CEC-MS coupling was reported by Gordon *et al.* [67] in 1994 separating steroid mixtures on 3μm ODS-silica. Earlier works [68] used pressure assisted electrochromatographic (p-CEC) systems, which were more reliable, but could not provide the full efficiency of CEC due to the mixed effect of the electroosmotic and pressure driven flow. These first CE-MS works used CFFAB interfaces and a FAB ionisation source but soon most of the work, as in the case of CZE, has been carried out with ESI [27]. The first ESI applications were reported by Hugener *et al.* [69], Schmeer *et al.* [70] and Lane *et al.* [71] separating food colours on 5μm C-18 and peptides on 1.5μm ODS-silica respectively.

Besides the general considerations for CE-MS coupling, such as; the maintenance of a stable electrical connection, to complete the CE circuit, and the simultaneously supply of the electrospray potential, and the avoidance of buffer diminution at the column outlet, CEC-MS also has additional issues, which have to be addressed.

The first problem is the minimum distance required to connect commercial CE systems with MS instruments. The required capillary length can be as high as 1m, which is not practical in CE(C) separations due to the long elution times. This results not only from the longer distance but also from the reduced electrical field strength due to the increased electrical resistance of the system, with accompanying band broadening.

The second and main problem is bubble formation. Although this can be avoided in stand-alone CEC systems, by pressurising [72], both the inlet and outlet of the capillary, this is not a possibility with the atmospheric pressure

of ESI sources. Beside Joule heat, the main sources of bubble formation are the capillary junction/connection - if it is applied in the system - and the frit between the packed section and the open section of the rest of the capillary.

Several researchers have reported [73,74] the use of the packed end of the CEC capillary as the spraying outlet. In this way the effluent can be directly sprayed into the ion source. A further development of this configuration was the application of packed tapered capillaries [75,76]. The possible tapered outlets are illustrated in Figure 3.5. Lord *et al.* [75] found that the liquid flow throughout, in both the drawn (external tapers) and melted then ground (internal tapers) capillaries were as good as the common sintered frits. This allows the packing, as the orifices were circa 10pm in both cases, and were sufficient to retain 3pm silica particles. The electrical contact was established by coating the tapers.

Figure 3.5 Packed external (a) and internal (b) taper for CEC-MS interface

Although packed tapers can reduce or eliminate bubble formation, they are prone to blockage and their fragility is a serious problem (especially with external tapers) as any breakage to the tip will result in the loss of the packing material. Using zero dead volume unions and connecting tubes as transfer lines after the terminating frit of the packed section is another approach to CEC-MS interfacing. In this set-up the spraying tip is separated from the packed capillary and can be individually replaced. This set-up can suffer from buffer depletion effects and band broadening [77].

3.6 Study of CE-MS Nanospray Interfaces for VG Quattro-I. Mass Spectrometer

As described previously, nanospray (NanoESI) is an obvious choice for ionisation method in CE/CEC as it requires no additional flow and nebuliser gas, since it uses the same flow rate as produced in CE/CEC. The aim of this preliminary work was to develop and optimise a simple NanoESI-MS coupling for general CE and CEC applications. The performance of various nanotips has been investigated to determine their reliability for future applications.

3.6.1 Experimental

Apparatus. All experiments were performed on a VG Quattro-I Mass Spectrometer (Micromass, UK), equipped with an ESI source, coupled with a commercially available CE interface (Ash Instruments, UK) as shown in Figure 3.6. This specially made interface was chosen for testing the different coupling techniques due its practical advantages, such as the smaller design which allowed easier positioning and the application of much shorter capillaries, and thus analysis time. Although, the accuracy and reproducibility (especially sample loading) of the CE part of the interface are worse than in a commercial CE instrument, the CE interface uses the original VG ESI ion probe, which allows the direct application of the coupling method to professional CE instruments once an adequate interface has been developed.

Due to the design of the VG Quattro MS instruments, the nanospray operation required the modification of the ion probe and therefore the ion source as well. The high voltage counter electrode, also known as "chicane lens" had to be removed due to the longer ion probe required to reach the lens orifices (Figure 3.7). Consequently the first skimmer became the counter electrode during nanospray operation.

Figure 3.6 Photograph of the Ash Instrument's CE interface with high voltage power supply for VG Mass spectrometers

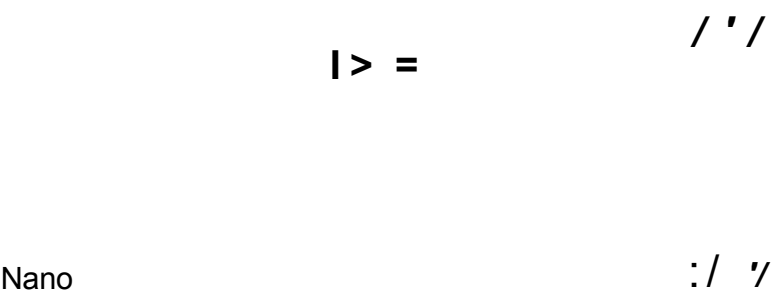

Figure 3.7. Comparison of inlet probe positioning in ESI source with the chicane lens and the nanosource with the skimmer lenses and hexapole in the VG Quattro-I mass spectrometer.

Chemicals. **Test samples of 3-substituated pyridines (amino-, cyano-, ethyl-, chloro- and acetyl-pyridines) were purchased from Sigma-Aldrich (Dorset, UK). The solvent used was HPLC grade acetonitrile, purchased from Aldrich (Dorset, UK). All the water used was distilled and then de-ionised (MilliQ**

grade) prior to the measurements (Millipore, Herts, UK). Chemicals used were HPLC grade ammonium acetate, hydrochloric acid and sodium hydroxide (BDH Chemicals Ltd., Dorset, UK). Fused silica capillaries were purchased from Composite Metals Services (Worcester, UK).

3.6.2. Discussion

To compare the performance of the different nanospray interfaces and determine their reliability for this thesis, a test mix of 3-substituated pyridines was used. Hydrodynamic infusion (25mbar, O.lmin) of the sample, diluted in the running buffer (20 mM ammonium acetate pH 2.5), was performed at a concentration of 10 p-g/mL for CZE-MS analysis. Test compounds were detected by SIR of [M+H]+.

Maintaining perfect electrical connection is the crucial factor in coupling CE instruments to MS, since EOF is generated by a potential difference between the two ends of the capillary. Thus a stainless steel Valeo union (1/16") to which the column and the stainless steel nanospray needle were connected (Figure 3.8) was tested at first for interface set-up. To obtain sufficient electrical contact as well as the liquid junction in the union, the tip end was also painted with conductive silver.

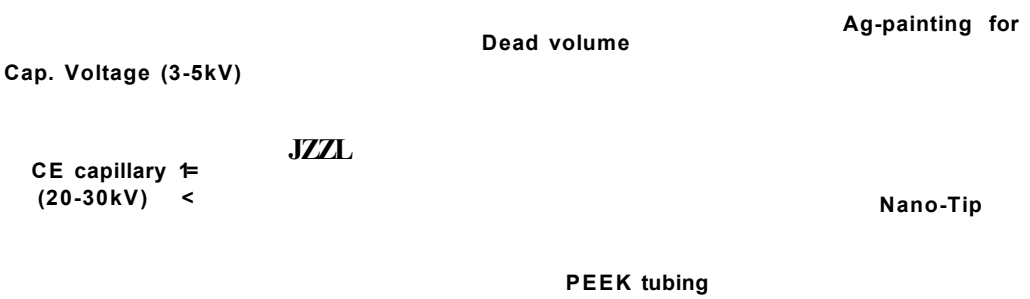

Figure 3.8. Schematic of capillary and spraying needle connection in a nanospray interface using a stainless steel (1/16") Valeo union.

This interface turned out to be poor in practice. As pulsating spray was observed, this poor performance was caused by insufficient electrical

contact. The formation of bubbles in the dead volume of the union (theoretically 5nl which can be larger due to imperfect PEEK tubing and/or silica capillary cutting) has been previously suggested on stainless steel due to electrolytic formation of hydrogen by high voltage [78,79]. The pulsating gas formation also caused fluctuations in the EOF (and on many occasions stopped it) as the electrical contact was broken every time a bubble formed in the liquid junction. Consequently this led to an unstable operation and as a result, separations became irreproducible and retention times greatly varied. Applying a small pressure (5-25mbar) to the capillary inlet did not improve the performance of the interface, which indicated the continuous high bubble formation rate. However it was also noted that both the simple Ash CE interface had poor performance to continuously maintain constant low pressure, thus limiting the possibility of assisting the flow with supplementary pressure.

To prevent these problems a method was required that butted two pieces of fused silica (separation capillary and spray tip) and allowed the ESI voltage to be applied to the very end of the spray tip. The initial set-up (Figure 3.7), had to be used due to the requirement of the VG inlet, thus the stainless steel Valco union (0.25mm-bore) was drilled out, to enlarge its internal orifice and hence allow the insertion of the polyimide coated silica capillaries (Composite Metals Services), with an outer diameter of 375μm, used for all of what described in this thesis. The spray voltage and electrical contact were made through conductive silver paint between the ion-probe and the nano tips (as in Figure 3.8).

Three different nanospray tips, which were devised and studied for this set-up, gold sputter coated, conductive silver painted paint drawn fused silicas (ID: 50 μm) and internally gold-coated glass micropipettes.

The minimum length of the spray tip was determined by the VG Quattro source inlet to be 20cm. Thus fused silica capillaries were drawn to a sharp

point using a suspended weight on the capillary and heating the capillary at a fixed height with a Bunsen micro-burner until it stretched. Capillaries were cut with a ceramic capillary cutter and tapered. To stabilise the coating on the surface, capillaries were cleaned and derivatised by the method of Kriger [80] prior to gold sputter coating, which was then performed using standard procedures by the Material Research Institute of Sheffield Hallam University. Conductive silver painting nano-tips required no prior derivatisation, they were simply painted prior to analysis. The tips were then butted to the separation capillary using a Microtight union (a plastic union designed specially for fused silicas) outside the inlet.

Figure 3.9. Photographs of different nanospray tips. (A) Gold sputter coated and (B) Conductive silver painted drawn silica tips and (C) Internally gold-coated glass micropipette.

Despite the advantage of derivatisation [80], gold sputtered capillaries showed very short lifetime (~1 day), as the gold layer (~0.5|um) sputtered

and peeled off of during operation (Figure 3.9 (A)). On the other hand, silver painted drawn silica capillaries exhibited a stable surface coating and thus long lifetime (3-4 days) due to thick coating layer (estimated width ~20-50μm). However, it easily produced electrical discharges on edges of the rough silver surface (Figure 3.9 (B)), which reduced its analytical performance compared to the gold sputtered tips due to the unstable and poorer ion signals (Figure 3.10 and 3.11). The application of supplementary pressures was restricted by the design of the Ash CE interface.

In an attempt to eliminate the difficulties observed with drawn silica tips, which required the additional capillary connection, internally coated glass micropipettes (commercially available from Teer Coating Ltd, UK.) were also utilised. Although, these micropipettes are designed for direct sample infusion for nanospray set-up, it was decided to take advantage of the possibility of directly fitting the separation capillary into the nanospray tip itself as shown in Figure 3 (C). The clamping of the capillary required great care to avoid breaking out the end. To maintain good electrical contact, the polyimide coating was removed from the end of the capillary and a small amount of the running buffer liquids injected to the Micropipette before inserting the separation capillary into at final position. Although the need for extra capillary connection was eliminated, the application of these tips was found to be more difficult in practice, as insufficient positioning of the separating capillary inside the nano-tip led to buffer backflow into the tip. Supplementary pressure was unsuitable in this case as it made this backflow even worse. Thus repositioning the capillary and nanotip was often required. If correct set up was obtained and left undisturbed very good signals were achieved (figure 3.12.). However, the overall lifetime of the micropipettes was only similar to gold sputtered drawn capillaries (<1 day). This was not unexpected as these micropipettes were designed as disposable nanotips for direct sample infusion.

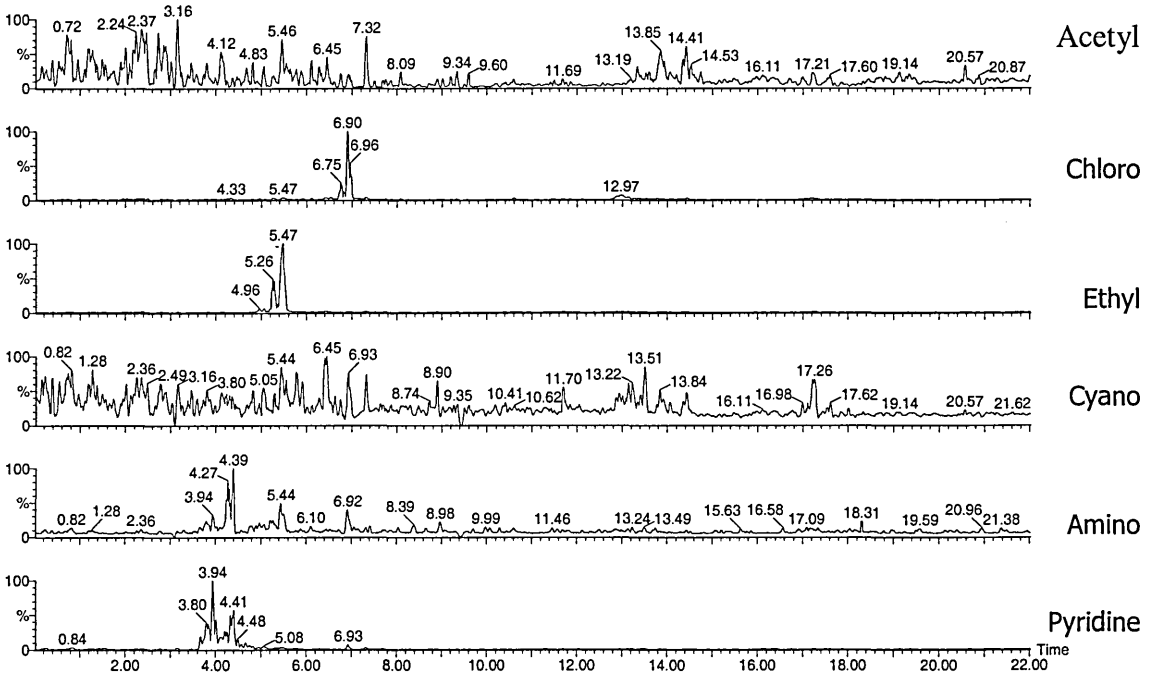

Figure 3.10. CZE-MS mass chromatogram. Gold coated drawn capillary interface. 75cm silica capillary (ID 50μ). Voltage (CE) 30kV, (tip) 3.5kV, (cone) 25V. Sample 10μg/ml 3-pyridine mixture. (35pg injected, 25mbar 0.1min)

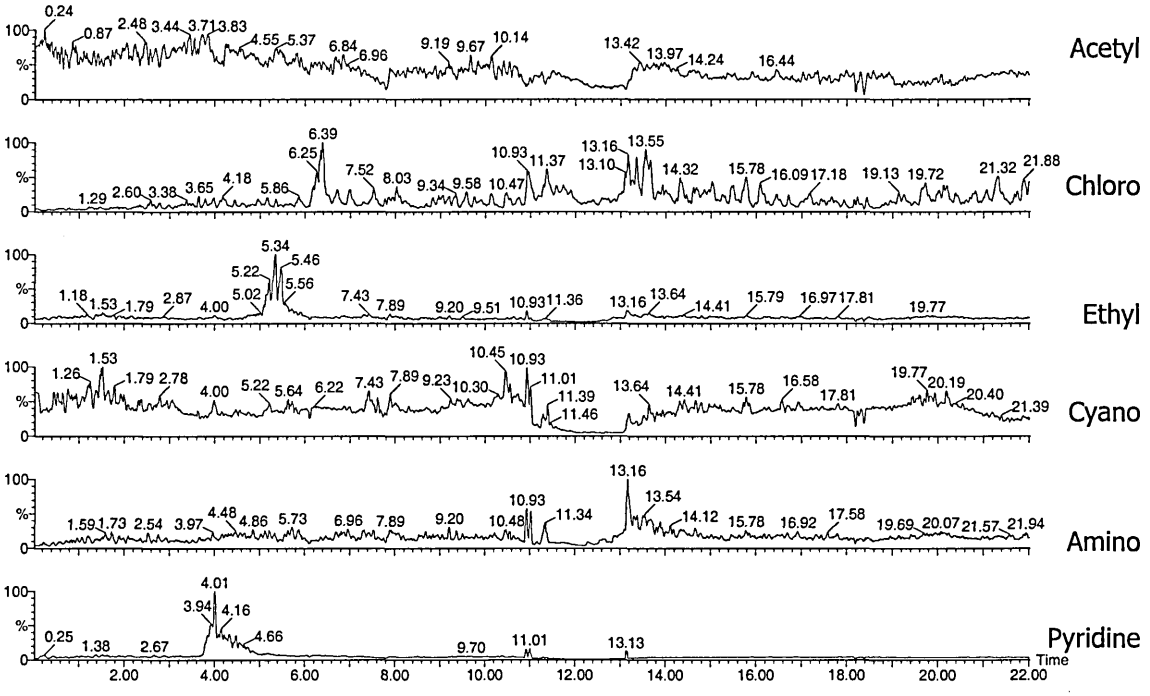

Figure 3.11. CZE-MS mass chromatogram. Silver painted drawn capillary interface. 75cm silica capillary (ID 50μ). Voltage (CE) 30kV, (tip) 3.5kV, (cone) 25V. Sample 10μg/ml 3-pyridine mixture. (35pg injected, 25mbar 0.1min)

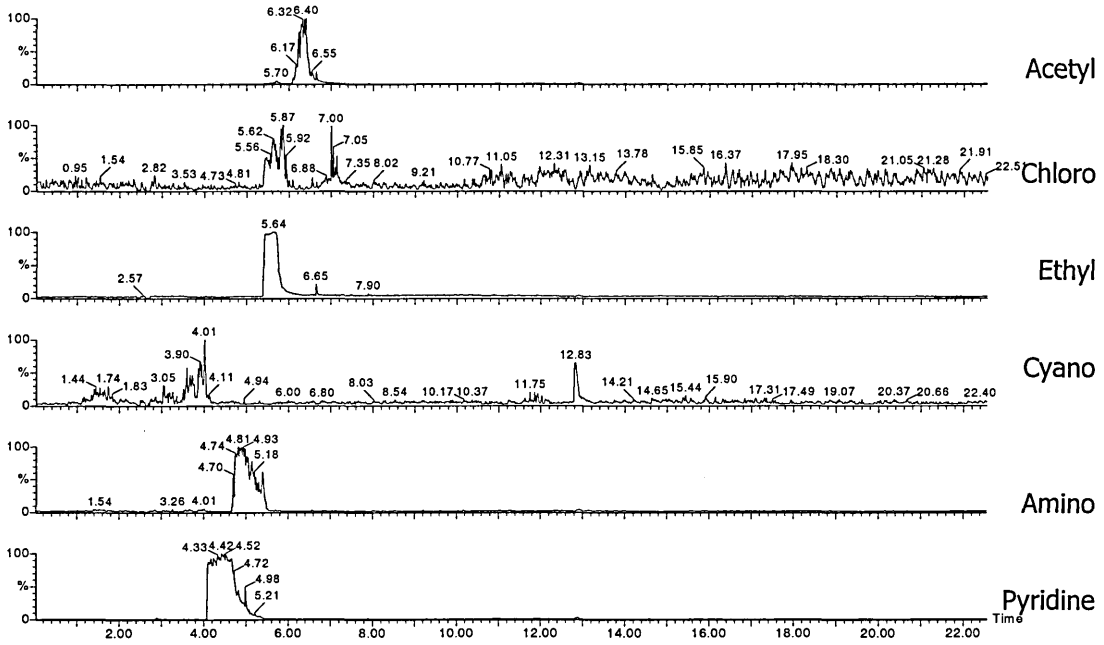

Figure 3.12. CZE-MS mass chromatogram. Micropipette (internally coated) capillary interface. 75cm silica capillary (ID 50μ). Voltage (CE) 30kV, (tip) 3.5kV, (cone) 25V. Sample 10μg/ml 3-pyridine mixture. (35pg injected, 25mbar 0.1min)

3.6.3 Conclusion

Four different tips have been investigated, for sheathless CE-MS analysis. Substituted pyridine solutes have been separated and detected using CZE-Nanospray-MS. Initial set-ups were found to be generally difficult and time-consuming. The stainless steel unions and tips were simple to use, however no results were obtained due to bubble formation and severe electrical discharges and had to be replaced by plastic union and silica tips. The best tips were commercially available Micropipettes, which required no extra capillary connection, but extreme care had be taken for internal positioning of the separating capillary.

The overall results indicated that sheathless set-ups for a MS instrument, which is not designed and dedicated for Nanospray application, were unreliable. It was difficult to manufacture a good spray tip and obtain sufficient electrical connectivity for CE coupling which resulted in poor signal

detection and non-reproducible elution times. It was concluded, that sheathless CE-MS coupling techniques required significant development, which was not part of the aims of this thesis. Thus, the further work in this study was carried out using the coaxial sheath liquid interface.

3.7 Summary

The high separation efficiency of CE makes it an attractive technique for the separation of complex mixtures, but its low concentration limits of detection are still a major drawback [31]. The selectivity of the MS may compensate for the lack of resolution and separation of non-resolved compounds achieved through HPLC and CE.

Although, initial work were based on CFFAB ionisation this has been superseded by ESI, due to its generality and ease of use. Up-to present most CE-MS work has used quadrupole analysers due to their widespread availability and the tandem MS possibility.

Most reported applications use co-axial CE-MS coupling due to its simple and reproducible construction. Sensitivity problems, due to sample dilution by the sheath liquid, can generally be solved by application of different pre-concentration methods [7, 81] which are known and available in CE. Another possible solution to this problem is the use of nano-ESI/MS coupling. Although, the search for robust, mechanically stable nanotips with long-life coatings is still in progress. The availability of commercial tips reflects the increase of research performed with this coupling.

However, recent trends in analytical chemistry in miniaturisation [82], sub-attomole detections, analyses of minute sample volumes, in-vivo/in cell and biological analyses and proteomic analysis [83] all suggest that there may be a rapid increase in CE-MS development and applications in the future due to the potential of this technique.

References

1 Olivares J.A., Nguyen N.T., Yonker C.R. and Smith R.D.; *Anal. Chem* 59 (1987) 1230

2 Cai J. and Henion J.; *J. Chrom. A.* 703 (1995) 667

3 Ding J., Vouros P.; *Anal. Chem. News & Features.* (1999) 378A

4 von Brocke A., Nicholson G., Bayer E.; *Electrophoresis* 22 (2001) 1251

5 Aguilar C., Hofte A.J.P., Tjaden U.R., Van Der Greef J; *J. Chrom. A.* 926 (2001) 57

6 Thompson T.J.,Foret F.,Vouros P., Karger B.L.; *Anal. Chem.* 65 (1993) 900

7 Palmer M.E., Smith R.F., Chambers K., Tetler L.W.; *Rapid Comm. Mass Spectrom.* 15 (2001) 224

8 Heitmeier S. and Blaschke G.; *J. Chrom. B.* 721. (1999) 93

9 Chen Y.R., Wen K.C., Her G.R.; *J. Chrom. A.* 866 (2000) 273

10 Lazar I.M. and Lee M.L.; *J. Microcol. Sep.* 11 (1999) 117

11 Tsai C.Y., Chen Y.R., Her G.R.; *J. Chrom.* A. 813 (1998) 379

12 Varesio E.,Cherkaoui S. and Veuthey J.L.;*J. High Res. Chrom.* 21 (1998) 653

13 Stöckigt J., Sheludko Y., Unger M., Gerasimenko I., Warzecha H., Stöckigt D.; *J. Chrom. A.* 967 (2002) 85.

14 Ramseier A., Siethoff C., Caslavaska J., Thormann W.; *Electrophoresis.* 21 (2000) 380

15 Perkins J. R. and Tomer K. B.; *Anal. Chem.* 66 (1994) 2835

16 Henion J.D., Mordehai S.A, and Cai J.; *Anal. Chem.* 66 (1994) 2103

17 Hofstadler S.A., Wahl J.H., Bakhtiar R., Anderson G.A., Bruce J.E. and Smith R.D.; *J. Am. Soc. Mass Spectrom..* 5 (1994) 894

18 Thomlinson A.J., Benson L.M., Johnson K.L. and Naylor S.; *J. Chrom.* 621 (1993) 239

19 Takada Y., Otsuka K. and Terabe S.; *J. of Pharma. Biomed. Analysis* 30 (2003) 1889

20 Caprioli R.M., Moore W.T., Martin M., DaGue B.B., Wilson K. and Moring S.; *J. Chrom.* 480 (1989) 247

21 Chang S.Y. and Yeung E.S.; *Anal. Chem.* 69 (1997) 2251

22 Zhang H. and Caprioli R. M.; *J. Mass Spectrom.* 31 (1996) 1039

23 Lee E.D.; Mück W.; Henion J.D. and Covey T.R.; *Biomed. Environ. Mass Spectrom.* 18 (1989) 844

24 Wachs T; Sheppard RL; Henion J. *J. Chrom. B.* 685 (1996) 335

25 Jussila M., Sinervo K., Porras S.P. and Riekkola M.L.; *Electrophoresis* 21 (2000) 3311

26 Pleasance S., Thibault P. and Kelly J. J.; *Chrom.* 591 (1992) 325

27 Choudhary G., Apffel A., Yin H. and Hancock W.; *J. Chrom. A.* 887 (2000) 85

28 Smith R.D., Barinaga C.J. and Udseth H.R.;*Anal.Chem.* 60 (1988) 1948

29 Tetler, L. W., Cooper, P. A. and Powell, B. *J. Chrom.* A 700 (1995) 21

30 Palmer M.E., Tetler L.W. and Wilson I.D.; *Rapid Comm. Mass Spectrom.* 14 (2000) 808

31 Tomer K.B.; *Chem. Rev. Am. Chem. Soc.* 101 (2001) 297

32 Nú Eez O., Moyano E. and Galceran M.T.; *J. Chrom. A* 974 (2002) 243

33 Kebarle, P.; *J. Mass Spectrom.* 35 (2000) 804

34 Soga T. and Heiger D.; *Anal. Chem.* 72 (2000) 1236

35 Foret F., Thompson T.J., Vouros P., Karger B.L., Gebauer P. and Bocek P.; *Anal. Chem.* 66 (1994) 4450

36 Lazar I.M., Lee E.D., Rockwood A.L. and Lee M.L.; *J. Chrom. A* 829 (1998) 279

37 Hau J. and Roberts M.; *Anal. Chem.* 71 (1999) 3977

38 Lausecker B., Hopfgartner G. and Hesse M.; *J. Chrom. B.* 718 (1998) 1

39 Van Berkel G.J., Zhou F. and Aronson J. T.; *Int. J. Mass Spectrom Ion Process.* 162 (1997) 55

40 Smith R. D., Udseth H. R., Barinaga C. J. and Edmonds C. G.; *J. Chrom.* 559 (1991) 197

41 Moseley M.A., Deterding L, Tomer K.B and Jorgenson J.W.; *Anal. Chem.* 63 (1991) 109

42 Siethoff C., Nigge W. and Linscheid M. ; *Anal. Chem.* 70 (1998) 1357.

43 Banks J.F.; *J. Chrom. A* 712 (1995) 245

44 Moseley M.A., Jorgenson J.W., Shabanowitz J., Hunt D.F. and Tomer K.B.; *J. Am. Soc. Mass Spectrom.* 3 (1992) 289

45 Schramel O., Michalke B. and Kettrup A.; *Fresen. J. Anal. Chem.* 363 (1999) 452

46 Feng H.T., Yuan L.L., and Li S.F.Y.; *J. Chrom.* A 1014 (2003) 83

47 Larsson M., Sundberg R. and Folesstad S.;*J. Chrom.* A 934 (2001) 75

48 Banks J.F.; *Electrophoresis* 18 (1997) 2255

49 Smyth W. F.; *TrAC.* 18 (1999) 335

50 Jauregui O., Moyano E. and Galceran M.T.;*J. Chrom. A* 896 (2000) 125

51 Henion J.D., Mordehai A.V. and Cai, J.; *Anal. Chem.* 66 (1994) 2103

52 Wilm M. and Mann M.; *Anal. Chem.* 68 (1996) 1

53 Wahl J.H. and Smith R.D.; *J. Cap. Elec.* 1 (1994) 62

54 Moini M.; *Anal. Bioanal. Chem.* 373 (2002) 466.

55 Bateman K.P., White R.L., and Thibault P.; *Rapid Comm. Mass Spectrom.* 11 (1997) 307

56 Hsieh F, Baronas E, Muir C. and Martin SA.; *Rapid Comm. Mass Spectrom.* 13 (1999) 67

57 Chen Y.R., Tseng M.C., Chang Y.Z. and Her G.R.; *Anal. Chem.* 75 (2003) 503

58 Fang L; Zhang R; Willaims ER; Zare RN.; *Anal. Chem.* 66 (1994) 3696

59 Cao P. and Moini M.; *J. Am. Soc. Mass Spectrom.* 8 (1997) 561

60 Kelly J. F., Ramaley L. and Thibault P.; *Anal. Chem.* 69 (1997) 51

61 Chang Y.Z., Yet R.C., and Her G.R. ; *Anal. Chem.* 73 (2001) 5083

62 Kriger M.S., Cook K.D., and Ramsey R.S.; *Anal. Chem.* 67 (1995) 385

63 Valaskovic G.A., and McLafferty F.W.; *J. of Am. Soc. Mass Spectrom.* 7 (1996) 1270

64 Barnidge D. R., Nilsson S., Markides K. E., Rapp H. and Hjort K.; *Rapid Comm. Mass Spectrom.* 13 (1999) 994

65 Maziarz E.P., Lorenz S.A., White T.P., and Wood T.D.; *J. Am. Soc. Mass Spectrom.* 11 (2000) 659

66 Wetterhall M., Nilsson S., Markides K.E., and Bergquist J. ; *Anal. Chem.* 74 (2002) 239

67 Gordon DB., Lord G.A. and Jones D.S.; *Rapid Comm. Mass Spectrom.* 8(1994) 544

68 Verheij E.R., Tjaden U.R., Niessen M.A. and van der Greef J.; *J. Chrom.* 554 (1991) 339

69 Hugener M., Tinke A.P., Niessen W.M.A, Tjaden U.R. and van der Greef J.; *J. Chrom.* 647 (1993) 375

70 Schmeer K., Behnke B. and Bayer E.; *Anal. Chem.* 67 (1995) 3656

71 Lane S.J., Boughtflower R., Paterson C. and Morris M.; *Rapid Comm. Mass Spectrom.* 9 (1995) 1283

72 Steiner F. and Scherer B.; *J. Chrom.* 887 (2000) 55

73 Ding J. and Vouros P.; *Anal. Chem.* 69 (1997) 379

74 Taylor M.R., Teale P., Westwood S.A. and Perrett D.; *Anal Chem.* 69 (1997) 2554

75 Lord G.A., Gordon D.B., Myers P. and King B.W.; *J. Chrom.* 768 (1997) 9

76 Rapp E. and Bayer E.; *J. Chrom. A.* 887 (2000) 367

77 Rathore A.S., and Horváth Cs.; Anal. Chem. 70 (1998) 3069

78 Herring C.J. and Qin J. *Rapid Comm. Mass Spectrom..* 13 (1999) 1

79 Jones R.C., Ferro M., Summerfield S.G., and Gaskell S.J.*; J. Mass Spectrom.* 33 (1998) 1261

80 Kriger M.S., Cook K.D. and Ramsey R.S.; *Anal. Chem.* 67 (1995) 385

81 Baidoo E.K, Clench R.M., Smith R.F. and Tetler L.W.; *in press*

82 Tachibana Y., Otsuka K., Terabe S., Arai A., Suzuki K. and Nakamura S.; *J. Chrom. A.* 1011 (2003) 181

83 Wittke S., Fliser D., Haubitz M., Bartel S., Krebs R., Hausadel F., Hilmann M., Golovko I., Koester P., Haller H., Kaiser T., Mischak H. and Weissinger E.M.; *J. Chrom. A.* 1013 (2003) 173

CHAPTER 4

Examination of C_{18} stationary phases for the capillary electrochromatographic separation of acidic, neutral and basic compounds.

4 Examination of stationary phases

4.1 Introduction

Today more than 600 different stationary phases (of which more than 80% are reverse phase) are available [1] for liquid chromatography. Differences are found both between similar phases supplied by different manufacturers and also between batches of the same phase. Stationary phases used in capillary electrochromatography (CEC) [2,3,4] have a special importance because they both participate in the separation via the classical partitioning mechanism and also contribute to the mechanism by which liquid is transported through the capillary system. The flow of the mobile phase, called the electroosmotic flow (EOF), is a result of the effect of the high voltage across the capillary, on the solution double layer at the silica surface, which is generated by deprotonated silanol groups [5,6,7,8]. Thus characterisation of the stationary phases is even more important in CEC than in HPLC. This could provide information that allows the choice of the optimum stationary phase for the required applications. Although the enormous variety of commercially available stationary phases provides great possibilities for solving various analytical problems, it may also limit the transfer of developed methods between them. This is because they may have different chromatographic performance. However, there is no general database or universal characterisation test [1], which might enable this to be predicted. Hence the evaluation of these phases is important.

4.2 Silica-based stationary phase particles

Stationary phase particles consist of a support media and a thin layer of bonded organic adsorbent. Although other support materials exist (*i.e.* alumina, porous graphitic carbon and polystyrene-divinylbenzene), silica gel is the most extensively used. This is due to the high efficiency and mechanical strength it provides over any other material used in chromatography, along with the relative ease of its functionalisation.

Two types of silica are produced depending on the manufacturing procedure. Each has different physical and chromatographic properties. Particles made by precipitation of soluble silicates, called sil-gels or xerogels, have higher surface areas, higher porosities and irregular pore shapes with variable wall thickness. Particles made by aggregating silica-sol particles, called sol-gel silicas, have lower surface areas, lower porosities and more regular pores with thicker walls defined by surrounding silica-sol micro particles [9]. A comparison of stationary phases prepared by both procedures showed that phases prepared from sol-gel silicas are more durable than xerogel silicas [10]. Further classification exists among older, less pure silicas called A type and newer, highly purified so called B type silicas. The newer phases are less acidic than the A types, give better peak shape and efficiencies and are useful for ionisable compounds, especially basic analytes.

Silica also has its disadvantages. The main limitation of silica is its restricted pH range (pH 2-8), due to the rapid solubility of the silica above pH 9, and especially the cleavage and hydrolysis of the siloxane (Si-O-Si) bond through which the stationary phase is bonded to the support. However, intensive studies by Kirkland *et al.* [9,11,12] showed that the pH stability of ODS silica is influenced by the nature and concentration of the buffer salt as well as the nature of the organic solvent in the mobile phase, by the presence of metal impurities in the silica and by temperature. With appropriate conditions such as low temperature, low concentration of organic buffers and the use of acetonitrile rather than methanol in the mobile phase, densely bound silica, which contains metal impurities, is stable towards high pH. To improve the stability of silica-based stationary phases several modifications of stationary phase bonding have been reported. Polymer encapsulation [13] and horizontal polymerisation [14] were found to provide higher stability towards high pH, while bidentate stationary phases have shown [15] greater stability than monofunctional stationary phases at all pH.

A further problem arises from the activity of the residual silanols on the silica surface towards basic compounds. This can cause serious peak tailing and irreversible sample retention. It was established in HPLC long ago, that free silanol groups on the surface of the stationary phases influence the separation [16,17,18,19].

Amorphous silica can have three kinds of residual silanols [20] on the surface: free (isolated) silanols, geminal silanols (where two hydroxyl groups are bonded to silica) and vicinal silanols (when neighbouring silanol groups are associated with each other by secondary hydrogen bonds). These are shown in Figure 4.1.

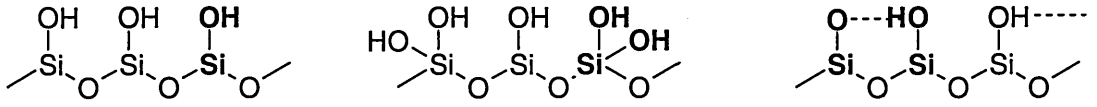

Figure 4.1. Different types of silanol groups on the hydrated silica surface

The concentration of surface silanols on a fully hydroxylated surface is approximately 8 μmol/m^2 (4.8 Si-OH/nm^2). Bonding the silica with the smallest C_1 ligand (trimethyl) results in the reaction of only about 51% of the silanols, due to steric hindrance effects among the alkyl chains. As is expected, this value decreases rapidly with the size of the ligand (*i.e.* the reaction percentage of the silanols with C_{18} dimethyl silane is 34-42% and with C_{18} diisopropyl silane 25-27%) [21,22]. Thus all bonded phases contain a range of residual silanols (about 4 μmol/m^2), which give rise to a range of chromatographic effects. However, these residual silanols have different interaction effects. The geminal and vicinal silanols are less acidic than free silanols and consequently they interact much less with the analyte [20]. Free silanols are able to interact strongly with basic compounds and are responsible for undesired ion-exchange interactions in reverse phase chromatography. The concentration of free silanols on the silica surface is estimated to be less than 1% of the total amount of residual silanols [20].

Several ways of masking unwanted silanols are known, however not all silanol groups on the surface can be reacted because of steric hindrance by the bonded phase ligands. Reduction of silanol activity can be carried out by one of the following methods [20, 23, 24]:

1, ***Endcapping***, which is carried out subsequent to phase bonding, using a small silane such as trimethylchlorosilane (TMCS) or hexa-methyldisilasane (HMDS). The latter modification was shown to be suitable for basic compounds, while the first was appropriate for acidic analytes [25]. Unfortunately, these small end-capped molecules cannot block all residual silanols and can be readily hydrolysed at low pH [21].

2, ***Shielding***. The protection can be steric, by using silane with bulky ligands (*e.g.* diisobutyl or propyl) or electrostatic, using a bonded silane containing amino groups, which may be charged under acidic or neutral conditions. These positive charges, located close to the surface, will repel positively charged samples. Bidentate phases [15] have a similar shielding effect due to their ethylene or propylene bridging groups

3, ***Base deactivation*** or rehydroxylation, which involves heating the silica followed by refluxing it in acid or bases. This will result in a reduction of free silanols and an increase in the amount of bonded silanols on the surface [31].

4, ***Polymerisation*** involves reacting the silica surface using tri-functional silane and alkoxysilane during the stationary phase manufacture forming a Si-O-Si bridging layer parallel to the surface (horizontal polymerisation [14]) or coating with a thin layer of organic silicone polymer with subsequent introduction of long alkyl chains (polymer encapsulation [13]).

5, ***High purity silica*** is used as the base material as certain metal contaminants can complex with chelating solutes, and others (especially aluminium in the silica lattice) affect the acidity of surface

silanols. Metal removal can be achieved by intensive acid treatment of the silica support before bonding the stationary phase ligand [22, 23].

Alternatives for the reduction of ion-exchange interactions include the modification of the mobile phase by adjusting pH [26] and/or the use of anti-tailing or silanol masking additives such as triethylamine or dimethyl-octylamine. Such additives (when $pK_{a\ [additives]} >> pK_{a\ [bases]}$) adsorb strongly on to the surface silanols and consequently reduce their undesired interactions with the analytes. The ion suppression mode can be achieved both at low pH (when $pH < pK_{a\ [silanols]}$) for reducing the ionisation and neutralising the residual silanols or at high pH (when $pH > pK_{a\ [bases]}$) for the basic analytes.

The influence of residual silanol groups and other properties of the stationary phases, such as trace metal content, particle size and shape *etc.*, on separation efficiency has been widely studied in HPLC [27, 28, 29]. Previous studies of HPLC stationary phases have indicated a relationship between "physical" properties, such as carbon loading and surface coverage, and chromatographic properties, such as capacity factor (k), selectivity (α), retention *etc.* [30, 31, 32].

The surface area of the bonded phase is a major factor in chromatographic performance: the larger the surface area the greater the capacity factor. Although the capacity factor of the analytes increases in proportion to the surface area selectivity is however not affected by small differences in the surface area.

The percentage bulk carbon data obtained by elemental analysis gives the overall concentration of carbon in the stationary phase *i.e.* both surface carbon and carbon located in the pores. Since the surface is the place where the most important chromatographic interactions are thought to occur, and some inner pores may be inaccessible to solutes, such data give only

approximate information. Surface specific techniques, such as X-ray Photoelectron Spectroscopy (XPS) and Secondary Ion Mass Spectrometry (SIMS), have been used to obtain complementary information [31]. Brown *et al.* [33] observed significant correlations between capacity factor and alkyl chain length, the C:Si atomic ratio and C% obtained from XPS and SIMS analyses. They confirmed that surface specific techniques generate potentially useful data for the prediction of chromatographic behaviour.

Differences in the physical properties of the "same" columns from different manufacturers, as well as between columns from the same manufacturer, but from different batches, have required the development of general characterisation tests [27,34]. These chromatographic characterisations [35] of different stationary phases can generally be divided into three classes, depending on whether they are based on empirical [26,28,33], retention model (QSRR) [27,36,37] or thermodynamic methods [38,39].

However, there is still no universal or universally accepted test to evaluate chromatographic performances [34].

4.3 Stationary phases in CEC

In CEC, studies have predominantly focussed on the effects of the experimental conditions *e.g.* pH, voltage, ionic strength of the buffer, organic solvent percentage, *etc.* [40,41,42,43] on separation efficiency. The main reason for this is the generation of the crucial transportation mechanism by the stationary phase. Reliable mobile phase flow is required to achieve separation or reproducible results and acceptable analysis times, therefore most investigations have mainly focused on the earlier mentioned parameters, which are the predominant influences on the EOF. The EOF is almost solely derived from the packing particles, as shown by Dittmann *et al.* [44], who used polyvinylalcohol (PVA) coated capillaries to eliminate the possible capillary wall contribution. This was later confirmed by other groups

[6,41,45,46]. The same group investigated [44,47] whether changes in mobile phase composition and stationary phase variations yield the same predictable effects on retention and selectivity in CEC as in HPLC. They employed alkyl parabens and PAH test mixtures with acetonitrile, methanol and tetrahydrofuran organic modifiers and five (Hypersil and Spherisorb) C_{18} stationary phases. It was concluded that the effects of solvent properties on EOF in CEC separations are within certain predictable limits, however changes in the surface properties of the stationary phases are unpredictable, even those induced by changing the mobile phase.

Cikalo *et al.* [43] have carried out studies to compare the open and packed sections of the capillary in CEC. The effects of all the basic parameters on the linear velocities obtained were reported using thiourea and naphthalene test compounds on Spherisorb ODS1 stationary phase. Column conductivity, a largely overlooked parameter, was studied [48] on Spherisorb SCX and C_{18} (ODS1) stationary phases at various pH. Little difference was observed between them at high pH, but several problems were reported at low pH. Studies with various SCX packed sections showed that the linear velocities changed little with the packed length at neutral pH, but at extreme pH the velocity decreased with length. Additionally, Cikalo *et al.* demonstrated [43] that different stationary phases can behave in a similar fashion under the right conditions and that the length of the packed section is likely to be an important parameter. However they also highlighted that there is no adequate explanation for the discrepancies between theoretical and experimental observations.

Previous work on the comparison of stationary phases for CEC has mainly focused on the separation of basic compounds [49,50,51,52,53] since pharmaceuticals are often basic and CE is used widely in the pharmaceutical industry.

The separation of mixtures of basic compounds is often a challenge in chromatography due to the surface adsorption effects described earlier. In this previous work on basic compounds the effect of pH, percentage organic modifier and the use of ion suppressors have been considered. Similar studies on acidic samples have been presented by Euerby *et al.* [54]. The use of amine additives in the CEC separation of bases (which is common practice in LC when non-end-capped stationary phases are used) has been studied by Hilhorst *et al.* [49]. The work showed that the use of amines to mask silanol groups enhanced CEC performance, however the presence of some silanols was vital for the separation.

Separations of acidic compounds are more problematic in CEC due to the similar charge states of the analyte and the silanols. At high pH this could lead to reduced partitioning with the stationary phase due to repulsion from the silanoate groups. Another difficulty arises from the fact that anionic acids tend to migrate towards the anode (out from the detection window) and if the generated EOF is not greater than their electrophoretic mobility they cannot be detected or even electrokinetically loaded into the capillary. This was observed by Huber *et al.* in the gradient CEC separation of some phenylthiohydantoin-amino acids [55]. Application of low pH and ion-suppression conditions [56] can overcome these problems but also leads to long analysis times due to the reduced EOF. The advantage of mixed mode (SCX/C_{18}) phases for faster separation for acidic compounds was first presented by Euerby *et al.* [57]. The number of applications of SAX phases in CEC is much smaller than SCX, but for some acidic compounds has been successfully presented [58,59]. In parallel with the use of mixed and reverse mode phases, recent work has included the development of new packing materials with the specificity and selectivity necessary for the recognition of biologically important substances. Recently, Ohyama *et al.* [60] studied pH effects in the CEC analysis of barbiturates, on a 3-(*N*-substituted)-aminopropyl modified silyl silica gel packed column.

It can be concluded, therefore, that the physical and chemical properties of stationary phases have an even more complex effect on the chromatographic behaviour of packed capillaries in CEC systems than in HPLC. To date, however, studies of CEC separations have mainly focused on theoretical aspects, not practical applications. This is probably because of the difficulty in obtaining fully reproducible and reliable packed CEC columns [63].

4.4 Aims of this work

The experimental work reported in this chapter uses the same approach to stationary phase study as Barrett *et al.* [30-33] and investigates the electrically driven separating behaviour of five commercially available HPLC packing materials for the separation of pharmaceutically relevant weakly basic, non-polar and weakly acidic compounds under CEC conditions. Physical properties of the phases, such as bulk carbon content, surface carbon content and surface area, are related to chromatographic properties, including capacity factor, plate number, electrophoretic mobility and peak asymmetry to investigate the possibility of obtaining a rapid and easier classification than generally used in liquid chromatography.

4.5 Experimental

Apparatus. All experiments were carried out on a Crystal CE System (Prince Technologies, Emmen, The Netherlands) equipped with DAx v6.1 control and data handling software (Prince Technologies) and with an ATI UNICAM 9200 UV/Vis detector (ATI Unicam, Cambridge, UK).

Instrumental analysis. All x-ray photoelectron spectral data for elemental surface analysis were produced on a Kratos Axis-162 instrument (Kratos, Manchester, UK) using aluminium K_α x-rays (E=1486.6 eV). Scanning Electron Microscopic (SEM) images were recorded on a Philips XL40 instrument, with an electron gun operating at 7.5-12.0 kV. X-ray and SEM

analyses were carried out at the Material Research Institute at Sheffield Hallam University. The x-ray gun operated at 15 kV and 5 mA. Samples for XPS analysis were prepared using an indium mirror technique. Bulk carbon data were obtained from elemental analyses carried out by Medac Ltd (Egham, UK)

Chemicals. Test samples of pyridine, biphenyl and barbital derivatives were purchased from Sigma-Aldrich (Dorset, UK). Basic chemical and chromatographic properties of the compounds are shown in Table 4.6.
The solvent used was HPLC grade acetonitrile, purchased from Aldrich (Dorset, UK). All the water used was distilled and then de-ionised (MilliQ grade) prior to the measurements (Millipore, Herts, UK). Chemicals used were HPLC grade ammonium acetate, sodium phosphate, hydrochloric acid and sodium hydroxide (BDH Chemicals Ltd., Dorset, UK).

Chromatography. The C_{18} stationary phases (Xtec, Exsil, Platinum, Hypersil) used in this study were supplied by Prof. P. Myers, University of Leeds. Basic properties of the phases, supplied by the manufacturers, are listed in Table 4.1.
Fused silica capillaries were purchased from Composite Metals Services (Worcester, UK). Capillaries were packed in the laboratory using the slurry packing method [61,62,63] with a Shandon Packer (UK). Frits and the detection windows were formed [61] using a capillary burner (Glaxo-Wellcome, UK). Prior to analysis all packed capillaries were conditioned overnight, by gradually applying voltage (from 2kV to 30kV) across the capillary until a stable current was observed.

CEC parameters and conditions were as follows:

Column	Total length:	75 cm
	Effective length:	60 cm
	Inner diameter:	50 μm
	CEC packed length:	25 cm

CEC separations were performed using an applied voltage of 30 kV at ambient temperature. The test compounds (200 μg/ml) were dissolved in acetonitrile (ACN) and/or water and injected electrokinetically (10 kV for 6 s). The detection was at a wavelength of 205 nm.
The data presented are the average values determined from three consecutive analyses of the given test analytes on the specified stationary phase.

It should be noted, that the chromatographic studies of each test mixture were carried out on new columns, packed with the studied stationary phases to give a uniform packed bed quality, thus results can be standardised. Although, this could be an additional source of variation in the obtained results due to the packing reproducibility (discussed in section 4.7), the practical problems observed during method development resulting in modification of the mobile phases (*i.e.* column dry out) necessitated this approach. The multiple disconnection of the column from the CE instruments and the re-application of high pressure after, were unfavourable as this can change the packed bed quality due to the repeated application of high pressure to the once equilibrated packed bed. This can lead to more compact stationary phase at first, but will also lead to the presence of a void in the packed bed as the particles will reorganise themselves under electric field. As silica particles are negatively charged they try to migrate in the opposite direction to the EOF. The result will be the formation of discontinuities in the stationary phase, whose dead volume reduce the chromatographic performance due to the parabolic flow profile and mixing in the voids (see also in Section 2.5.1.2)

Mobile phases used were as follows:

Basic: ACN-5mM aqueous sodium phosphate buffer (25:75) ; pH=8.0
Neutral: ACN-20mM aqueous TRIS buffer (70:30) ; pH=7.0
Acidic: ACN-5mM aqueous sodium phosphate (40:60) ; pH=3.5

Mobile phases were prepared by mixing an adequate volume of organic solvent and buffer solution, the pH was adjusted by adding an appropriate amount of 0.1M hydrochloric acid, then filtered (0.2μm Acrodisk, UK) and degassed in an ultrasonic bath for 2 min before use. Ammonium acetate and sodium phosphate stock solutions were made by dissolving an appropriate amount in 100mL MilliQ H_2O. These stock solutions were mixed with the appropriate volume of organic solvent to obtain the running buffer.

4.6 Result and Discussion

4.6.1 Physicochemical properties of silica

As chromatographic separations are based on the partitioning of the analyte between the mobile and silica based stationary phase, the characterisation of the silica is very important. Basic information is supplied by the manufacturers, as listed in Table 4.1. These data usually are averages of a number of batches of stationary phases.

Stationary Phase	Pore size [Å]	Pore volume [ml/g]	Surface area [m^2/g]	Surface modification
Exsil 17/339	100	0.51	200	None
Exsil 26/106	100	0.51	200	None
Hypersil 3 ODS	120	0.7	170	Endcapped
Platinum EPS	100	0.51	200	Base deactivated
Xtec ODS 1	80	0.49	200	None

Table 4.1. Column manufacturer's data on the physical properties of stationary phases used in this study

Several methods are available to obtain further information to enable the complete characterisation of the alkyl-bonded silica stationary phases. The oldest and simplest technique was the determination of the bulk carbon

content, by elemental analysis of the stationary phase particles which gives information about the percentage composition of the carbon both on the particle's outer surface and in the pores of the silica (Table 4.2.)

Stationary Phase	Bulk Carbon [%]	Surface carbon [%]
Exsil 17/339	11.62	30.97
Exsil 26/106	10.66	32.52
Hypersil 3 ODS	9.91	28.07
Platinum EPS	4.19	13.41
Xtec ODS 1	6.28	21.40

Table 4.2. Carbon content of a range of stationary phases determined by elemental and XPS analysis (for experimental conditions see section 4.5)

In the case of CEC both the most important chromatographic interactions and the generation of the EOF are thought to occur on the surface of the silica particles. Consequently, determinations were carried out by a surface-specific technique as well, *i.e.* as X-ray photoelectron spectroscopy (XPS). This was also important for crosschecking the unexpectedly high differences in the carbon content between the two batches of the same Exsil stationary phase. These data are shown in Table 4.3.

Stationary Phase	Surface Si [%]	Surface O [%]	Surface O/Si	Surface C [%]
Exsil 17/339	24.02	45.03	1.875	30.97
Exsil 26/106	26.44	41.04	1.552	32.52
Hypersil 3 ODS	24.94	46.98	1.884	28.07
Platinum EPS	28.00	58.59	2.092	13.41
Xtec ODS 1	30.00	48.60	1.62	21.40

Table 4.3. Surface composition data determined by XPS analysis (for experimental conditions see section 4.5)

Using the percentage bulk carbon data and equation 4.1, the bonded phase coverage or bonding density (N) for an ODS (Figure 4.2) stationary phase can be calculated [64]. This gives a better representation of the alkyl moieties available for chromatographic interactions. These data are shown in Table 4.4. These data support the hypothesis that the surface modified phases have less alkyl ligand available for separation. However, the large differences between the bonding densities for the two batches of Exsil were unexpected. This observation already shows the importance of stationary phase characterisation, as it appears that even manufactures of the same stationary phase can be unreliable.

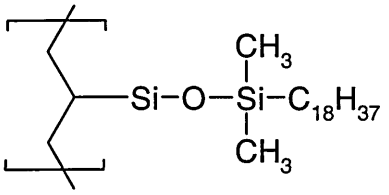

Figure 4.2. Structure of dimethyloctadecylsilyl-bonded silica

$$N = \frac{10^6 P}{(1200n - P(M-1))S} \qquad (4.1)$$

N = bonded phase coverage [μmol/m^2]; P = percentage of bulk carbon; n = the number of carbons in the bonded silane chain (for ODS is 20); M = molecular weight of the silane chain of the substrate (for ODS is 327) in [g/mol]; S = surface area of the non-bonded silica in [m^2/g].

Stationary Phase	Bonded Phase Coverage [μmol/m^2]
Exsil 17/339	2.875
Exsil 26/106	2.597
Hypersil 3 ODS	2.807
Platinum EPS	0.926
Xtec ODS 1	1.430

Table 4.4. Calculated bonded phase coverage values using equation 4.1

4.6.2 Effect of stationary phase chemistry on the EOF

EOF is a consequence of the surface charge predominantly on the stationary phase particles with a negligible contribution from the capillary wall. For (fused) silica surfaces EOF is controlled by the numerous silanol groups (SiOH). The more efficient the bonding the less silanol groups remain free. Therefore the EOF properties of the stationary phases depends upon number of these free silanol groups, the bonded surface coverage and any masking technique used (*e.g.* end-capping). Since in our study all stationary phases were C_{18} with 3μ particle size and the same surface area the observed differences in EOF will be related to the bonding density, and the presence of end-capping.

	μ_{eof} [cm^2/kVs]				
	Xtec	**Exsil 17**	**Exsil 26**	**Hypersil**	**Platinum**
pH=3.5	0.121	0.107	0.121	0.100	0.128
pH=7.0	0.178	0.135	0.190	0.122	0.189
pH=8.0	0.241	0.132	0.118	0.167	0.289

	Si%	**O%**	**RSQ C(s)%**	**C(b)%**	**N[μmol/m^2]**
pH=3.5	0.217	0.441	0.477	0.529	0.683
pH=7.0	0.088	0.278	0.277	0.329	0.467
pH=8.0	0.604	0.808	0.963	0.965	0.900

Table 4.5 Calculated electroosmotic mobilities and correlation coefficients with stationary phase properties. (Mobile phase compositions are shown on page 131)

As expected, separations carried out at high pH showed the highest EOF (Table 4.5). However, each test mixture required a different mobile phase, as no composition was found to give separation for all the three different test mixtures. Thus the electrophoretic information is not directly comparable in the three different cases as the μ_{EOF} of any CEC system is also influenced by the organic content, the buffer concentration and ionic strength of the buffer

in the eluent *etc.* (see Chapter 1.6). Although, the pH is the most crucial factor to determine the generation of EOF.

The EOF results obtained show no correlation with either the surface oxygen or surface silica concentrations. However, there is a significant correlation observed with the bonded phase coverage and/or carbon loading (Figure 4.3). The higher the surface coverage the more compact the "carbon layer" above the silica surface (and thus the shielding of the surface silanols), the lower the generated EOF. This effect was clearly demonstrated by the two different batches of the same Exsil phase where that with the larger amount of surface carbon, and with the lower surface oxygen content, generated the lower EOF.

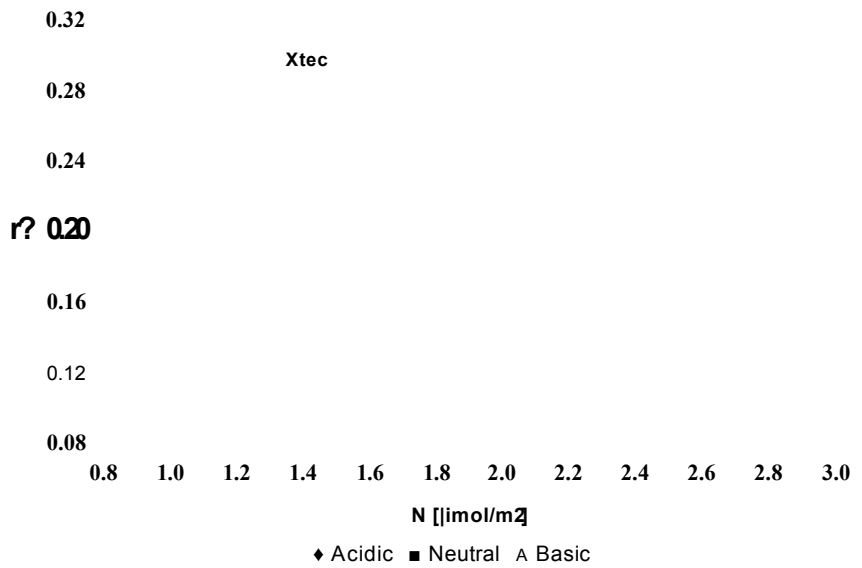

Figure 4.3 Relationship between electroosmotic mobilities and bonded phase coverage (for details see Table 4.4 and 4.5)

This shielding effect was also shown by the fully endcapped Hypersil phase which generated a low EOF. This has also been observed by other groups [65]. Quite the opposite was observed with the base-deactivated Platinum EPS silica, which gave the highest EOF in all cases. The reason for this appears to be related to the manufacture of this phase. The manufacturing

procedure of this phase [66] uses a unique base-deactivation approach. Instead of maximizing the phase coverage of the silica to hide the particle surface, the method controls the exposure of the silica surface, thus providing a dual mode separation medium with both polar and non-polar sites exposed to the sample. This is claimed to extend polar selectivity (hence the name). This method can be clearly seen to lead to significantly lower bonded phase coverage (as well as carbon loading) and higher surface oxygen values for this phase.

Although a clear trend was observed between the physicochemical properties of the stationary phases and the generated EOF, the poor correlation factors, the significant differences in them in relation to the use of mobile phases with higher pH (which mobile phase system gives better correlation) indicates and that the ionisation of the surface by the mobile phase influences more strongly the resultant EOF, than the origin of the silica based stationary phase.

4.6.3 Chromatographic properties

The most direct information for stationary phase characterisation is only provided by chromatographic tests. However, there is no generally accepted characterisation test and there are many different solutes used in many different characterisation tests [67,68,69]. Our test mixtures (Table 4.6) were chosen to model a wide range of different type of samples (also covering wide range of pK_a values) typically analysed by reversed-phase HPLC.

Under electrically driven conditions any charged species take part in electrophoresis according to their electrophoretic migration. To eliminate this simultaneous interfering separation process, as well as reducing ion-exchange interactions with the stationary phase for the favour of

partitioning, ion suppression was used. This was expected to provide clear reversed-phase chromatography.

	Log P		**Log P**	**pK_a**		**Log P**	**pK_a**
4-Acetyl	3.4	3-Amino	0.17	6.10	**Barbital**	0.60	7.43
4-Methoxy	n/a	**Pyridine**	0.60	5.19	Pheno-	1.47	7.49
Biphenyl	3.7	3-Acetyl	0.62	3.30	Butethal	1.60	8.00
4-Methyl	4.2	3-Chloro	1.43	2.84	Amo-	2.01	8.07
4-Bromo	4.6	3-Bromo	1.60	2.84			
4-Ethyl	4.7	3-Ethyl	1.78	5.80			

Table 4.6 Chemical properties of the test compounds used in this study [32].

Therefore, the test compounds were analysed predominantly in their non-ionised form at the appropriate pH (Section 4.2). Although is not the case in this study, it should be noted that this approach could be unfavourable for acidic compounds in CEC if a pH value less than 3 required, due to the reduced EOF generation.

4.6.4 Peak Asymmetry

Peak asymmetry is regarded as a direct indicator of the secondary interactions between the sample and the stationary phase. These interactions are assumed to be caused by the free silanol groups (or silanoate groups under CEC conditions) and to a lesser degree by the metal impurities of the packing material.

Several other factors can, however, also cause peak tailing (*i.e.* sample overloading, buffering problems), thus care in the analytical conditions used is required. But the most important – especially in CEC, where capillary packing is still the major error factor – is the packed bed quality of the stationary phase particles.

The observed peak asymmetry factors were well within the practically acceptable range of 0.95-1.5 (Table 4.7) for most of the test compounds, indicating that the separation was based on reverse-phase partitioning.

A(s)	Xtec	Exsil 17/339	Exsil 26/106	Hypersil	Platinum
Acetyl	1.02	1.10	1.14	1.06	0.84
Methoxy	0.94	1.28	1.08	0.96	0.90
Biphenyl	0.94	1.34	1.16	1.03	0.90
Methyl	1.04	1.24	1.16	1.04	1.02
Bromo	0.91	1.08	1.05	0.98	0.94
Ethyl	0.91	1.37	1.05	1.01	0.94
Barbital	1.22	1.03	1.33	0.99	0.97
Pheno	1.09	0.79	1.07	0.87	0.85
Butethal	1.03	0.96	1.25	0.91	0.94
Amo	0.93	0.99	1.10	0.92	0.91
Amino	1.80	3.39	2.01	3.51	1.64
Acethyl	1.18	1.90	1.98	2.96	1.33
Pyridine	1.39	1.90	1.98	5.37	1.46
Chloro	1.49	1.75	1.59	5.20	1.17
Bromo	1.57	2.46	1.89	2.23	0.88
Ethyl	2.93	2.46	1.89	2.23	1.65

Table 4.7. Asymmetry factors for the test compounds. (For experimental conditions see Section 4.5. For calculation see Section 1.4.6. Representative electropherograms are shown in Appendix II.)

As expected, some basic compounds showed worse peak asymmetries on all stationary phases. These were the ones with high ionisation percentage at the mobile phase pH of 8.0 - such as 3-amino-(11.2%), 3-ethyl pyridine (5.9%) and pyridine (1.56%) - but even the worst obtained asymmetry values (3.51, 2.93 and 5.37 respectively) were much lower than those reported for HPLC separation at the same pH (15.88, 4.27 and 15.56 respectively [32]). Despite the higher organic content in the mobile phase (which is assumed to facilitate access of solutes to the residual silanols by the better solvation of the alkylsilane layer, and therefore degrades reverse phase behaviour towards basic analytes [70]), the better peak shapes

observed demonstrates the advantage of the flat flow profile of CEC over laminar flow in HPLC. These better peak shapes were observed for all stationary phases, a clear indication of this.

Barrett *et al.* [32] reported that the observed A_s values increased with higher bonding density and alkyl-chain length. That is probably because the use of a shorter carbonyl chain can cause better surface/silanol masking. A similar observation was made with the neutral and basic analytes, as their A_s values increased towards higher and bulk and surface C% (thus bonding density). The more densely bonded the silica surface the higher steric interactions expected between the alkyl chains. This can lead to uneven orientation and allocation of the C_{18} chains when interactions in the uncovered areas can be responsible for the peak broadening. However, the acidic analyte mixture showed no correlation with bonding density, which limits the significance of this finding.

The two end-capped stationary phases gave apparently contradictory data for the basic analytes. While Platinum showed good results (although not much better than the unmodified phases), the Hypersil phase exhibited the highest peak tailing. As the reproducibility data (section 4.7) for this phase was not significantly different to that for all other phases, this cannot connected solely to packing problems. Hence, this indicates that the surface modification was insufficient for endcapping in the case of Hypersil.

4.6.5 Efficiency

The first observation was, as expected, that significantly much better efficiencies were obtained by CEC than those typically obtained for HPLC. It was also expected that the neutral system would exhibit the highest efficiency whilst the barbiturates and the pyridines would exhibit similar efficiencies. However the pyridines showed much higher variation between the phases.

It is known that asymmetry and plate numbers are greatly influenced by the quality of the packed bed. This may be the reason for the observation that no meaningful correlation was observed with surface properties of the stationary phase particles. However, some tendency can be observed with surface oxygen content. The acidic system showed greater efficiencies with higher surface oxygen percentage. This may be explainable by the greater repulsion between the solute and the surface analytes, which provides more retention for the acids in the C_{18} layer. The neutral system gave a similar efficiency regardless of the surface oxygen content. On the other hand, pyridines showed very high variation, which could indicate the presence of several secondary effects during the separation.

N	Xtec	Exsil 17/339	Exsil 26/106	Hypersil	Platinum
Acetyl	60593	58642	56065	57519	56635
Methoxy	28676	62633	49730	54511	42586
Biphenyl	28676	61956	49137	50497	42586
Methyl	43045	28200	41810	28180	33671
Bromo	37554	47550	37349	44547	22820
Ethyl	37554	50121	36863	43352	22820
Barbital	34359	33287	33496	52314	56851
Pheno	29969	21150	27329	41375	41612
Butethal	33206	25528	31312	40644	39752
Amo	18559	19587	20439	24023	37335
Amino	36343	16728	23921	29669	25942
Acethyl	47381	32417	16972	14179	56690
Pyridine	34891	10476	9799	3971	38759
Chloro	44722	40243	31833	13548	24989
Bromo	42270	26784	28476	7420	22849
Ethyl	24162	26784	28476	7420	29563

Table 4.8. Plate numbers for the test compounds.(For experimental conditions see Section 4.5. For calculation see Section 1.4.2)

4.6.6 Retention factor

Retention factor in reversed-phase chromatography indicates the hydrophobic or partitioning type interactions with the organic stationary

phase. The surface area of the stationary phase, which is a major factor in determining retention, was therefore kept constant in our study, to enable comparison of different bonding properties.

Higher surface carbon means higher amount of stationary phase for partitioning type interaction by the alkyl-ligands thus results higher retention volume. Thus a linear relationship is expected between the observed retention factors (generally reported by its logarithm) and the surface carbon content and with bonding density. The results of barbital and biphenyl test mixtures were consistent with this prediction. (Table 4.9).

log k	Xtec	Exsil 17/339	Exsil 26/106	Hypersil	Platinum
Acetyl	-0.68	-0.39	-0.44	-0.64	-0.77
Methoxy	-0.60	-0.21	-0.26	-0.45	-0.72
Biphenyl	-0.60	-0.17	-0.21	-0.41	-0.72
Methyl	-0.46	0.00	-0.05	-0.23	-0.64
Bromo	-0.37	0.09	0.05	-0.14	-0.52
Ethyl	-0.37	0.13	0.09	-0.08	-0.52
Barbital	-1.10	-0.96	-1.10	-1.10	-1.22
Pheno	-0.70	-0.52	-0.70	-0.72	-0.89
Butethal	-0.54	-0.38	-0.55	-0.59	-0.80
Amo	-0.40	-0.21	-0.41	-0.44	-0.66
Amino	-1.49	-1.30	-1.22	-1.52	-1.00
Acetyl	-0.95	-1.10	-0.96	-1.10	-0.74
Pyridine	-0.70	-0.70	-0.59	-0.74	-0.54
Chloro	-0.26	-0.03	-0.01	-0.20	-0.17
Bromo	-0.14	0.07	0.09	-0.10	-0.07
Ethyl	0.05	0.07	0.09	-0.10	0.08

Table 4.9. Logarithmic retention factors for the test compounds.
(For calculation see Section 1.4.5, for experimental conditions Section 4.5.)

As expected, the neutral biphenyls provided the most linear relationship with carbon content, (averages of the individual analytes correlation factors of log k - $C_{(s)}$% : R^2=0.993) while acidic (average R^2=0.716) and especially the basic solutes showed minimal correlations (average R^2=0.338). A similar, but

weaker relationship was found with bonding density. These results indicate that the separation of all the neutral solutes are governed by reverse-phase retention only, while the basic solutes showed significant deviation from this, which can indicate secondary interactions.

Hydrophobicity or hydrophobic selectivity (α_{CH2}) was used to measure the selectivity between alkylbenzenes differentiated by specific molecular increments, generally one methylene group. This should provide a measure of the surface coverage of the phase, as selectivity is dependent on the ligand density. Previously several groups have reported good linear correlation with surface properties. Claessens *et al.* [71] compared the hydrophobicity for a range of different test compounds. They found that hydrophobic selectivity data (unlike silanol activities) are generally interchangeable and can be used for column classification. Thus our test compounds were also expected to be appropriate for the generation of information about hydrophobic selectivity.

Using biphenyl as reference, 4-methyl- and ethyl-biphenyl as test compounds, our data agreed with these previous findings. As expected, better correlation was obtained using the ethyl derivative, surface carbon data than with surface coverage (Table 4.10).

	Xtec	**Exsil 17**	**Exsil 26**	**H3**	**Platinum**		
			α			r^2 (BPhC)	r^2 (C(s)%)
Me	1.40	1.47	1.48	1.50	1.21	***0.832***	*0.859*
Et	1.72	2.00	2.03	2.12	1.58	***0.952***	*0.834*

Table 4.10. Hydrophobic selectivities of the different stationary phases and their correlation factor with bonding density and carbon content. (Reference compound was Biphenyl. For calculation see Section 1.4.5.; for stationary phase properties see Table 4.2 and 4.4)

As was expected, Platinum with the lowest carbon content give significantly lower hydrophobicity, while the two batches of the same stationary phase

gave similar selectivity. However, this was unexpected due to the unpredicted differences in their bonding density, which indicates that no simple relationship exists between hydrophobicity and carbon loading. This was also observed in the case of different stationary phases with similar % carbon [71].

Correlation of log P with log k

In an ideal reverse phase stationary material the resolution should correlate with log P (octanol-water partition coefficient) for every compound. Any deviation indicates the occurrence of non-hydrophobic interactions. The neutral and acidic system, showed very strong linear relationships between log k and log P as show in Table 4.11.

	Xtec	Exsil 17	Exsil 26	Hypersil	Platinum
Acidic	0.9824	0.9903	0.9865	0.9875	0.9956
Neutral	0.9910	0.9564	0.9556	0.9570	0.9854
Basic	0.9489	0.9470	0.9459	0.9410	0.9743

Table 4.11 Correlation coefficients obtained from log P vs. log k plots
(For details see Table 4.6 and 4.9)

Retention factor and log k vs. log P data showed that the stationary phases give consistent separation performance in the case of each type of solutes. These results were unexpected. While the base deactivated Platinum column gave the closest performance to be ideal reverse-phase stationary phase, the endcapped Hypersil column showed similar performance to the Exsil columns, which are without surface modification. The Xtec phase showed the least ideal reversed-phased performance. These data were consistent with the obtained asymmetry values, where the Platinum and Xtec presented the two extremities while the other columns gave similar chromatographic performance.

The log P - log k correlation results would also appear to indicate that the test compounds are retained on the stationary phases by primarily hydrophobic, reversed-phase type mechanism, with some secondary interactions present in the separations of basic pyridines. However, the indication of the possible secondary interactions with basic analytes from log P – log k comparison are much less than obtained from C% – log k correlation information. The overall better performance for acidic solutes over the neutral analytes was also unexpected. It may be the result that the other test mixtures contained more solutes, covering wider range of different analytes.

4.6.7 Column selectivity

The selectivity of two columns can be compared by a plot of the logarithmic values of retention factors for the test compound mixtures on each column. If the selectivity of the columns is the same the data points will fall into a straight line with a correlation coefficient of 1. The higher the deviation from the best fit the more different the two columns are. In typical separation conditions, a 2% change in retention factor (or 3% in separation factor, 1 standard deviation) results in 0.2–0.4 units change in resolution. This has a negligible effect on separation [72]. Thus a value of ≥ 0.983 (corresponding to 0.012 log k units of SD) implies equivalent selectivity or interchangeable columns. The obtained correlation coefficients for the three test mixtures are shown in table 4.12.

The results are in agreement with the log P verses log k comparison, however it provides a direct and thus more powerful method for column comparison.

As expected the columns packed with the same silica from different batches, give the same separation efficiency for all the three types of compounds. The base deactivated Platinum phase gave significantly different performance,

which can be clearly seen from these comparisons as well. Table 4.12 also shows that the endcapped Hypersil column has very similar chromatographic separation performance to the Exsil phases. As the physicochemical properties of the Hypersil phase are very similar to Exsil phases (also indicated by the similar EOF obtained), this unexpected result can only be explained by the poor application of the endcapping procedure.

	Xtec	**Exsil 17**	**Exsil 26**	**Hypersil**	**Platinum**
			Neutral test		
Xtec	1				
Exsil 17	0.9591	1			
Exsil 26	0.9598	1.0000	1		
Hypersil	0.9570	0.9996	0.9993	1	
Platinum	0.9661	0.9008	0.9026	0.8994	1
			Acidic test		
Xtec	1				
Exsil 17	0.9998	1			
Exsil 26	1.0000	0.9999	1		
Hypersil	1.0000	0.9999	1.0000	1	
Platinum	0.9985	0.9994	0.9987	0.9988	1
			Basic test		
Xtec	1				
Exsil 17	0.9361	1			
Exsil 26	0.9563	0.9968	1		
Hypersil	0.9777	0.9798	0.9924	1	
Platinum	0.9823	0.9713	0.9774	0.9764	1

Table 4.12 Correlation between log k_A vs. log k_B plots of the different columns.

Similar information can be obtained from the slope value of the same log k_A–log k_B plots, where the higher deviation from unity indicate the higher differences in the chromatographic behaviour between the compared columns. These values are also shown in Table 4.13.

	Xtec	Exsil 17	Exsil 26	Hypersil	Platinum
			Neutral test		
Xtec	1				
Exsil 17	1.4727	1			
Exsil 26	1.5282	1.0373	1		
Hypersil	1.5607	1.0607	1.0224	1	
Platinum	0.7803	0.5011	0.4835	0.4719	1
			Acidic test		
Xtec	1				
Exsil 17	1.0913	1			
Exsil 26	0.9961	0.9125	1		
Hypersil	0.9577	0.8774	0.9614	1	
Platinum	0.7873	0.7216	0.7904	0.8222	1
			Basic test		
Xtec	1				
Exsil 17	1.0222	1			
Exsil 26	0.9641	0.9317	1		
Hypersil	1.0080	0.9551	1.0301	1	
Platinum	0.7155	0.6735	0.7239	0.6998	1

Table 4.13 The slope unit of log k_A vs. log k_B plots of the different columns.

4.7 Column Reproducibility

To better interpret the stationary phase data, the reproducibility of the column packing procedure was studied.

Most of the problems in CEC are associated with the frits (Chapter 2.5.1.1.) as the applications of the packed columns rely on porous but also strong frits. If the frits are over sintered they can be stable, strong but non permeable for liquid flow. If the silica particles not sintered to each other and to the capillary wall the frit cannot hold the stationary phase during the mobile phase flow.

At the beginning of this project several serious problems were experienced with packing, a situation that was only resolved after the application of a new capillary burner, confirming that the source of the problem was indeed the frit formation. This was also studied by comparison of scanning electron microscopic images (SEM) of different frit manufacturing parameters (burning temperature and time) but the discussion of that project is not part of this thesis.

However, packing was still a difficulty throughout out this study, thus similar analysis were also carried out on the frits of the working capillaries used in this study to check the frit making procedure. It was observed in the earlier study, that SEM images can give clear information on the origin of frit failures. Insufficient sintering leads to holes in the frit which make it weak, while application of too long burning and/or too high temperature results in impermeable, blocked frits as clearly shown in Figure 4.4.

However, when the SEM images of frits from the good columns used in this stationary phase study were compared, no significant differences were observed which could be linked to their analytical performances. This is clearly presented in Figure 4.4 C and D where two quite different operational frits are shown. While C represent a "uniform" frit (which was found among the used columns), D (from an earlier column) is quite different in appearance. In that frits sintered particles, which are melted together at their contact points (marked with blue) and thus assure the necessary strength of the frit are presented together with the particles with highly

porous appearance, which are over-molten (marked with red). If they are in majority the frit will be impermeable, but their presence alone does not define frit failure.

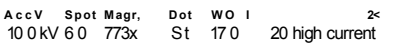

Figure 4.4. SEM images of failed (A - weak, B - over burnt) and operational frits (C-D)

After the investigations of the frits, it was concluded that SEM provided no useful information, as no significant differences were found between the frits, which could have been linked to the performance of the individual columns.

Hence replicate analyses using five columns, packed with the same stationary phase were used to analyse the effect of the packing procedure on the reproducibility of the column's performance. For test analytes the basic

pyridine mixture was chosen since these are the type of compounds where analyte-surface interaction are the most important (as previously discussed). For the same reason, the stationary phase was chosen which was that without surface modification (*i.e.* Xtec). This was to try eliminating other factors that can influence the chromatographic performance of the separation of basic analytes, and thus highlight any packing inconsistency. After conditioning with the appropriate mobile phase the basic mixture was tested on each of the five columns with five consecutive runs. The obtained reproducibility results are shown together in Table 4.14.

A

		Xtec	Exsil 17	Exsil 26	Hypersil	Platinum
A(s)	**Pyridine**	8.8	33.2	48.4	28.8	10.7
N		26.0	6.9	5.0	29.1	8.6
k		7.7	1.4	0.6	7.0	0.1

B

	Xtec	Xtec 1	Xtec 2	Xtec 3	Xtec 4	Xtec 5
A(s)	8.8	5.6	6.3	9.8	18.4	16.5
N	26.0	3.4	16.4	13.8	15.3	3.1
k	7.7	2.2	6.6	6.6	5.3	5.9

Table 4.14. RSD% (n=5) data of chromatographic of the test compounds. (A) Analyses using new columns for each test compounds (B) Replicate analyses on Xtec columns. CEC columns were packed for 20cm of the given 3μm stationary phases particles. Conditions stated in 4.5.

As can be seen the obtained results are generally higher than would be considered acceptable for a robust chromatographic application (RSD should be less than 3% for validated methods). The observed variability between the columns is a clear sign of the packing or conditioning inconsistency, rather than frit manufacture from the SEM results which showed no significant differences among the frits, as described earlier. These problems however are not unreported in the literature, as one of the main drawbacks of this technique is column failure.

Comparison between the different test mixtures showed that the basic compounds gave greater variability (Table 4.15). Although, this is not fully unexpected due to the known possible secondary interactions with pyridine, even when the ion-suppression mode was applied, this and the high variation between the analytical parameters and as well as the different test mixtures, indicates that other factors than packing inconsistency may also be responsible for the observed low reproducibility.

		Xtec	Exsil 17	Exsil 26	Hypersil	Platinum
A(s)	Biphenyl	4.4	1.3	4.6	3.0	2.5
	Barbital	7.4	2.5	5.6	6.6	0.2
	Pyridine	8.8	33.2	48.4	28.8	10.7
N	Biphenyl	10.5	5.8	3.9	2.2	3.1
	Barbital	3.2	4.4	2.2	8.5	1.0
	Pyridine	26.0	6.9	5.0	29.1	8.6
k	Biphenyl	5.8	0.9	0.2	4.6	7.2
	Barbital	1.7	1.4	1.3	1.4	0.3
	Pyridine	7.7	1.4	0.6	7.0	0.1

Table 4.15. RSD% (n=5) data of chromatographic of the compounds from the different test mixtures. Analyses using new columns for each test compounds. CEC columns were packed for 20cm of the given 3μm stationary phases particles. Conditions stated in 4.5.

However, if we calculate the average score of the order (1-5) of the observed standard deviations, the obtained results shows that the base-deactivated Platinum phase gave the best reproducibility, the two batches provide similar variation, while the unmodified phase with the lowest bonding density (Xtec) showed the most variation between the different columns. Surprisingly, the end-capping of the Hypersil phase does not exhibit the expected advantage of the surface modification, it gave similar variations among the separation of the acidic, neutral and basic compounds as the Xtec

phase. The poor end-capping quality of this phase was already highlighted in it very poor analytical performance towards basic analytes.

4.8 Conclusions

The aim of this of this work was to examine the effect of the physicochemical properties of different stationary phases on the CEC separation of neutral, weakly acidic and weakly basic solutes with self-packed CEC columns.

The generation of EOF was influence by the availability of surface silanols as a clear trend was observed with surface carbon and bonded phase coverage properties. The higher correlations with surface carbon and bonding density over surface oxygen content indicates the importance of the availability of the free silanols (which are responsible for the generation of EOF) for the mobile phase ions. The more densely bonded phases can cover, hence shield these silanols, resulting less EOF. However, the better correlations obtained towards higher pH of the mobile phase indicates that the pH effect plays a more significant role in the generation of EOF.

The results showed that the surface coating of the stationary phases governs the retention of the test compounds used in this study. More densely bonded phases give better separation due to the better coverage of the surface, reducing unwanted silanol effects. However, peak asymmetries and column efficiencies show poorer correlations. Asymmetries are also strongly influenced by other parameters such as sample overloading, buffering efficiency, extra column effects and packed bed quality. A reproducibility study carried out with several capillaries packed with the same stationary phase showed that the reason for the poor correlation could be connected to the quality of the packing, while SEM analysis showed that this is not due to frit problems. Although this study used a relatively small number of replicate analyses it highlights that the main disadvantage of CEC is the personal manufacturing of the columns for the applications. However, personal

capillary packing is usually required as only few CEC columns are commercially available (comparison to HPLC columns), which are also generally expensive.

Overall, it can be concluded that no simple relationship was observed with the physicochemical properties. However, these properties of the bonded silica material can give useful preliminary information to distinguish between different stationary phases, highlight the inconsistency among several batches of the same material, but it can be fully utilised only if a reliable packing can be achieved.

References

1 Claessens H.A.; *TrAC.* 20 (2001) 563

2 M. Pursch, LC. Sander; *J. Chrom. A* 887 (2000) 313

3 Liu C.Y.; *Electrophoresis* 22 (2001) 612

4 Jiskra J., Claessens H.A. and Cramers C.A.; *J. Sep. Sci.* 26 (2003) 1305

5 Crego A.L., Gonzales A. and Marina M.L.; *Crit. Rev. Anal. Chem.* 26(4) (1996) 261

6 Cikalo M.G., Bartle K.D., Robinson M.M., Myers P. and Euerby M.R.; *Analyst* 123 (1998) 87R

7 Knox J.H. and Bouughtflower R.; *TrAC* 19, 11 (2000) 643

8 Bartle K.D. and Myers P.; *J. Chrom. A* 916 (2001) 3

9 Kirkland J.J.; *LC-GC* 14 (1996) 486

10 Claessens H.A.; van Straten M.A. and Kirkland J.J.; *J. Chrom. A* 728 (1996) 259

11 Kirkland J.J.; van Straten M.A. and Claessens H.A.; *J. Chrom. A* 691 (1995) 3

12 Kirkland J.J.; *J. Chrom. Sci.* 34 (1996) 309

13 Kobayashi S., Tanaka I., Shirota O., Kanda T. and Ohtsu Y.; *J. Chrom. A* 828 (1998) 75

14 Wirth M.J., and Fatunmbi H.O.; *Anal. Chem.* 65 (1993) 822

15 Kirkland J.J., Adams J.B., van Straten M.A. and Claessens H.A.; *Anal. Chem.* 70 (1998) 4344

16 Bij K.E., Horváth Cs., Melander W.R and Nahum A.; *J. Chrom.* 203 (1981) 65

17 Köhler J. and Kirkland J.J.; *J. Chrom.* 385 (1987) 125

18 Nawrocki J. and Buszewski B.; *J. Chrom.* 449 (1988) 1

19 Cox G.B.; *J. Chrom. A* 656 (1993) 353

20 Nawrocki J.; *J. Chrom. A* 779 (1997) 29

21 Kirkland J.J., Glajch J.L. and Farlee R.D.; *Anal. Chem.* 61 (1989) 2

22 Zhuravlev N.D, Siepmann J.I. and Schure M.R.; *Anal. Chem.* 73 (2001) 4006

23 Nawrocki J.; *Chromatographia*, 31 (1991) 177

24 Nawrocki J.; *Chromatographia,* 31 (1991) 193

25 Lochmüller C.H. and Marshall D.B.; *Anal. Chim. Acta* 142 (1983) 63

26 McCalley D.V.; *J. Chrom. A* 769 (1997) 169

27 Claessens H.A. van Stratena M. A., Cramersa C. A., Jezierskab M. and Buszewski B.; *J. Chrom.* A. 826 (1998) 135

28 Kaliszan R., van Straten M.A., Markuszewski M., Cramers C.A. and Claessens H.A.; *J. Chrom. A* 855 (1999) 455

29 Euerby M.R. and Petersson P.; *J. Chrom. A* 994 (2003) 13

30 Barrett D.A., Brown V.A., Davies M.C. and Shaw P.N.; *Anal. Chem.* 68 (1996) 2170

31 Barrett D.A., Brown V.A., Watson R.C., Davies M.C., Shaw P.N., Ritchie H.J. and Ross P.; *J. Chrom. A* 905 (2001) 69

32 Barrett D.A., Brown V.A., Shaw P.N., Davies M.C., Ritchie H.J. and Ross P., *J. Chrom. Sci.* 34 (1996) 146

33 Brown V.A., Barrett D.A., Shaw P.N., Davies M.C., Ritchie H.J, Ross P., Paul A.J. and Watts J.F.; *Surface and Interface Analysis* 21 (1994) 263

34 Rogers S.D. and Dorsey J.G.; *J. Chrom. A* 892 (2000) 57

35 Claessens H.A; *TrAC* 20(10) (2001) 563

36 Sándi Á and Szepesy L.; *J. Chrom. A* 818 (1998) 1

37 Sándi Á and Szepesy L.; *J. Chrom. A* 818 (1998) 19

38 Cole L.A. and Dorsey J.G.; *Anal. Chem.* 64 (1992) 1317

39 McCalley D.V.; *J. Chrom. A* 902 (2000) 311

40 Asiaie R., Huang X., Farnan D. and Horváth Cs.; *J. Chrom. A* 806 (1998) 251

41 Wen E., Asiaie R. and Horváth Cs.; *J. Chrom. A* 855 (1999) 349

42 Jiskra J., Cramers C.A., Byelik M. and Claessens H.A.; *J. Chrom. A* 862 (1999) 121

43 Cikalo M.G., Bartle K.D. and Myers P.; *J. Chrom. A* 836 (1999) 35

44 Dittmann M. and Rozing G.; *J. Micro Sep.* 9 (1997) 39

45 Rathore A.S. and Horváth Cs.; *Anal. Chem.* 70 (1998) 3271

46 Smith N. and Evans M.B.; *J. Chrom. A* 832 (1999) 41

47 Dittmann M. and Rozing G.; *J. Chrom. A* 744 (1996) 63

48 Cikalo M.G., Bartle K.D. and Myers P.; *J. Chrom. A* 836 (1999) 25

49 Hilhorst M.J., Somsen G.W. and de Jong G.J.; *J. Chrom. A* 872 (2000) 315

50 Dittmann M.M, Masuch K and Rozing G.P.; *J. Chrom. A* 887 (2000) 209

51 Wei W. and Luo G.A.; *J. Chrom. A* 817 (1998) 65

52 Smith N.W.; *J. Chrom. A* 887 (2000) 233

53 MacKillop A.G.; *Anal. Chem.* 71 (1999) 497

54 Euerby M.R., Johnson C.M., Smyth S.F., Gillott N., Barrett D.A. and Shaw P.N.; *J. Microcol. Sep.* 11(4) (1999) 305

55 Huber C.G., Choudhary G. and Horváth Cs.; *Anal. Chem.* 69 (1997) 4429

56 Robson M.M., Cikalo M.G., Myers P., Euerby M.R. and Bartle K.D.; *J. Microcol. Sep.* 9 (1997) 373

57 Euerby M.R., Johnson C.M. and Bartle K.D.; *LC-GC* 16 (1998) 386

58 Zhang J., Huang X., Zhang S., Horváth Cs.; *Anal. Chem.* 72 (2000) 3022

59 Scherer B. and Steiner F.; *J. Chrom. A* 924 (2001) 197

60 Ohyama K., Wada M. Lord G.A., Ohba Y., Fujishita O., Nakashima K., Lim C.K. and Kuroda N.; *Electrophoresis* 25 (2004) 594

61 Paterson C. J., Boughtflower R. J., Higton D. and Palmer E.; *Chromatographia* 46 (1997) 599

62 Angus P.D.A., Demarest C.W., Catalano T., Stobaugh J.F.; *J. Chrom. A.* 887 (2000) 347

63 Colón L.A., Maloney T.D. and Fermier A.M.; *J. Chrom. A* 887 (2000) 43

64 Sandler L.C. and Wise S.A.; *Anal. Chem.* 56 (1984) 504

65 Zimina T.M, Smith R.M. and Myers P. ; *J. Chrom.* 758 (1997) 191

66 Alltech Associates, Inc. *HPLC catalogue* (2003) pp.387

67 Visky D., Heyden Y.V., Iványi T., Baten P., De Beer J., Kovács Zs., Noszál B., Dehouck P., Roets E., Massart D.L. and Hoogmartens J.; *J. Chrom. A* 1012 (2003) 11

68 Sander L.C., Pursch M. and Wise S.A.; *Anal. Chem.* 71 (1999) 4821

69 Gilroy J.J., Dolan D.W. and Snyder L.R.; *J. Chrom. A* 1000 (2003) 757

70 Welsch T., Frank H. and Vigh G.*; J. Chrom.* 506 (1990) 97

71 Claessens H.A., van Straten M.A., Cramers C.A., Jezizrska M. and Buszewski B.; *J. Chrom. A* 826 (1998) 135

72 Lewis J.A., Lommen D.C., Raddatz W.D., Dolan J.W., Snyder L.R., and Molnár I.; *J. Chrom.* 592 (1992) 183

CHAPTER 5

Separation of Anionic Nonylphenol Ethoxylate Type Surfactant Mixtures by Capillary Electrophoresis – Mass Spectrometry

5.1 Introduction

Surfactants are amphiphilic compounds *i.e.* they have both hydrophilic and hydrophobic characteristics. Each molecule has a polar, water soluble end, the so called "head", and a long alkyl-chain, the "tail". The dual structure is the most important characteristic of surfactants. It gives them their ability to change the surface properties of water, forming foams and micelles. In aqueous systems, surfactants tend to accumulate at interfaces *e.g.* solid/liquid, gas/liquid or liquid/liquid interfaces with different polarities and reduce the surface tension. Their name originated from this activity, as a shortening of "*Surface-active agent*".

Because of the characteristic behaviour of surfactants to orient at surfaces and to form micelles, surfactants perform certain basic functions. However, each surfactant can excels in certain functions and has others in which it is deficient. Their special chemical properties are the basis of their numerous, multi-purpose applications such as solubilisation, emulsification, detergency, wetting, dispersing and (de)foaming. Although there is similarity in these functions, in practice the surfactants differ widely. In emulsification, for example - the selection of surfactant or surfactant system will depend on the materials to be used and the properties desired in the end product. Selection of surfactants, orders of addition and relative amounts of the two phases determine the class of emulsion.

Solubilisation is a function closely related to emulsification. As the size of the emulsified droplet becomes smaller, a condition is reached where this droplet and the surfactant micelle are the same size. At this stage, an oil droplet can be pictured as being in solution in the hydrophobic tails of the surfactant and the term solubilisation is used.

The function of cleaning or *detergency* is a complex combination of all the previous functions. The surface to be cleaned and the soil to be removed

must initially be wet and the material such as soils suspended, solubilised, dissolved or separated in some way so that it will not just re-deposit on the surface.

Detergents, which are often confused with surfactants are mixed substances containing surfactants and other components, which improve their performance and stability.

The surface active properties can be adjusted for different purposes by varying the hydrophilic/hydrophobic part of a surfactant and this makes them one of the major groups of industrial organic chemicals.

Surfactants main applications are in household cleaning (laundry, kitchen) and personal care (soaps, shampoos, cosmetics), industry (cleaning, extraction, textile, paper, food) and agriculture (pesticide emulsions and suspensions). These markets, especially household cleaning, are continuously growing. The annual world surfactant and soap production was almost 30 million tonnes in 1996 with a value of over $ 14 billion (excluding soap) and was expected to grow at 3.5% [1-3].

The estimated annual surfactant production in 2000 - which had in fact a continuous 1.6 % growth over the last decade - and the distribution of production in Western Europe are shown in Table 5.1.

These large figures have led to a growing concern about the environmental and human health effects of surfactants. There was particular concern following the work of Jobling and Sumpter [5] who showed that alkylphenol polyethoxylates have oestrogenic effects in nature. The oestrogenic property of alkylphenols were found earlier [6], but only recent research has highlighted these effects [7].

	1000 Tonnes	%	total %
1. Anionics			
LAS	434	43.5	17.5
Alkane sulphonates	75	7.5	3.0
Alcohol sulphates	99	9.9	4.0
Alcohol ethersulphates	305	30.6	12.3
Other anionics	85	8.5	3.4
Total anionics	998	100.0	**40.2**
2. Non-ionics			
Alkylphenol ethoxylates	116	9.4	4.7
Alcohol ethoxylates	747	60.7	30.1
Other ethoxylates	160	13.0	6.4
Amine oxides	14	1.1	0.6
Other nonionics	194	15.8	7.8
Total non-ionics	1231	100.0	**49.6**
3. Cationics			
Esterquats and imidazolinium salts	151	72.9	6.1
Other cationics	56	27.1	2.3
Total cationics	207	100.0	**8.3**
4. Amphoterics			
Betaines	33	70.2	1.3
Imidazolines	5	10.6	0.2
Other amphoterics	9	19.1	0.4
Total amphoterics	47	100.0	**1.9**
Total Surfactant	2483	-	100.0

Table 5.1. Surfactant production in Western Europe in 2000 [4].

Also in 1993 Sharpe and Skakkebaek [8] found a connection between the oestrogenic effect of alkylphenol polyethoxylate and decreasing sperm number in males living in the industrialised world. This led to widespread interest in surfactant determinations in natural and sewage water. A report by Consultants in Environmental Sciences (CES) in 1993, commissioned by the UK Department of the Environment, showed that in 1992 the vast majority, 83%, of UK nonylphenol ethoxylate production ended up in the environment, with 37% in the aquatic media [9]. An obvious cause for

concern. Surfactant elimination from sewage is carried out through a biological process as a result of their biodegradation. In this way 95% of the waste surfactants can be removed. As a result, their biodegradation has been widely studied [10].

5.2 Classification of surfactants

The charge of the polar group is used to classify surfactants as either anionic, cationic, amphoteric or non-ionic compounds (Figure 5.1.)

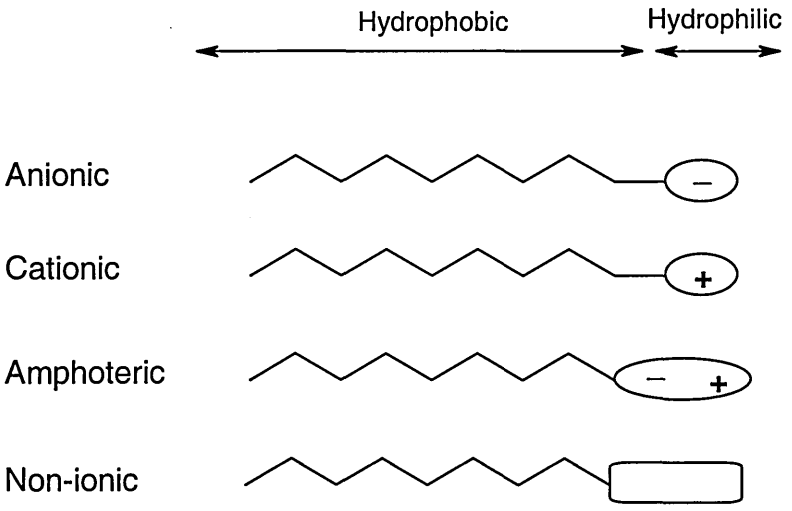

Figure 5.1. Types of surfactants

5.2.1 Anionic surfactants

Anionic surfactants are negatively charged in aqueous solutions due to the presence of a hydrophilic moiety, which can carry a negative charge on, for example, a sulfonate, sulphate, and carboxylate or phosphate group. The associated cations add the water (Na^+, K^+, NH_4^+) and/or oil (alkali earth metal ion, NH_4^+) solubility. They have been used for the longest time among all the surfactants, and soaps have been known since ancient times. However, despite their negative effect on the environment, they are used in large quantities due to their low cost and very good surface active performance. Commercial anionic surfactants are mixtures of homologues

with different alkyl chain lengths. Surfactants with C_{12}-C_{15} alkyl chains have been found to have the best surfactant properties.

Some surfactant groups have different isomers, such as linear alkylbenzenesulphonates (LAS), which give them further complexity and widens their application. The largest volume of anionic surfactants are used in consumer products such as laundry detergents, cleaning and dishwashing agents along with personal care products. Industrial cleaning agents are also an important application of anionic surfactants. By volume, the most produced groups of anionic surfactants are fatty acid soaps, which alone are still the most important group of all the surfactants.

5.2.2 Cationic surfactants

Cationic surfactants are positively charged in aqueous solutions. The hydrophilic part is an amino or quaternary ammonium group. In commercial products mainly the quaternary ammonium compounds are used.

Commercial raw materials are normally derived from natural oils, this leads to surfactants, which are homologous mixtures of compounds with different alkyl chain lengths. In household products, cationic surfactants are primarily used in fabric softeners as they are antistatic. As cationic surfactants have antibacterial activity they are also used as disinfectants and biocides (*e.g.* alkyldimethylbenzylammonium salts (ADMBAX)). By volume, the most important cationic surfactants in household products are the alkyl ester ammonium salts.

Cationic surfactants generally adsorbs strongly to several material (minerals, glass, plastics *etc.*) as they usually have negative surface charge. This ability makes them ideal emulsifiers, as they make the different material surfaces hydrophobic.

5.2.3 Amphoteric surfactants

Surface-active compounds with both acidic and basic properties are called amphoteric surfactants. Amphoteric surfactants include two main groups, *i.e.* amino acid derivatives such as betaines and real amphoteric surfactants based on fatty alkyl imidazolines. The key functional groups in the chemical structures are the quaternized nitrogen and the carboxylic group. Betaines are characterized by a fully quaternized nitrogen atom and do not exist as anions in alkaline solutions. This means that betaines are present only as 'zwitterions'. There is another group of amphoterics called "imidazoline derivatives" because of the formation of an intermediate imidazoline structure during the synthesis. This group contain the real amphoteric surfactants that form cations in acidic solutions, anions in alkaline solutions, and 'zwitterions' in mid-pH range solutions. Amphoteric surfactants are mainly used in personal care products (*e.g.* hair shampoos and conditioners, liquid soaps, and cleansing lotions) due to their mildness and high and stable foaming properties. The total volume of their consumption among the surfactants is relatively small (Chapter 5.1), but is increasing with the demand for milder surfactants. They are also used in mixtures with anionic surfactants to improve their mildness. By volume, the most important groups of amphoteric surfactants today are the of alkylamido and alkyl betaines.

5.2.4 Non-ionic surfactants

These surfactants do not ionise in aqueous solutions. Commercial non-ionic surfactants are normally a mixture of homologous structures composed of alkyl chains that differ in the number of carbons and with hydrophilic moieties the number of ethylene oxide (ethoxylate, EO), propylene oxide (propoxylate, PO) and butylene oxide (butoxylate, BO) units. Non-ionic surfactants are widely used in consumer products *e.g.*, laundry detergents, cleaning and dishwashing agents, and personal care products. Non-ionic surfactants are also widely used in cleaning agents formulated for the

industrial and institutional sector. By volume, the most important non-ionic surfactants are alcohol ethoxylates and alcohol alkoxylates.

5.3 Analysis of surfactants

Several methods for surfactant determination using gas chromatography (GC) and high performance liquid chromatography (HPLC) have been published. These techniques generally offer adequate resolution and speed, although, like all techniques, both have their disadvantages. GC requires the sample to be volatile, HPLC columns have a short lifetime when used for surfactant analysis and both have high mobile phase consumption. Most CE separation of surfactants are still just compared to available LC and GC methods. The increasing number of applications of CE for the separation of different types of surfactants will be reviewed in the following section.

5.3.1 Anionic surfactants

Most CE investigations of surfactants have been concerned with the analysis of anionics, and mainly the linear alkylbenzenesulphonates (LAS). Due to their high world-wide consumption and discharge into wastewater, their environmental effects and degradation has been the subject of extensive investigation [10,11-13].

One of the earliest CE studies used phosphate and borate buffers with acetonitrile (ACN) as the organic modifier [14]. ACN was chosen because it increases the stability of longer alkyl chain LAS and at low concentrations (<40%) its effects on viscosity and EOF are small, resulting in only slight increases in migration times [15,16].

Pietrzyk demonstrated, for both CE [16] and LC [17], that the resolution of complex mixtures of sulfonate and sulphate surfactants can be significantly improved with the use of a high ionic strength mobile phase and an

electrolyte that provides a specific cation such as Mg^{2+} [16]. However addition of metal ions can cause precipitation of long-chain derivatives.

CE has been reported to give poor discrimination between structural isomers within each homologue where the benzene sulfonate ring is at a different carbon position along the alkyl chain.

Detection is often problematic because of the absence of an detector active chromophore in the alkane sulphonates and alkyl sulphates (*e.g.* non-aromatic type surfactants). Indirect detection can provide good detection limits in these cases [16,21]. The earliest CE studies of alkyl sulphonates were carried out by Jandik and Jones [18,19] using indirect UV detection in benzoate and naphthalanesulphonate electrolytes.

Detection sensitivity can be also improved by on-column sample (pre)concentration techniques such as sample stacking. Ding and Liu presented [20] the first application of large volume sample stacking for CE separation of anionic surfactants, where 100-fold enrichments were obtained over general CZE separation.

Cassidy and Salimi-Moosavi [22] compared data from previous studies carried out in aqueous systems with data from non-aqueous systems, and investigated the effect of cation additives. They could detect alkanesulphonates up to C_{10} and alkyl sulphates up to $C_{12\text{-}14}$ in the studied surfactant samples (C_{16} and C_{18} mixtures respectively). The observed sample loss was explained by hydrophobic adsorption of the analytes on the capillary wall and by ion-ion interactions that cause precipitation of the longer chain surfactants. They used methanol as the solvent because its solvating properties were expected to reduce these hydrophobic interactions. Indirect detection at 214 nm with p-toluenesulphonate was applied since it had a mobility close to those of the alkyl sulphates and alkane sulphonates. Their non-aqueous system showed good peak shapes for all of the species,

although the highest efficiencies were obtained using a $MeOH/H_2O$ mixture with different ratios for short and long chain surfactants. The importance of ion pairing effects was demonstrated by the relative change in mobility, and consequently in retention time, with increasing concentration of the studied Ca^{2+} ion. The change was greater for alkane sulphonates, which show a greater tendency for ion pairing than alkyl sulphates.

Shamsi and Danielson [23] have used CE with indirect photometric detection as a complementary technique to reverse phase ion chromatography (RPIC) for the separation and identification of mono- and di-esters of C_1-C_6 aliphatic organophosphates and ethoxylated polyphosphates. CE, with positive polarity configuration, eliminated the interference with inorganic anions (usually Cl^- and F^-) in real samples, since these high mobility ions migrate much slower than the surfactants. This interference cannot be solved in RPIC, where sample pre-treatment is required. They observed 50-500 times better efficiencies for CE when compared to RPIC. The resolution of the CE method for ethoxylated polyphosphates was improved with the use of diethylenetriamine (DETA) as a buffer additive, which worked as an EOF suppressor and reduced possible H-bonding interactions of the phosphates with the silica capillary surface.

Heinig *et al.* [24] presented a full comparison of CE and HPLC methods for the analysis of the most important anionic, cationic and non-ionic surfactants. They concluded that CE has the advantage over HPLC in the case of anionic surfactants, where separation can be achieved without sample preparation. However, the high efficiency of CE could not be achieved for non-ionics, because of their complexity. The detection sensitivity of CE methods is also lower than HPLC due to the very small diameter of the capillaries used (Chapter 1.8.2.1).

The first separation of chiral biodegradation intermediates of LAS in waste waters was published by Giger *et al.* [25], who used a conventional CE

capillary and 20 mM citrate buffer (pH 4.0) containing 60 mM α-cyclodextrin. A detection limit of 1-18μl/L was reported after solid phase extraction on graphitised carbon black and sample stacking.

Riu *et al.* presented [26] and compared a CE-UV/MS method of trace analysis of LAS from coastal and wastewaters to LC-ESI-MS. They found an average 27% difference in the LAS concentrations in the same samples, between the two different separation methods. They concluded that the higher concentrations obtained by CE-UV separation are the result of co-eluting positional isomers of LAS substances.

Desbène and Rony [27] have reported the analysis of an extremely complex industrial anionic surfactant mixture resulting from the sulphonation of oil fractions (WITCO TRS 10-80), using MEKC. They examined the influence of SDS concentration and the ratio and nature of organic co-solvents, such as ACN, 2-propanol, methanol and THF. Despite the longer retention time, due to the organic solvent's lower ε / η ratio (Chapter 1.3 and 1.6.2), 2-propanol was found to be a better co-solvent, with a lower percentage content required to fully separate C_1-C_{16} alkylbenzene homologues compared to acetonitrile.

5.3.2 Cationic surfactants

Despite the fact that CE can be successfully applied in anionic surfactant separation, as discussed earlier, cationic surfactant separations have rarely been investigated by CE. There are two main reasons. Firstly, cationic surfactants tend to strongly adsorb onto the negatively charged inner capillary surface. Secondly, they can form micelles, even at low concentrations, as they have low solubility in pure aqueous systems. The result is severe peak tailing and insufficient resolution.
Several studies on cationic surfactant separation report that the use of organic solvents, *e.g.* as THF [24,28-30], methanol [31], ACN [22] as

electrolyte additives is essential. Of these the use of THF was generally found to give the best resolution and analysis time. The use of ACN was reported to have little effect on EOF and consequently analysis time, in contrast to the use of 2-propanol where the effects were large. However in all cases the use of organic modifiers yielded electropherograms with relatively poor peak resolution. Piera [29] also reported that the use of 50 (v/v)% THF led to current loss across the capillary (although this effect has not been reported by others).

As cationic surfactants generally lack a chromophore, indirect UV detection has been generally used for detection [28,30].

5.3.3 Non-ionic surfactants

Uncharged, non-ionic surfactant samples cannot be separated by simple CE as they have no electrophoretic mobility and will migrate together with the EOF. Therefore additional interactions with buffer constituents are necessary to obtain CE separations.

Ironically, the use of surfactants themselves *e.g.* sodium dodecylsulphate (SDS), can solve the problem of separation of non-ionic surfactants. Micellar electrokinetic chromatography (MEKC) and, less frequently, capillary gel electrophoresis (CGE) are the two techniques which are generally used for this purpose.

While the vast majority of MEKC separations have been performed using the partitioning of neutral samples into and out of the micelles to obtain the separation, structurally similar hydrophobic analytes are difficult to resolve due to their low solubility in water and high partition into the micelles. Organic modifiers (above 20 (v/v)%) added to the running buffer help the solubilization of the analytes and inhibit micelle formation. Under such conditions the different electrophoretic mobilities, on which separation is

based, are the result of hydrophobic interactions between analytes and SDS called solvophobic association [33], according to the principle and separation mode developed by Jorgenson [34].

Heinig *et al.* carried out studies with MEKC analysing alkylphenol type surfactants [24,35] and FAEs and alkyl polyglucosides (APG) mixtures [33]. They demonstrated [24] that the organic solvent content (*e.g.* ACN), required to provide sufficient resolution with SDS, depends on the average ethylene oxide units number. The higher the average EO number in APEO mixtures the lower their hydrophobicity, as their polarity is increased, thus a lower organic solvent content is necessary for their separation.

Wallington [36] demonstrated that the extremely high efficiencies of CGE (which has principally been employed in biological analysis of size-based separation of proteins and nucleic acids) can be applied to non-ionic ethoxylated surfactant separation.

In this technique, the analytes must be derivatized to produce charged species, which results in migration in the electric field according to their electrophoretic mobility. Several simple reactions are available. The most commonly used reagent is phthalic anhydride with imidazole [36,37] in pyridine. 1,2,4-benzenetricarboxilic anhydride (BTA) can also be used which produces more highly charged analytes and thus faster electrophoretic migration. The disadvantage of using BTA is the significantly longer reaction time (5 hours vs. 1 hour) required for derivatization. These reactions provide both the required ionisable group on the analyte molecule and hence the charge, and a good chromophore for direct UV detection (275 nm). The method can also be used for fatty alcohol ethoxylates (FAE).

Comparison of CGE data to previous CZE separations [14,37] indicates that in the case of low molecular weight ionic surfactants, similar resolution can be obtained. However CZE generally provides faster separations and could

yield quantitative data regarding the concentrations of non-ionic/ionic alkyl phenol ethoxylates in the sample. This is not possible with CGE. For high molecular weight surfactants, such as AP40P or PEG 4600, CGE has been shown [36] to provide much higher resolution, compared to CZE and HPLC. The disadvantages of the CGE technique are the long retention times (for example Wallington reported 75 min separation time for AP40P compared to 20 minutes by CZE) , its cost and the UV absorbance of the polyacrylamide gel below 230 nm. This reduces the detection sensitivity for ethoxylates or other type of analytes with absorbance maxima at low wavelengths.

As an alternative to cross-linked polyacrylamide gels, dilute solutions of polymers in the running buffer can be employed to provide the size discrimination in CE separations. Barry *et al.* [38] used 3 (w/w)% dextran and polyethylene oxide solutions in 60mM Tris-Taps running buffer (pH 8.3) to form a UV transparent polymer network for PEG separation, and obtained a successful separation of PEG 2000-4700 in 25 minutes. The separation selectivity and distribution comparison to Maldi TOF-MS separation showed comparable or better results for CE.

5.3.4 Amphoteric surfactants

No work appears to have been published describing the CE separation of alkyl/alkylamido betaine and imidazole type amphoteric surfactants and only a few publication on phospholipids [39]. This is probably due to their low production rate and low present importance amongst surfactants.

5.4 Aims of this work

In the present work capillary electrophoretic separations were investigated for the analysis of industrially important NPEO sulphate (NPEOSp) and sulphonate (NPEOS) anionic surfactants.

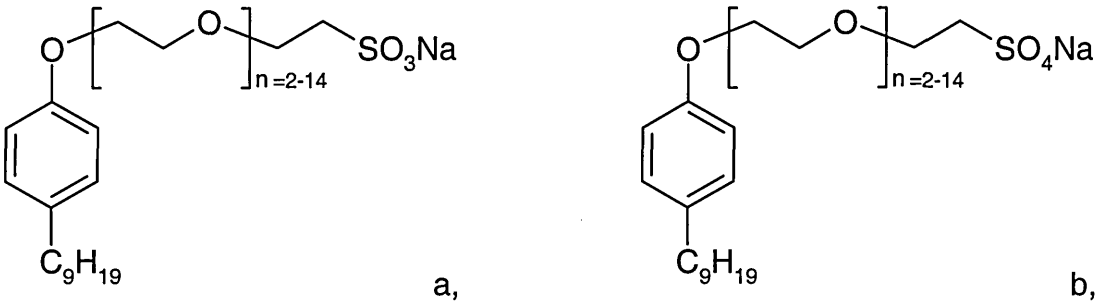

Figure 5.2. Structure of nonylphenyl ethoxy sulphonate (a) and sulphate (b) type surfactants

This was continuation of earlier work carried out in this laboratory, using HPLC [40]. To the best of this author's knowledge, no data on CE or CE-MS separations of NPEO sulphate and sulphonate type surfactants has been published.

5.5 Experimental

5.5.1 Reagents and Materials

A sample of a commercially available NPEOS surfactant manufactured by Hoescht was supplied by Dr. Tor Austad (Rogaland University Centre, Stavanger, Norway), Perlankrol surfactant mixture manufactured by Ackrol Chemicals (Manchester, UK) was purchased from Sigma-Aldrich (Dorset, UK). Solvents used were HPLC grade methanol and acetonitrile and were purchased from Aldrich (Dorset, UK). All the water used was distilled and then de-ionised (MilliQ grade) prior to the measurements (Millipore, Herts, UK). Chemicals used were HPLC grade ammonium acetate and hydrochloric

acid, sodium hydroxide, (BDH Chemicals Ltd., Dorset, UK), uracil and hexadimethrine bromide (HDB) (Sigma-Aldrich, Dorset, UK).

5.5.2 Equipment

All CZE measurements were carried out using a Crystal CE 310 (Prince Technology, The Netherlands) fitted with an ATI UNICAM 9200 UV/Vis detector (ATI Unicam, Cambridge, UK). UV detection was carried out at 205nm, with the signal being recorded with Dax v6.1 data acquisition software (Prince Technology, The Netherlands). Fused silica capillaries (Composite Metals Services, Worcs, UK) of 50μm I.D. and 375μm O.D. were used throughout. The detection windows were formed using a capillary burner (Glaxo-Wellcome, UK).

5.5.3 Sample and Buffer preparation

Ammonium acetate stock solution was made by dissolving an appropriate amount in 100mL MilliQ H_2O. These stock solutions were mixed with the appropriate volume of organic solvent to obtain the running buffer. The pH of the obtained running buffer was adjusted with 1M HCl solution. All surfactant samples were dissolved in MilliQ water.

5.5.4 CE conditions

Column:	Total length:	75cm.
	Effective length:	60cm.
Sample loading:	Hydrodynamic injection:	25mBar for 0.1min
Ramp:		10kV/sec
Run Voltage:		30kV.

5.5.5 Capillary (pre)treatment

All new fused silica capillaries were first washed with 1M NaOH solution (2000mBar, 5 minutes) to obtain a negatively charged inner surface. In reverse-CZE mode the capillaries were washed with 1M HDB solution after the first NaOH wash to coat the inner capillary wall to change the surface charge to positive. In the case of normal-CZE mode, between the measurements a short wash with 0.1M NaOH (2000mbar, 0.5 minutes) was carried out to clean and renew the charge of the inner surface.

5.5.6 Mass Spectrometer conditions

All CZE-MS measurements were carried out using a Quattro I mass spectrometer (Micromass, Manchester, UK), with an electrospray (ESI) source and coaxial ion-probe (Chapter 3). The sheath liquid was introduced by a Harvard Apparatus Model II (Harvard Instruments, USA) syringe driver, using Hamilton gas-tight syringes (Sigma-Aldrich, Dorset, UK) via a stainless steel Valco T-piece union (Sigma-Aldrich, Dorset, UK), as shown in Figure 4.1. The sheath liquid was the same as the running buffer used in CZE separation, and prior to use was thoroughly degassed by ultrasonication. The position of the CE capillary inside the sheath tube and the sheath liquid flow rate were determined experimentally by optimisation of the analyte signal. Additional parameters, such as drying, nebulising gas flow rates and source lenses, were optimised daily before the measurements.

Mass spectral data of deprotonated molecules were acquired in selected ion recording (SIR) mode with a 0.5 amu window across each m/z value using a 0.08s dwell time.

5.6 Results and Discussion

5.6.1 Nonylphenol ethoxylate sulphonates (NPEOS) and sulphates (NPEOSp)

In capillary electrophoretic separation methods, the observed liquid flow (EOF) is highly dependent on the pH of the mobile phase, which necessitates the use of buffer systems, to obtain stable flow and reproducible measurements. To make the CE system compatible with mass spectrometry, the buffer used must meet several requirements, which limit the available buffers. A good buffer for electrospray mass spectrometry, and hence for CE-MS, should be volatile and highly soluble in the organic solvents used (*e.g.* methanol or acetonitrile) since non-volatile buffers (*e.g.* inorganic buffers) contaminate the ion-source producing high background signal. Inorganic buffers, such as phosphate and borate *etc.*, tend to crystallise under the conditions used in mass spectrometry and even relatively low concentrations can block skimmer and nozzle orifices decreasing or destroying sensitivity. Recently developed mass spectrometers use a Z-shaped pathway into the ion source to overcome this problem. However, the VG Quattro-I used in these experiments uses direct entry which is sensitive to source contamination. Unfortunately the number of volatile buffers is small and they cover only a narrow pH range (between 3-6). This greatly reduces the possibilities in CE method development since buffers not only stabilise the pH of the CE system, but also strongly influence the generated EOF and consequently the separation and resolution as well. Ammonium acetate was chosen as the buffer system during these CE studies, as it has several advantages [41] beside its volatility, which make it widely used in MS studies.

Since NPEO sulphonate and sulphate ethoxymers are anionic their "normal" CZE analysis produces long separation times as negative ions have the least mobility towards the cathode at the detector side of the capillary. This also results in broader peaks, as Figure 5.3 shows for an NPEOS sample. The separation is worse than previous HPLC results [40] (Figure 5.6).

For anionic substances, such as NPEOS and NPEOSp, reversing the polarity and the direction of the electroosmotic flow causes sharper peaks with short migration times. Additional modification of the EOF can be achieved by dynamic or permanent modification of the capillary wall (Chapter 1.4), but dynamic coatings are not desirable in CE-MS work as they introduce polymeric modifiers into the running buffer and consequently into the ion source. For this reason, the capillaries were washed with 1M HDB solution for 5 minutes to generate a permanent, positively-charged coating on the capillary wall. This gives a stable and effective coating.

The separations of NPEOS and NPEOSp formulations, obtained using reverse CZE with a MeOH-50mM ammonium acetate (75:25) pH 5.6 buffer system at -30kV are shown in Figures 5.4 and 5.5 respectively.

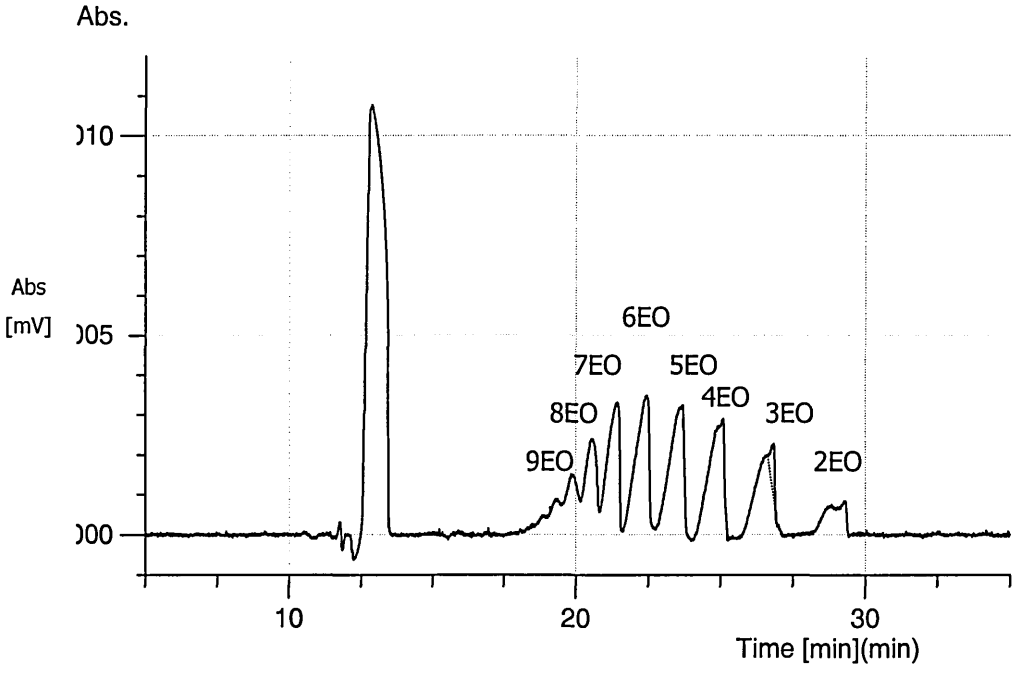

Figure 5.3. Normal mode CZE separation of NPEOS using a 75cm (ID.50μm) silica capillary with a mobile phase of ACN-25mM ammonium acetate (70:30) buffer system at pH=5. Running voltage +30kV. Sample of 49ng in total was injected hydrodynamically by 25mBar for 0.3min and detected by UV absorption at λ=205nm. The broad peaks correspond to the 9EO (t_r = 19.8 min) to 2EO (t_r = 29.3 min) containing oligomers in this electropherogram.

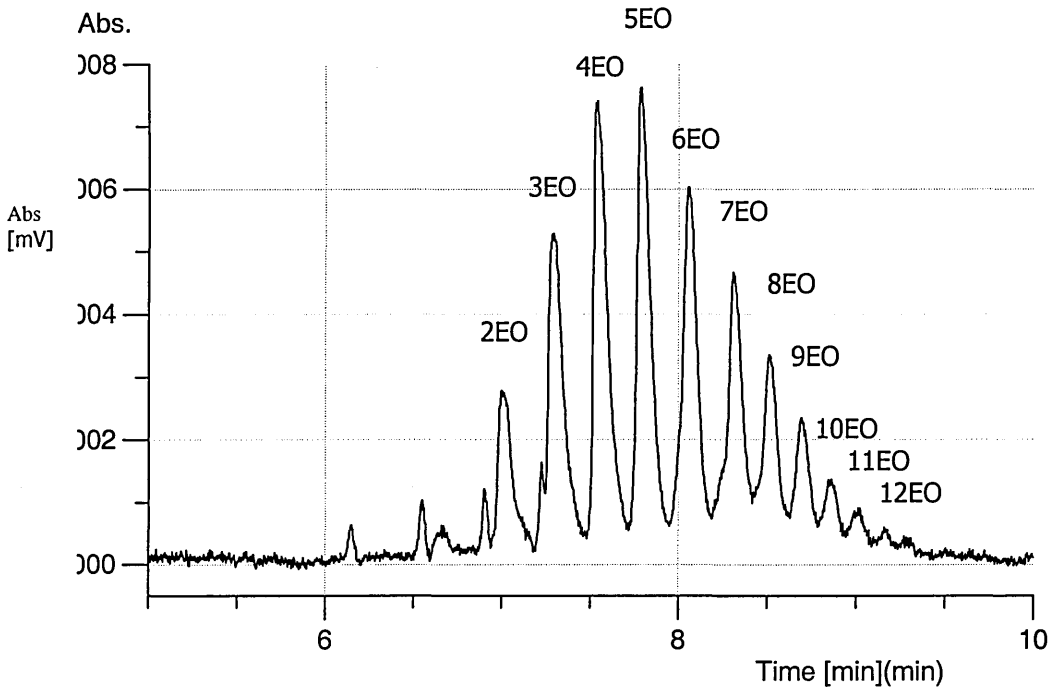

Figure 5.4 Reverse CZE electropherogram of NPEOS employing an HDB coated silica capillary with running voltage –30kV. Other conditions as described in Figure 5.3. The peaks corresponding to the 2 EO (t_r = 6.99 min) to 12 EO (t_r = 9.15 min) containing oligomers are clearly visible in this electropherogram.

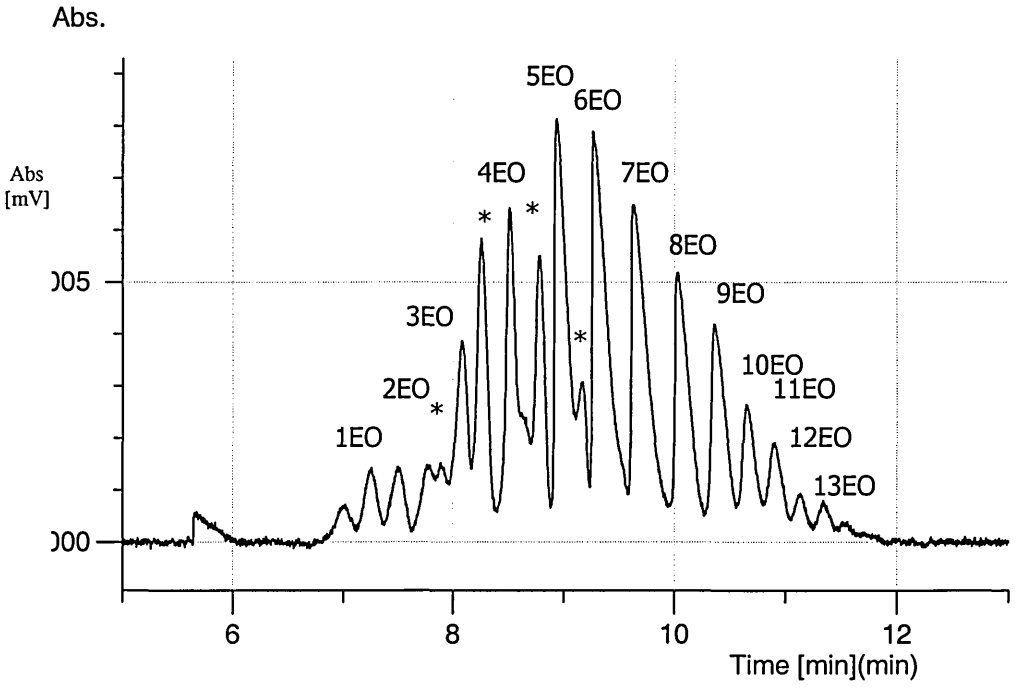

Figure 5.5. Reverse CZE electropherogram of NPEOSp employing a HDB coated silica capillary of 75cm with running voltage –30kV. Other conditions as described in Figure 5.3. The peaks corresponding to the 1 EO (t_r = 7.23 min) to 13 EO (t_r = 11.34 min) containing oligomers and the presence of hydrolytic byproducts (*), are clearly visible in this complex electropherogram.

These electropherograms show excellent resolution for both NPEOS and NPEOSp ethoxymers. This methodology is an improvement on the previously reported mixed-mode HPLC separations for NPEOS [40] (as can be seen from Figure 5.6) and NPEO [42]. It is also in better agreement with earlier studies [43] on the ethoxymer chain length distribution for this particular NPEOS formulation.

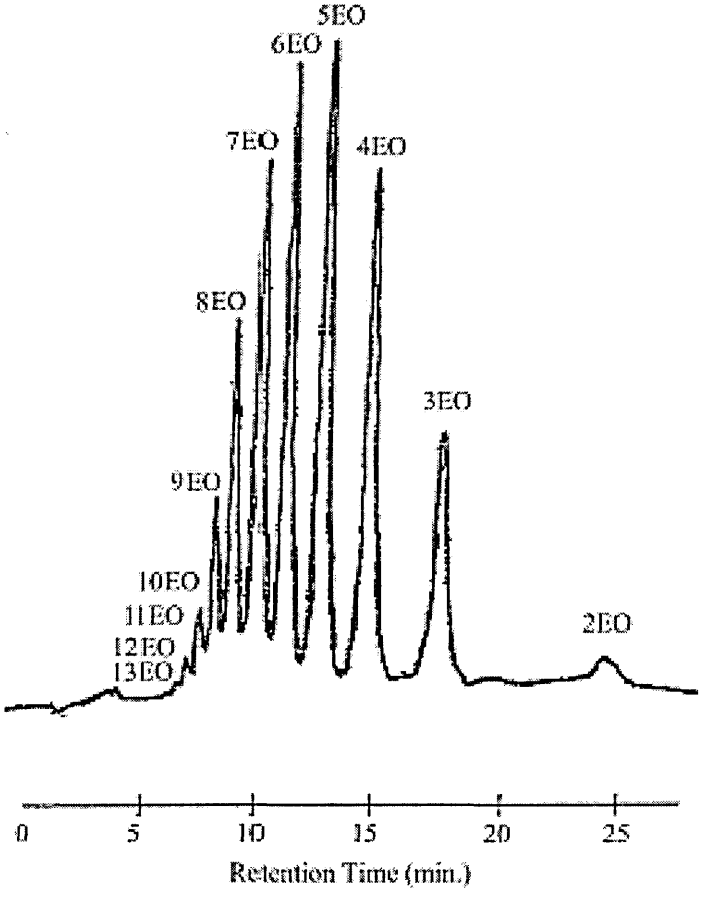

Figure 5.6. A representative chromatogram of reverse phase/mix mode HPLC separation of NPEOS, using a 50cm 5μ C8/SAX column. With permission from [40].

Figure 5.4. shows peaks components containing between 2 and 12 ethoxymer units in the NPEOS formulation migration times between 6.99 and 9.15 minutes.

Figure 5.5. shows the more complex electropherogram obtained from the NPEOSp formulation. This complexity, arises due to the ready hydrolysis of the ethoxy sulphates. They hydrolyse at low pH and with increasing temperature [44]. However, the relatively mild experimental conditions (pH=5.6, T=22ºC) would not fully explain the observed complexity of the mixture.

MS studies have shown that the Perlankrol surfactant mixture contains a distribution of nonylphenol-exthoxy sulphates and wide range of individual ethoxymer sulphates. The retention order of the individual ethoxymers was in high correlation with the fact that their mobilities decrease with the higher ethoxymer unit number and consequently the size of the whole molecule.

The determination of the average number of ethoxymer units or mole ratios of individual exthoxymers is a general way to describe surfactant formulations. These were calculated as weighted average of percentages of individual peak heights or areas (no differences was found between the two data) based on the equation 5.1 where N_i and P_i are the number of ethoxy units and the percentage of the *i*-th ethoxymer's peak height - based on the total peak height equivalent with 100% -, respectively:

$$N_w = \sum \frac{(N_i^2 P_i)}{N_i P_i} \qquad (5.1)$$

The values obtained are 6.46 for NPEOS and 6.45 for NPEO Sulphate. This is in good agreement with the previous results (6.0, 6.46 and 6.32) calculated from LC, LC-MS and MALDI data by Benomar *et al.* [40].

The average number of ethoxymer units calculated from reverse CZE electropherograms (as presented in Figure 5.4-5.5) for the NPEOS and NPEO Sulphate surfactant mixtures are shown in Figure 5.7 and 5.8 respectively.

It must be stated, that this calculation is a general way to compare data obtained with different analytical techniques, rather than a method to determine accurate mole ratios of individual ethoxymers.

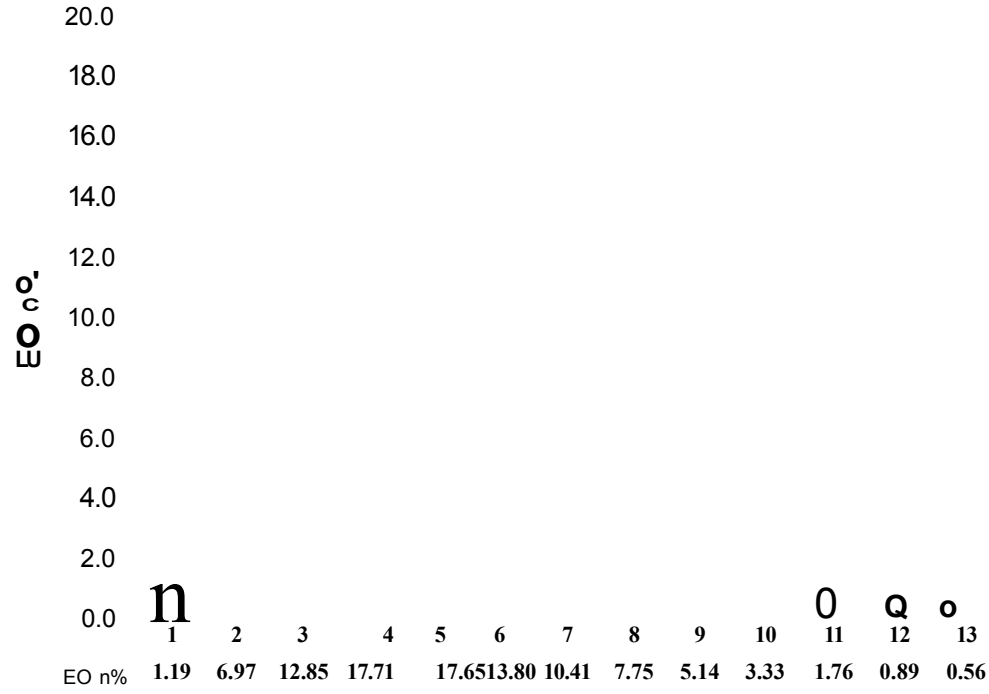

Figure 5.7. Average number of ethoxylate unit of NPEOS surfactant.

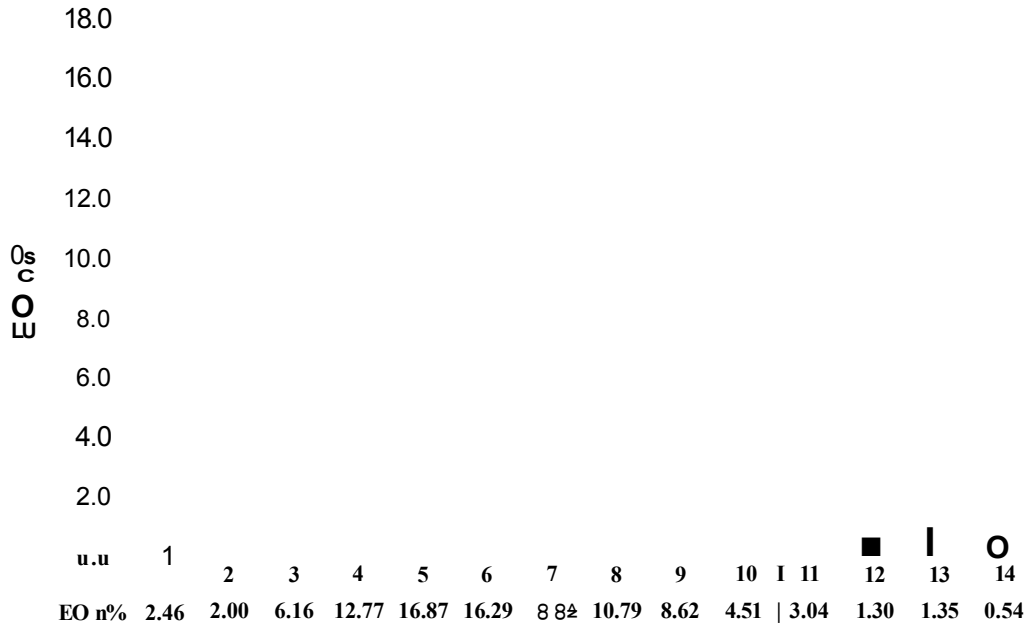

Figure 5.8. Average number of ethoxylate unit of NPEOSulphate surfactant. (Perlankrol).

5.6.2 Capillary Electrophoresis-Mass spectrometry of NPEOS

Capillary Electrophoresis-Mass spectrometry is a potentially very powerful technique, but several parameters must be optimised to obtain a good, working system.

The crucial problem is to achieve a perfect and stable electrical contact between the CE system and the MS interface during the measurements. Any disconnection, which can be caused by several factors, results in a loss of conductivity in the CE system. This stops the EOF flow and consequently the separation. This yields irreproducible results and even complete loss of signals.

During this study, the co-axial set-up invented by Smith *et al.* (Chapter 3), was used. The following parameters, which have direct or indirect influence on the electrical contact, had been optimised prior to the measurements.

5.6.2.1 Composition of sheath liquid

A widely used general solvent mixture for ESI, and consequently as a make-up flow as well, is 1:1 water - organic solvent (mainly methanol and acetonitrile) with 0.1% v/v organic acid (acetic / formic acid) to help the protonation of the analyte. Although, in our study, it was found that a mismatch in conductivity (ion strength) and viscosity (organic content) with the CE running buffer system, can cause crucial signal and EOF loss as well as instability. As the flow rate mismatch is a minimum of 1-2 orders against the EOF, the running buffer cannot overcome the effects arising from the sheath flow. Due to the severe negative effects with the solvent mixture, the sheath liquid was kept the same as the running buffer. The use of high buffer concentrations in the sheath flow (*i.e.* matching those of the running buffer) would not normally be considered desirable in MS. However, probably due to the very low flow rates, no problems were encountered in these studies. This agrees with observations reported by Vouros *et al.* [45]

5.6.2.2 Sheath liquid flow rate

The effect of the sheath flow rate was also investigated as it has two competing effects. Analyte sensitivity was optimised at 5 μL/min, using the stated running buffer above and 20 mbar additional pressure. As Figure 5.9 shows at higher flow rate the signal of the analyte ions decreased, due to dilution effects and at lower flow rates the spray became unstable and intermittent. This stopped the separation as insufficient electrical contact occurred resulting in the loss of the potential difference in the CE capillary.

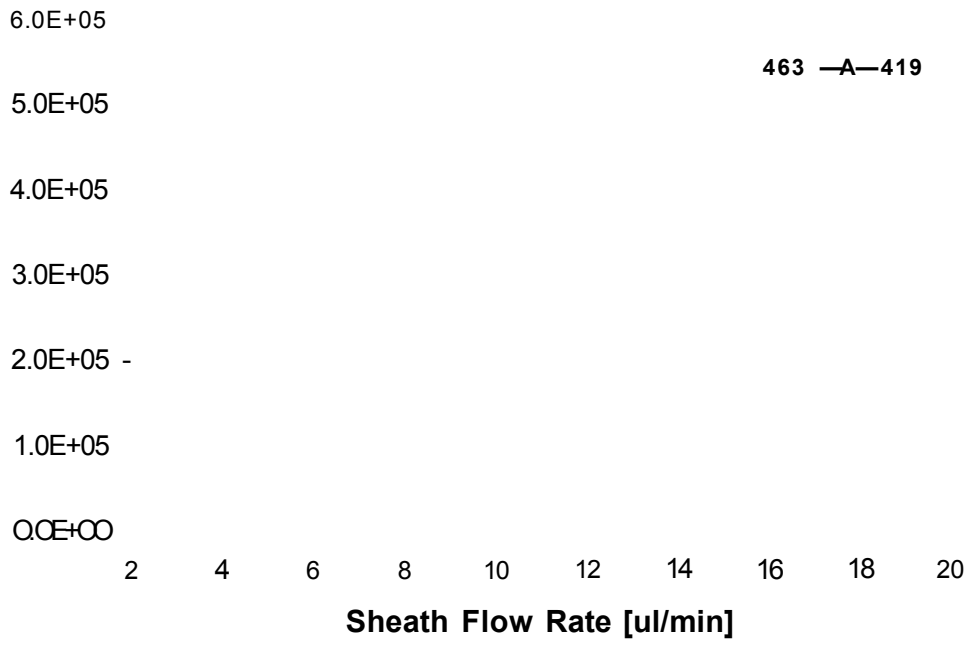

Figure 5.9. The effect of sheath flow rate on ESP+ signals of NPEOSp ions m/z 419, 463,551 and 653. Further details in Section 5.7.2.2. and 5.2.7.7.

5.6.2.3 Capillary position

The capillary position has been demonstrated to be the most critical parameter in CZE/MS coupling as the crucial electrical contact is produced via the sheath liquid at the end of the separation capillary. Our experience is strongly in contrast with previously published [46,47] work where an optimum of between 0.1 - 1.0 mm was found. Here it was found that the best peak area signals were produced when the separation capillary was slightly (-0.5mm) inside the sheath tube (Figure 5.10). The possibility of sheath counter ions migrating backwards into the separation capillary was predicted by Vouros [45]. This would be very possible in this capillary position, but was not observed in our system. This set up gives the best signal most likely due to continuous efficient mixing of the sheath liquid and analyte independently of the nebuliser gas flow rate.

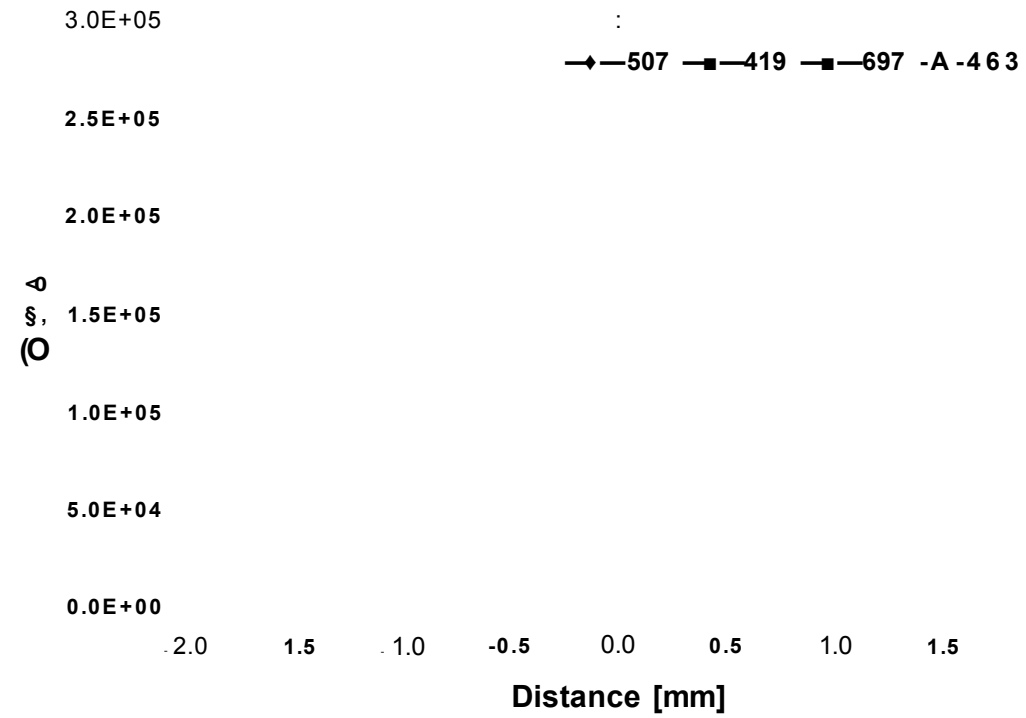

Figure 5.10. Effect of distance between CE capillary and sheath tube exit on ESP+ signal of NPEOSp ions of m/z 507, 419, 463 and 697. Further details in Section 5.7.2.3. and 5.2.7.7.

5.6.2.4 Applied additional pressure

Additional pressure is generally applied to the CE capillaries in CE-MS experiments as electrospray ionisation often causes a vacuum at the capillary exit, resulting in EOF and signal loss. Thus the applied pressure must be optimised. The data obtained show that higher pressure, as expected, reduced retention time (Figure 5.11). Resolution - calculated after Kirkland *et al.* [48] - was also decreased (Figure 5.12) due to the introduction of laminar flow, which causes peak broadening [Chapter 1.5.1]. The loss in resolution at low pressure is the result of EOF loss arising from the conductivity loss also due to the vacuum at the capillary wall. The very long retention times (34-40 minutes) are also proof of the absence of EOF under these conditions. The optimum value, 25mbar, gave the best resolution with the shortest separation time.

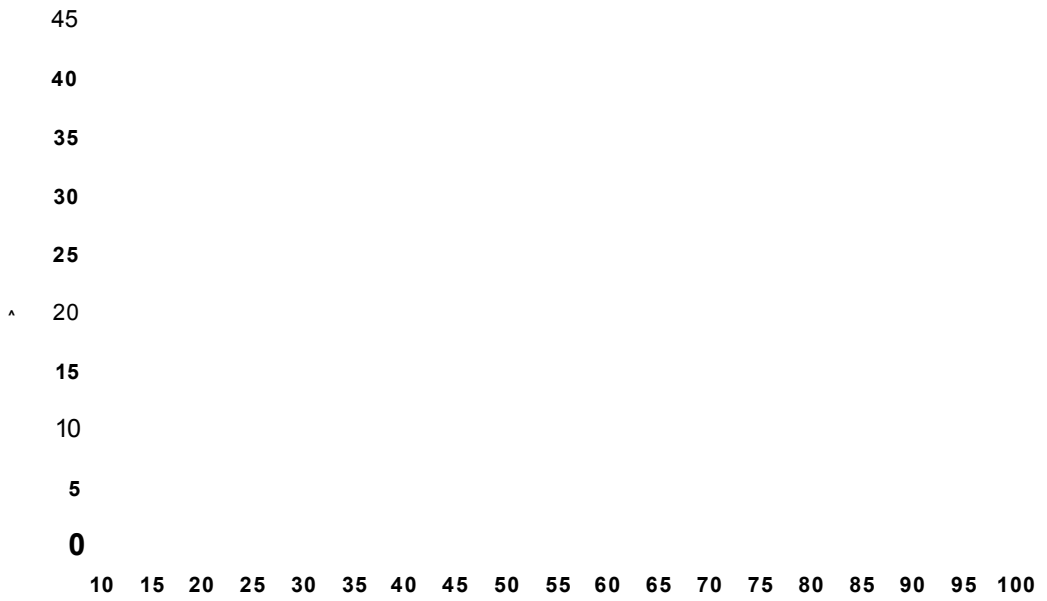

Figure 5.11. Effect of additional pressure on retention time on ESP+ signal of NPEOSp ion m/z 463. Further details in Section 5.7.2.4. and 5.2.7.7.

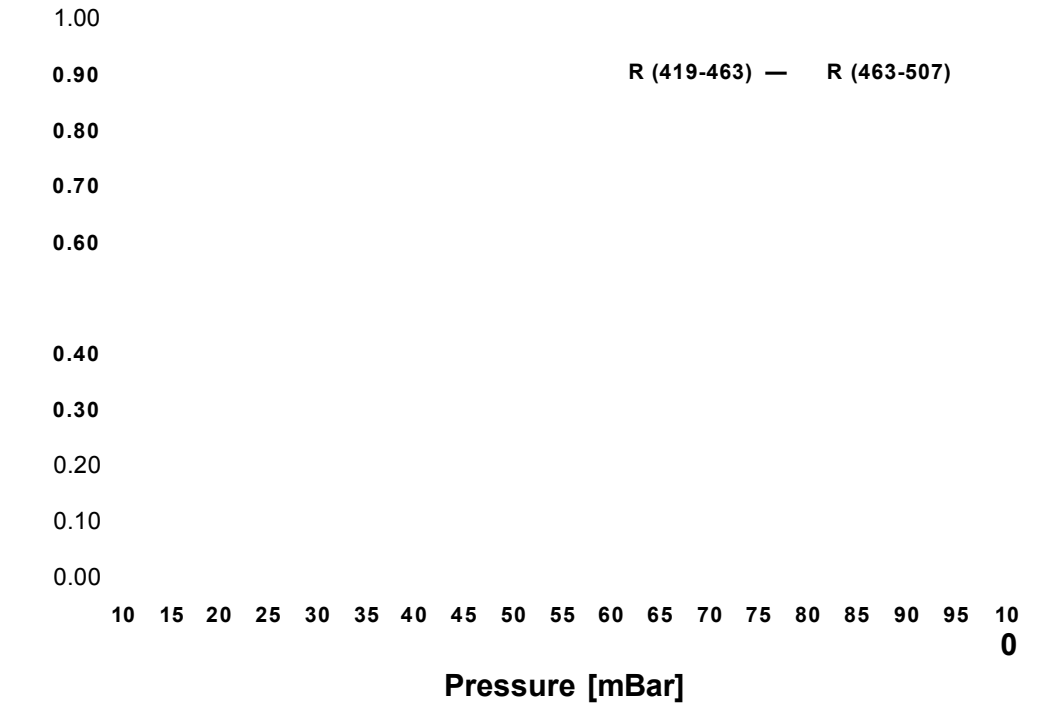

Figure 5.12. Effect of additional pressure on the resolution on ESP+ signal of NPEOSp ion m/z 419, 463 and 507. Further details in Section 5.7.2.4. and 5.2.7.7.

5.6.2.5 Nebuliser and drying gas flow rate

The nebulising gas flow rate was kept high (~40 L/hr) as lower flow rates dramatically changed the signals, resulting in loss of signal for the analyte. Higher flow rates also decreased signals of the analytes and increased solvent signals. Drying gas flow rates were half those commonly used for LC-MS *e.g.* in electrospray ionisation ~100L/hr is typically used. This was due to less liquid being introduced into the system.

5.6.2.6 Temperature

Source temperature was also reduced (50°C) compared to typical ESI conditions to minimise capillary drying effects, due to the reduced total liquid volume of the analyte.

5.6.2.7 Optimised parameters

The optimised mass spectrometric parameters, which were later used in this work, were found to be as follows:

Composition of the CE mobile phase and sheath liquid were ACN-25 mM ammonium acetate (70:30) at pH 5. Make-up flow was infused at 5 μL/min to the source, which was kept at 80°C. A 25mbar supplementary pressure was applied to separating silica CE capillary, which was positioned 0.5mm inside the sheath tube from the spraying end. Drying and nebulising gas were nitrogen with a flow rate of 40 and 50 L/hr respectively. The following voltages were applied in positive and negative mode respectively: +/-30kV (capillary), +/-3.5kV (tip) and +70V/-30V(cone).

5.7 CZE-MS Results

Direct ESP analysis of NPEOS gives three major groups of ions in positive mode. These groups, in decreasing sensitivity, correspond to the ionic species [M-Na+2H]+, [H2(0C2H4)nS03+H]+ and [C9Hi9(OC2H4)n]+. The sulphate formulation gives two major groups as [M-Na+2H]+ and [CH2(0C2H4)nS04+H]+, and two less intensive, equal ion groups ([CH2(0C2H4)nS03+H]+ and [(0C2H4)nS04+H]+) as shown in Figure 5.13.

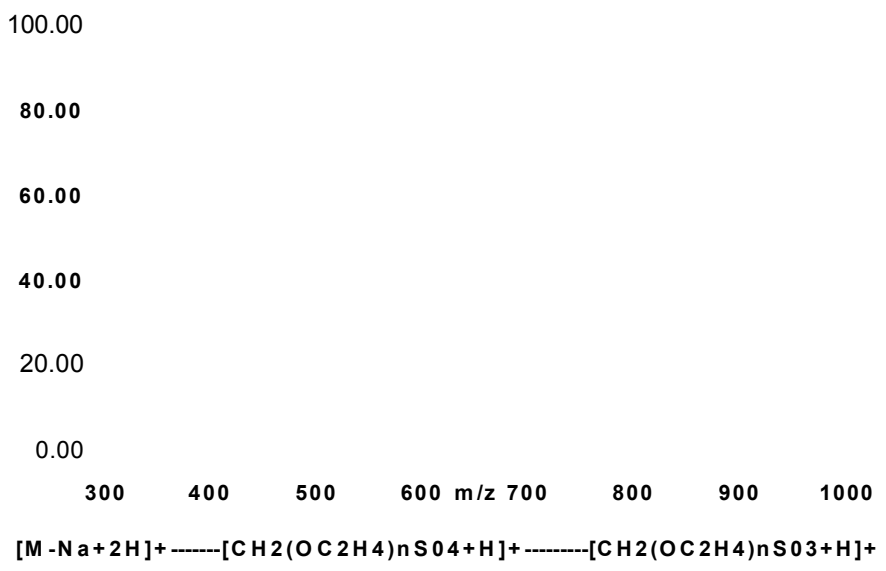

Figure 5.13. Percentage distributions of the observed ion types in Full scan ESP+ spectra of NPEOSp surfactant based on base peak m/z 653. (Details in Appendix III.)

Both spectra exhibit envelopes of the these ion types, corresponding to the distribution of ethylene oxide chain lengths (Appendix III. Figure 1-2). The observed ions are presented in Table 5.2.

Despite the similar operating condition, the observed ions are different from LC-ESP-MS data, where the [M-Na+H-i-NH4]+ ions were observed [9]. This shows that the concentration of ammonium acetate buffer, which was lOOmM in *Benomar's* method, strongly influences the detectable ion.

	Perlankrol				NPEOS		
n(EO) (C_2H_4O)	$[CH_2(OC_2H_4)_nSO_4+H]^+$	$[CH_2(OC_2H_4)_nSO_3+H]^+$	$[(OC_2H_4)_nSO_4+H]^+$	$[M-Na+2H]^+$	$[C_9H_{19}(OC_2H_4)_n]^+$	$[H_2(OC_2H_4)_nSO_3+H]^+$	$[M-Na+2H]^+$
1				389			373
2				433			417
3				477			461
4				521			505
5				565	*439*		**549**
6	375			**609**	*483*		593
7	419			653	*527*		637
8	463		*449*	697	*571*	435	681
9	**507**	*491*	*493*	741	*615*	479	725
10	551	*535*	*537*	785	***659***	523	769
11	595	*579*	*581*	829	*703*	567	813
12	639	*623*	***625***	873	*747*	611	857
13	683	*667*	*669*	917	*791*	**655**	901
14	727	***711***	*713*	961	*835*	699	945
15	771	*755*	*757*		*879*	743	
16	815	*799*	*801*		*923*	787	
17	859	*843*	*845*		*967*	831	
18	903	*887*	*889*		*1011*	875	

Table 5.2. Observed positive ions in [CE-ESI-MS+] measurement of nonylphenol ethoxysulphate (Perlankrol) and sulphonate (NPEOS) surfactant samples. The ions groups observed with minimal intensity are shown in italics, while the "base peaks" of the individual groups in bold.

In negative mode, only $[M-Na]^-$ ions were observed, at m/z 387, 431, 475, 519, 563, 607, 651, 695, 739, 783, 827 and 871 corresponding to 1 to 12 EO unit containing oligomers of NPEOSp and at m/z 371, 415, 459, 503, 547, 591, 635, 679, 723, 767, 811 and 855 corresponding to 1 to 12 EO unit containing oligomers of NPEOS type alkylethoxy surfactant (Appendix III. Fig.3-4) with base-peaks of 519 (4EO unit) and 547 (5EO units) respectively.

This method gives a very straightforward and clear identification of alkylethoxysulphate and sulphonate surfactants. The separation would be faster, however if reverse mode CZE could be used (as presented earlier in this chapter). Unfortunately on the VG Quattro mass spectrometer system used (due to the instruments and it's detector parameters), poor sensitivity is obtained in negative ion mode, which means usually that only 10-50% of the equivalent positive ion signal is obtained.

As the required total injected sample amount was high for full scan mode selective ion monitoring mode (SIM) a possible alternative mode in MS detection was chosen for CZE-MS (Figure 5.14-17). This mode gives higher sensitivity due to the longer detection time on individual ions than in full scan operating, although the possible ions must be identified prior the experiments.

Detection limits were calculated from the total surfactant amount injected (Eq. 1.40) onto the capillary hydrodynamically. Limit of detection was found to be 0.98ng on-column injection (CZE-UV = 2.00ng) of NPEOSp surfactant formulation and 1.14ng (CZE-UV = 2.25 ng) of NPEOS surfactant formulation. As these surfactant formulations are always mixtures of individual ethoxymers, LOD calculations have not been carried out for each ethoxymer. An estimation can be made using mole ratios of individual exthoxymers (calculated as described earlier). This gives a result of 8.45pg for the main component (EO6) of NPEOSp and 9.46pg for the NPEOS formulation.

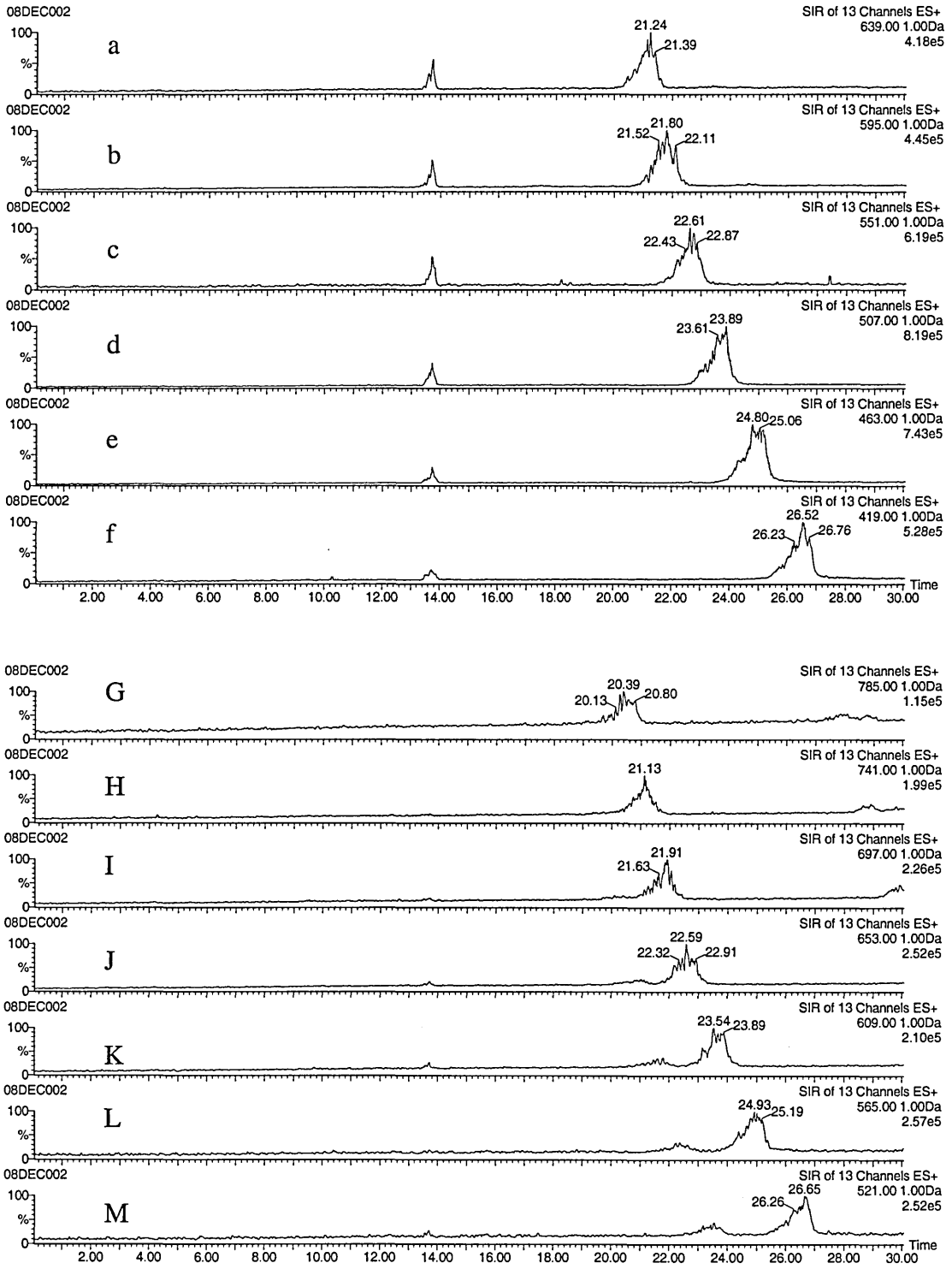

Figure 5.14. SIM ion chromatograms of NPEOSp surfactant formulation by [CZE-ESP+] analysis using the operational parameters as described in Section 5.6.2.7. Injected sample amount was 7.1ng.
The quasimolecular ethoxymer ions $[M\text{-}Na+2H]^+$ of 4EO (t_r = 26.65 min) to 10EO (t_r = 20.39 min) containing oligomers are shown in (G)-(M) in this chromatogram. The $[CH_2(OC_2H_4)_nSO_3+H]^+$ peaks (a-h) corresponding to the 7EO to 12EO containing oligomers.

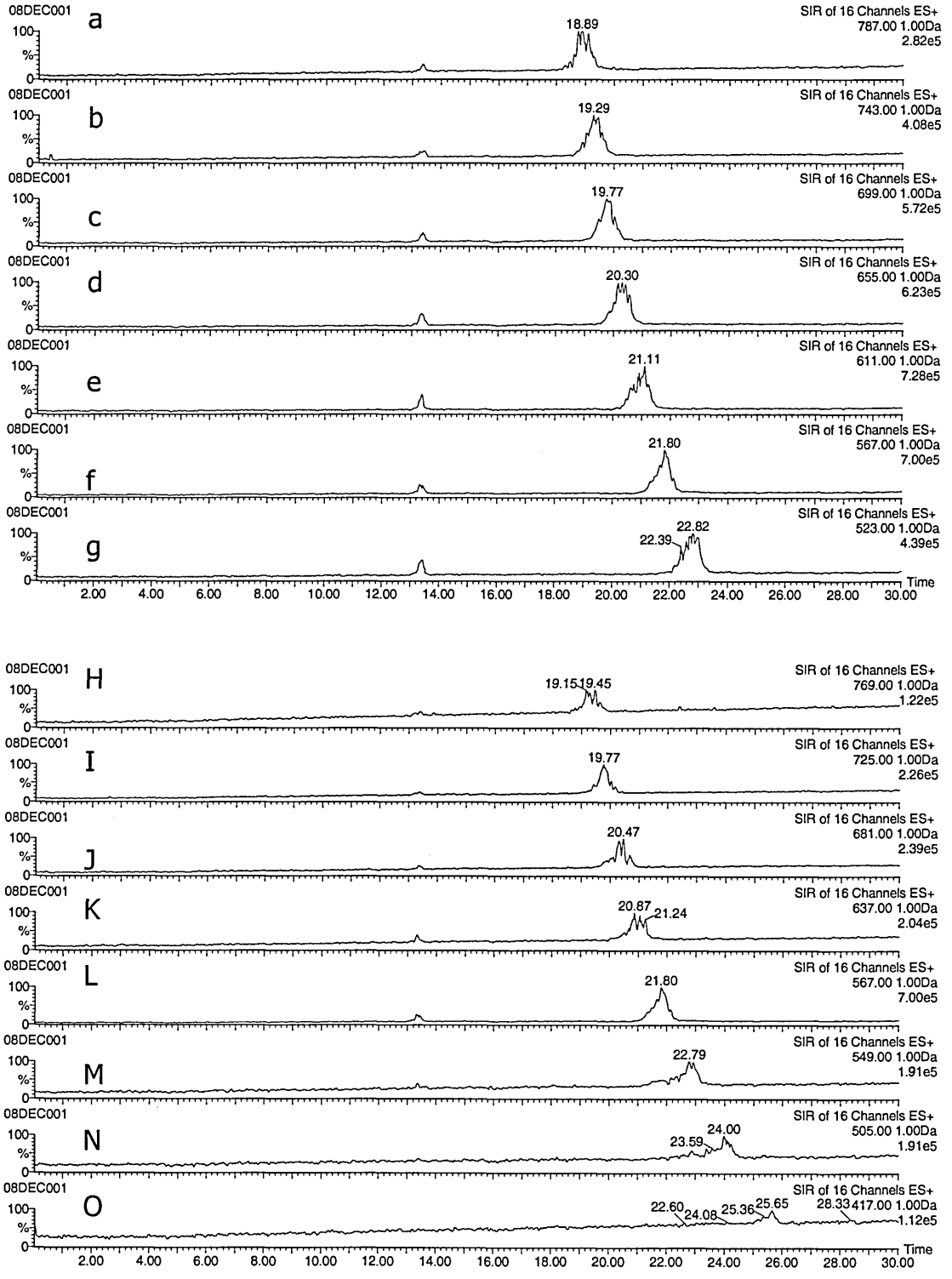

Figure 5.15. SIM ion chromatograms of NPEOS surfactant formulation by [CZE-ESP+] analysis using the operational parameters as described in Section 5.6.2.7. Injected sample amount was 7.1ng.
The quasimolecular ethoxymer ions $[M\text{-}Na+2H]^+$ of 2EO (t_r = 25.65 min) to 10EO (t_r = 19.15 min) containing oligomers are shown in (H)-(O) in this chromatogram. The $[H_2(OC_2H_4)_nSO_3+H]^+$ peaks (a-j) corresponding to the 16EO to 10EO containing oligomers.

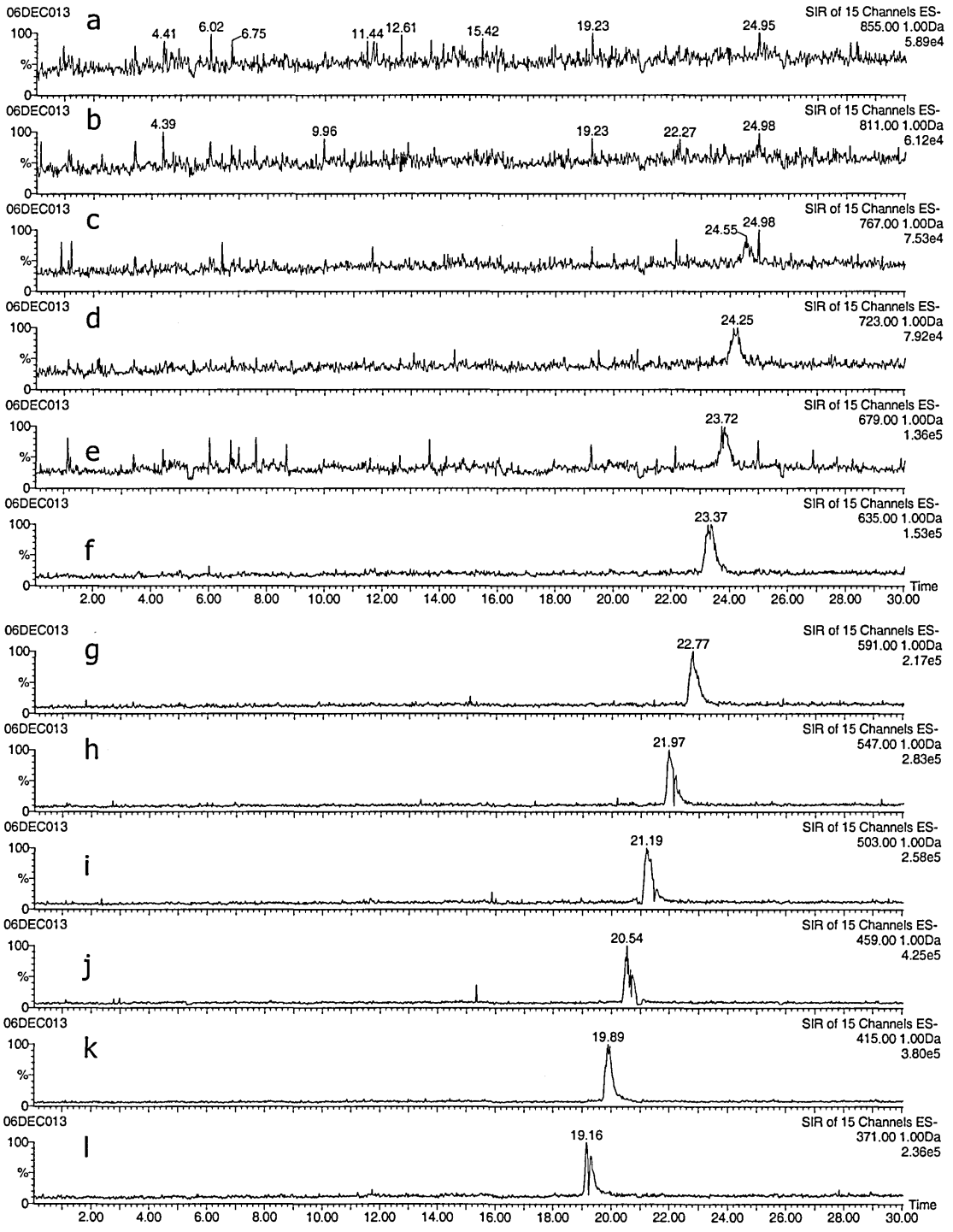

Figure 5.16. SIM ion chromatograms of NPEOS surfactant formulation by [CZE-ESP-] analysis using the operational parameters as described in Section 5.6.2.7.
(a)-(l) $[M-Na]^-$ ethoxymer quasimolecular ions. Peaks corresponding to 10 EO (t_r=24.55min) to 1 EO (t_r=19.16min) unit containing oligomers were detectable. 7.1ng sample injected.

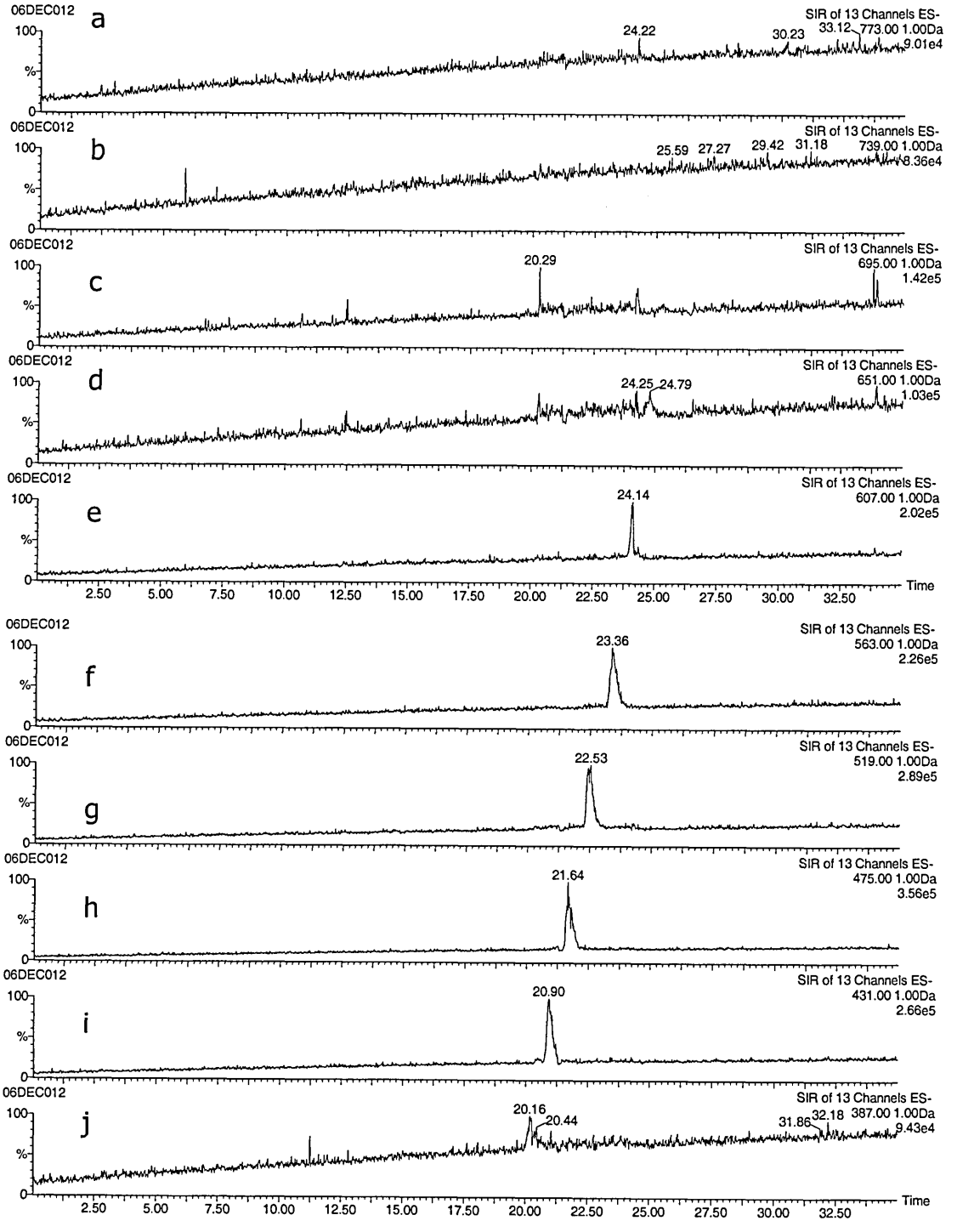

Figure 5.17. SIM ion chromatograms of NPEOSp surfactant formulation by [CZE-ESP-] analysis using the operational parameters as described in Section 5.6.2.7.
(a)-(j) $[M-Na]^-$ ethoxymer quasimolecular ions. Peaks corresponding to 7 EO (t_r=24.79min) to 1 EO (t_r=20.16min) unit containing oligomers were only detectable. 7.1ng sample injected.

5.8 Conclusions

The aim of this work was to develop CE separation techniques for NPEOS and NPEOSp surfactants. It was hoped that they would offer improvements over HPLC methods developed previously in this group.

The separation of NPEOS and NPEOSp ethoxymers has successfully been demonstrated for reverse CZE and CZE/MS methods using reverse CZE negative ion and normal CZE positive ion mode.

The calculated average number of ethoxymer units, with the resulted value of 6.46 for NPEOS and 6.45 for NPEOSp formulations, were in good agreement with previous data obtained by different methods.

Mass spectrometric data was obtained in both full scan and selected ion monitoring (SIM) mode. Due to the better sensitivity obtained with selected ion recording positive ion mode, it was chosen for the CZE-MS study. This experiment gave a detection limit of ~1 ng for the surfactant formulations, containing 13 EO unit with the average of 6 ethoxymers.

As use of a mass spectrometer allows separation by mass, perfect electrophoretic peak resolution is not as important as in spectro-photometricaly detected systems. This was clearly demonstrated with normal CZE coupled with MS as its UV equivalent method generated only poor peak specifications. The MS technique provided precise measurements of the molecular weight of the individual ion species present in the analyte.

References

1. Karsa D.R.; *Chem. Ind.* 9 (1998) 685
2. Morse P.M.; *Chem. & Engineering News*, February 1, (1999) 35
3. Berna J.L., Moreno A. and Bengoechea C., *J. Surfactants and Detergents* 1 (1998) 263-271
4. European Chemical Industry Council (CEFIC), *Cesio news* issue 5, 2001 November, Brussels.
5. Jobling S. and Sumpter J.P.; *Aquatic Toxicol.* 27 (1993) 361
6. Mueller G.C. and Kim U.H. *Endocrinology* 102 (1978) 1429
7. Soto A.*; Environ. Health Perspect.* 92 (1991) 167
8. Sharpe R. and Skakkebaek N.E., *Lancet* 341 (1993) 1392
9. CES 1993 for the Dept. of the Environment. *Uses, Fate and Entry to the Environment of Nonylphenol Ethoxylates*. CES Ltd. Beckenham, Kent (1993)
10. Painter H.A., *Detergents, the Handbook of Environmental Chemistry*, Springer-Verlag, Germany 1992. Anionic surfactants 1-88.
11. Krueger C.J, Radakovich K.M., Sawyer T.A., Barber L.B., Smith R.L. and Field J.A.; *Environ. Sci. Technol.* 32 (1998) 3954
12. Tolls J., Haller M., and Sijm D.T.H.M; *Anal. Chem.* 71 (1999) 5242
13. Rosen M.J., Fang L., Morrall S.W. and Versteeg D.J. .; *Environ. Sci. Technol.* 35 (2001) 954
14. Zweigenbaum J.; *Chromatogr.* 11 (1990) 9
15. Desbène P.L., Rony C., Desmazaières B. and Jacquier J.C.; *J. Chrom. A.* 608 (1992) 375
16. Chen S. and Pietrzyk D.J.; *J. Chrom. A.* 657 (1993) 2770
17. Pietrzyk D.J. and Zhou D.; *Anal. Chem.* 64 (1992) 1003
18. Romano J., Jandik P., Jones W.R. and Jackson P.E.; *J. Chrom. A.* 546 (1991) 411
19. Jandik P., Jones W.R., Weston A. and Brown P.R; *LC-GC* 9 (1991) 643
20. Ding W.H. and Liu C.H.; *J. Chrom. A.* 929 (2001) 143
21. Kuhr W.G. and Yeung E.; *Anal. Chem.* 60 (1988) 2642

22. Salimi-Moosavi H. and Cassidy R.M.; *Anal. Chem.* 68 (1996) 293
23. Shamsi S.A., Weathers R.M. and Danielson N.D.; *J. Chrom. A.* 737 (1996) 315
24. Heinig K., Vogt C. and Werner G.; *J. Chrom. A.* 745 (1996) 281
25. Kanz C., Nölke M., Fleischmann T., Kohler H.P.E. and Giger W.; *Anal. Chem.* 70 (1998) 913
26. Riu J., Einchhorn P., Guerrero J.A., Knepper Th.P and Barceló D.; *J. Chrom. A.* 889 (2000) 221
27. Desbène P.L. and Rony C.M.; *J. Chrom. A.* 689 (1995) 107
28. Weiss C.S., Hazlett C.S.. Datta M.H. and Danzer M.H.; *J. Chrom. A.* 608 (1992) 325
29. Pierra E., Erra P. and Infante M.R.; *J. Chrom. A.* 757 (1997) 275
30. Heinig K., Vogt C. and Werner G.; *J. Chrom. A.* 781 (1997) 17
31. Shamsi S.A. and Danielson N.D., ; *Anal. Chem.* 67 (1995) 4210
32. Lin C.E., Chiou W.C. and Lin W.C.; *J. Chrom. A.* 722 (1996) 189
33. Heinig K., Vogt C. and Werner G.*; Anal. Chem.* 70 (1998) 1885
34. Walbroehl Y. and Jorgenson J.W.; *Anal. Chem.* 58 (1986) 479
35. Heinig K., Vogt C. and Werner G.; *Fresen. J. Anal. Chem.* 357 (1997) 695
36. Wallingford R.A.; *Anal. Chem.* 68 (1996) 2541
37. Bullock J.; *J. Chrom. A.* 645 (1993) 169
38. Barry J.P., Radtke T.R., Carton W.J., Anselmo R.T. and Evans J.V.; *J. Chrom. A.* 800 (1998) 13
39. Raith K., Wolf R., Wagner J. and Neubert R.H.H.; *J. Chrom. A.* 802 (1998) 185
40. Benomar S.H., Clench M.R. and Allen D.W.; *Anal. Chimica Acta* 445 (2001) 255
41. Lim C.K. and Peters T.J.; *J. Chrom. A.* 316 (1984) 397
42. Scullion S.D., Clench M.R., Cooke M. and Ashcroft A.E.; *J. Chrom. A.* 733 (1996) 207
43. Austad T. and Fjelde I.; *Anal. Lett.* 25 (1992) 957
44. Tally L.D.; *SPE Res. Eng.* 3 (1988) 235

45. Foret F., Thompson T.J., Vouros P., Karger B.L., Gebauer P. and Booek P.; *Anal. Chem.* 66 (1994) 4450

46. Moseley M.A., Jorgenson J.W., Shabanowitz J., Hunt D.F. and Tomer K.B.; *J. Am. Soc. Mass Specrom.* 3 (1992) 289

47. Banks J.F.; *J. of Chrom. A.* 712 (1995) 245

48. Kirkland J.J. ed.; *Modern Practice of LC* Wiley, New York 1971

CHAPTER 6

Conclusions

6.1 Development of a CZE/UV Separation of Nonylphenol Ethoxylate type Surfactant mixture

A rapid and efficient separation of a nonylphenol ethoxylate surfactant mixture has been developed and optimised. As these types of surfactants are negatively charged, normal mode CZE resulted in long separation times with tailing peaks. To solve the problem, reverse mode CZE was applied after permanently coating the silica capillary with hexadimetrine bromide. A radical decrease in migration times and an increase in peak efficiencies were observed, which also resulted in a full resolution of fourteen components from the mixture. Mild analytical conditions (mobile phase, buffer and pH) had to be chosen to prevent hydrolysis of the analyte and make the system available for mass spectrometric work.

The HPLC separation method reported previously by our group, was successfully improved, indicating the usefulness of electrophoresis in the analysis of NPEOS and NPEOSp surfactants in oil recovery industry and/or environmental analysis.

The obtained data showed that both nonylphenol ethoxylate type surfactant formulations had a chain length of 2-13 ethoxymer units. The determined average numbers of the ethoxymer units were 6.46 for NPEOS and 6.45 for NPEOSp. These values are is in high agreement with previous HPLC result.

6.2 Analysis of Nonylphenol Ethoxylate Surfactants by CZE/MS

The separation of NPEO type surfactant mixtures has successfully been transferred from a CZE/UV to a CZE/MS method using a co-axial sheath-flow interface. The effect of operational conditions such as capillary positioning, sheath liquid and nebuliser gas flow rate, pressure was investigated.

Data was obtained in selected ion recording mode, which consumed much less sample (~1.14 ng and ~0.98 ng respectively), indicating the higher level of sensitivity obtained whilst using selected ion recording over full scan.

Mass spectrometric data was successfully studied in both positive and negative mode. The observed ion species were different from LC-ESP-MS data, showing the strong influences of the concentration of ammonium acetate buffer in the mobile phase.

6.3 Investigation of Stationary Phases for CEC

In CEC, the EOF is generated from the residual silanols on the surface of stationary phases. The quantity and availability of these surface silanols can be assigned to the physicochemical properties of the different stationary phases, which was clearly observed in the apparent trend with surface carbon and bonding density of the bonded silicas. The higher correlations with surface carbon and bonding density over surface oxygen content indicated the importance of the availability of the free silanols (which are responsible for the generation of EOF) for the mobile phase ions. The more densely bonded phases can cover, hence shield these silanols, resulting in a reduced EOF. However, this effect is greatly influenced, and can be overshadowed, by the pH and organic composition of mobile phases.

Chromatographic results showed that the surface coating of the stationary phases governs the reversed-phase type retention of the test compounds used in this study. More densely bonded phases gives better separation due to the better coverage of the surface, reducing unwanted silanol effects. Retention data obtained from the same analytical conditions were used to evaluate separation behavior of five different stationary phases were observed. Three different types of behavior were observed. This was consistent across all of the different types of test solute. The result showed that effect of surface modification (used for silanol masking in reversed-

phase chromatography) on analytical performance is not straightforward under CEC conditions as the endcapped phase showed similar performance as unmodified phases with similar bonding density.

Overall, physicochemical properties can provide useful information about the EOF generation capability of the stationary phases in CEC. Although a correlation with bonding density was found, physicochemical properties appear to have a much lower influence on chromatographic performance than the quality of the packed bed. While reversed-phase type retention mechanism can be characterized with surface properties, other properties of the quality of separation (such as efficiency and asymmetry), as well as reproducibility studies, demonstrated the near impossibility of packing CEC columns in a reproducible manner. This a severe limitation to the widespread adoption of this technique.

6.4 Overall Conclusions

In general terms, in the work carried out, CZE and CEC have been shown to be powerful separation techniques. However, these electrodriven techniques have major drawbacks that can be crucial in their suitability for applications.

CZE can provide extremely efficient separations but it is limited to charged species. It can be successfully connected to MS but specially designed integrated CZE and CEC-MS instrumentation still must be developed for the market, as at present interfacing requires long capillary lengths (due to the restraints in physical positioning caused by the designs of the MS instruments). This increases analysis time and thus reduces efficiencies. Stable and sufficient electrical connection and grounding are also a main difficulty, especially in the case of CEC-MS and the whole interfacing requires careful optimisation.

In CEC, the packing procedure, still generates the most problems. These often overshadow delicate stationary phase effects. Although conventional packing materials are widely available and can provide better chromatographic performance in electrochromatography than under pressure driven conditions, it seems – as indicated from the increasing number of publication on this field – the future of this technique would appear to rely on the application of continuous bed or monolithic columns formed in-situ.

Overall, electrically driven separation techniques can provide an exciting approach to the analysis for a wide range of analytes. CEC is still in a position of being only an interesting alternative (and mainly academic) method beside GC and HPLC. Although, it has the potential to become the analytical technique of the future, it is unlikely that CEC methods will replace the widespread applications of HPLC (or GC) and they will remain complementary techniques useful in sample limited situations and academic researches.

6.5 Future Work

There is big area that could be further developed from this work. The study of different stationary phases showed some encouraging results and better correlation with their physicochemical properties than was previously found. However, the available range of different stationary phases has limited the strength of our conclusions, thus it would be useful to continue this study with several phases and with several batches of the same phase from the same manufacturers. Further, it would be more interesting to compare phases which produced by several different silanol masking techniques (*i.e.* endcapping, shielding, base deactivation, polymerisation *etc.*) as these surface modification techniques methods has high influence on the generation mobile phase flow (*e.g.* EOF).

Although CZE-UV and CZE-MS techniques gave better analytical result than previous HPLC separations, it would be academically interesting to complete the analytical study for nonylphenol ethoxylate type surfactants by the application of CEC with mixed mode SAX stationary phases, which were previously reported being successful by our group in HPLC, but required a total of 50cm column length. This could also provide advantage to separate (and with combination with MS identify) other possible neutral by-products as well from. However, the main field of future work would be the performance test of the CZE method on crude samples from oil fields, testing whether the method powerful enough to simplify the presently used HPLC analyses where preliminary solid phase extraction is also necessary.

Meetings and conferences attended

Analytical Research Forum of RCS, University of East Anglia, Norwich

2001 July 16-18

Poster presentation of *"Applications of Capillary Electrophoresis and Capillary Electrochromatography Nano ESI-MS "*

25th Annual BMSS Conference, University of Southampton, Southampton

2001 September 10-12

Poster presentation of "*Optimisation of Coupled Capillary Electrophoresis and Capillary Electrochromatography Nano ESI-MS*".

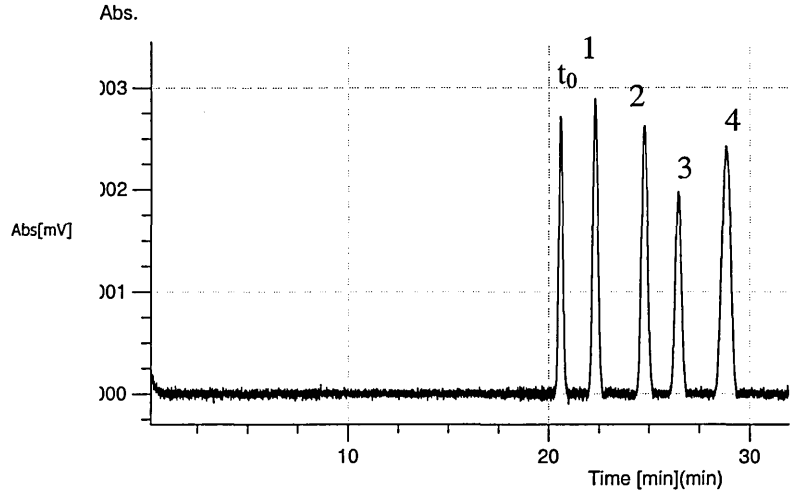

A

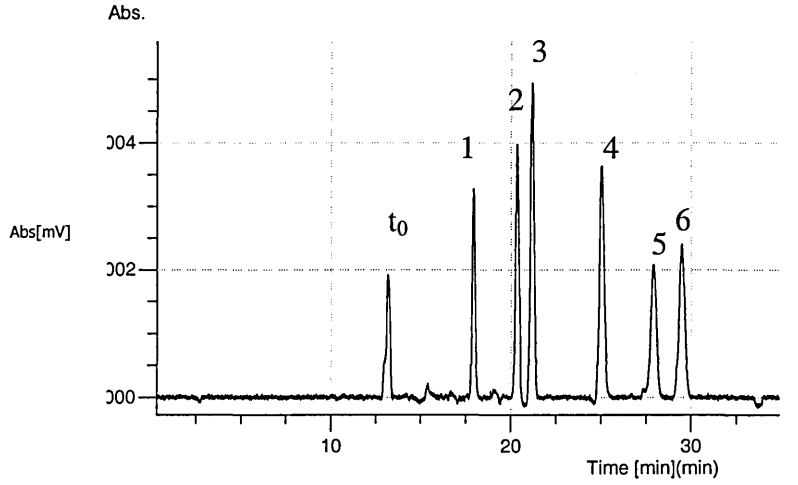

B

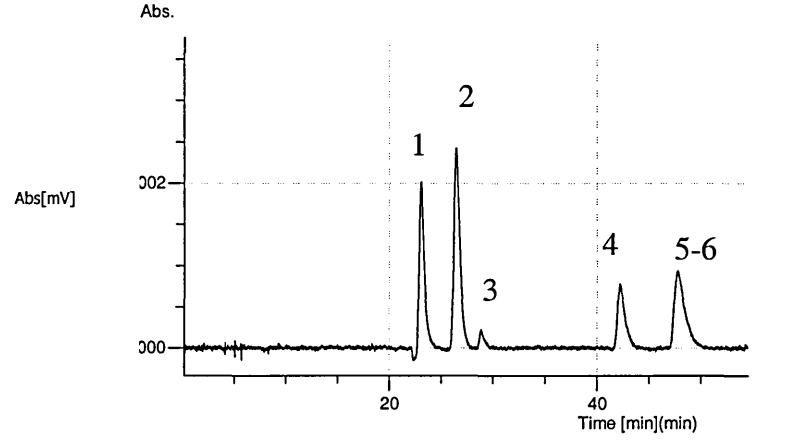

C

Appendix II. Figure 1. CEC separations of (A) barbital, (B) biphenyl and (C) pyridine test mixtures on **Exsil 26/106** stationary phase with uracil neutral marker (t_0). For CEC conditions see section 4.4 and Table 4.7.
The peaks correspond to [A]: (1) barbital, (2) phenobarbital, (3) butethal and (4) amobarbital; [B]: (1) acethyl-, (2) methoxy-, (3) biphenyl, (4) methyl-, (5) bromo- and (6) ethyl-biphenyls; [C]: (1) amino-, (2) acethyl-, (3) pyridine, (4) chloro-, (5) bromo- and (6) ethyl-pyridine.

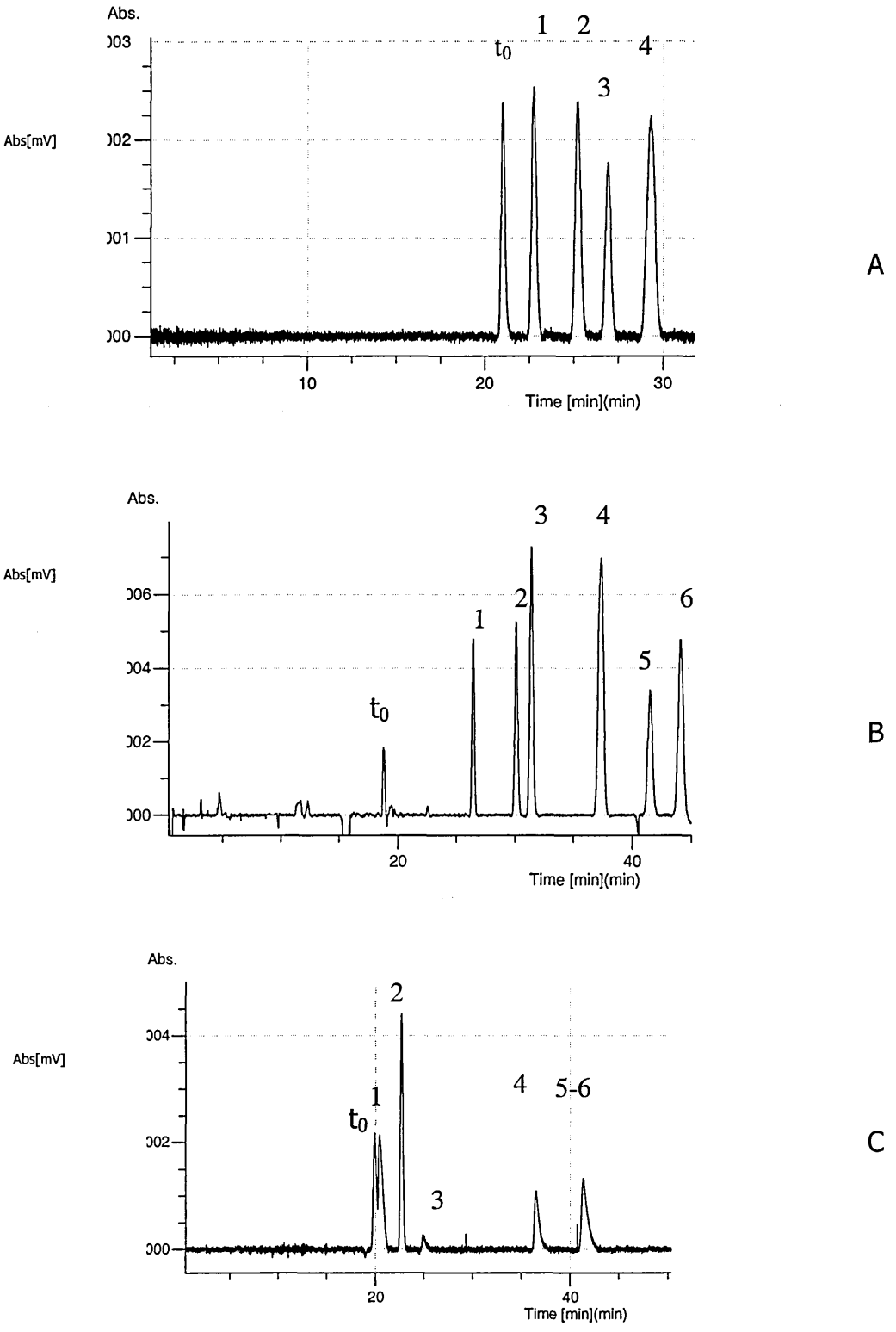

Appendix II. Figure 2. CEC separations of (A) barbital, (B) biphenyl and (C) pyridine test mixtures on **Exsil 17/339** stationary phase with uracil neutral marker (t_0). For CEC conditions see section 4.4 and Table 4.7.
The peaks correspond to [A]: (1) barbital, (2) phenobarbital, (3) butethal and (4) amobarbital; [B]: (1) acethyl-, (2) methoxy-, (3) biphenyl, (4) methyl-, (5) bromo- and (6) ethyl-biphenyls; [C]: (1) amino-, (2) acethyl-, (3) pyridine, (4) chloro-, (5) bromo- and (6) ethyl-pyridine.

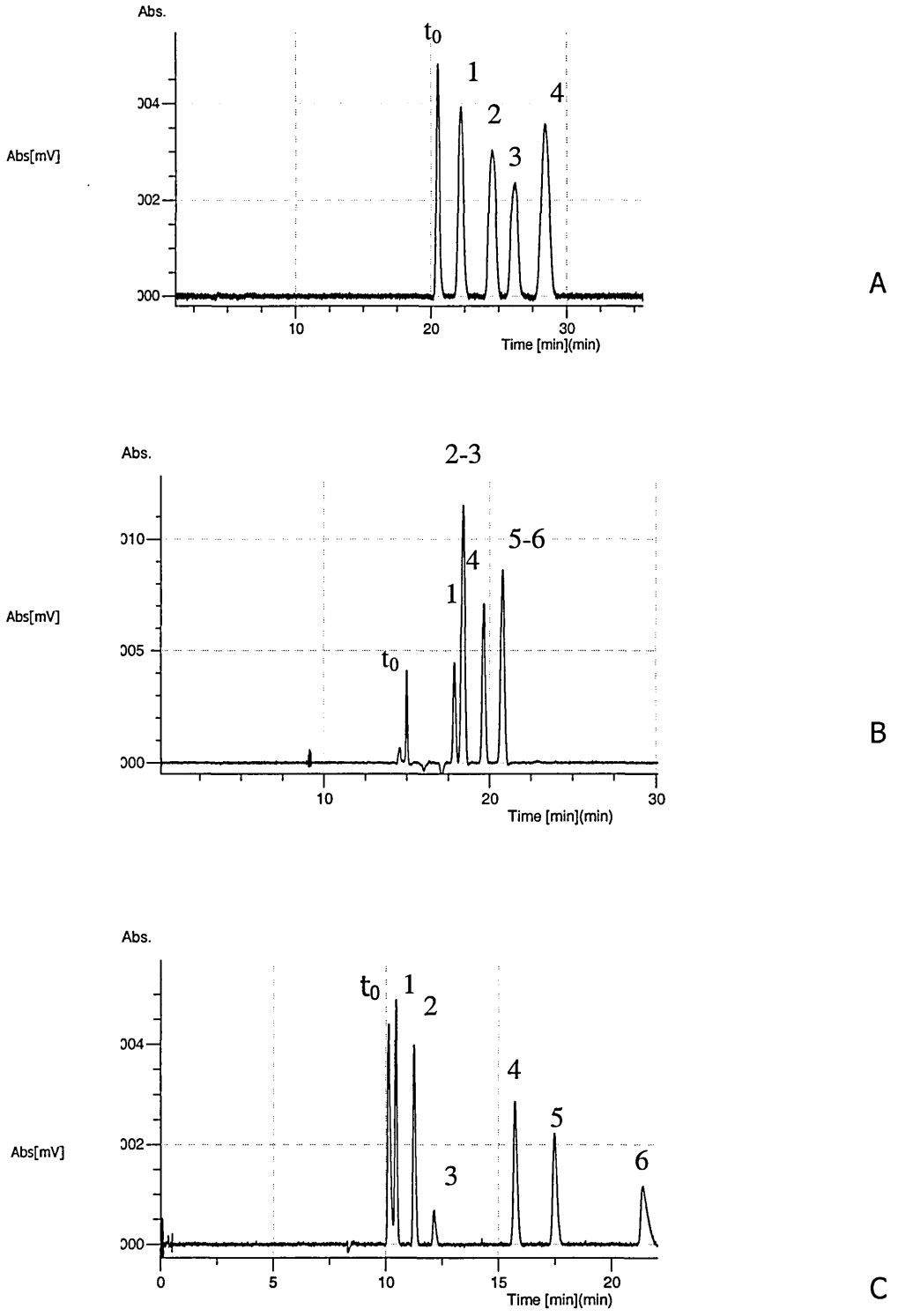

Appendix II. Figure 3. CEC separations of (A) barbital, (B) biphenyl and (C) pyridine test mixtures on **Xtec ODS1** stationary phase with uracil neutral marker (t_0). For CEC conditions see section 4.4 and Table 4.7.

The peaks correspond to [A]: (1) barbital, (2) phenobarbital, (3) butethal and (4) amobarbital; [B]: (1) acethyl-, (2) methoxy-, (3) biphenyl, (4) methyl-, (5) bromo- and (6) ethyl-biphenyls; [C]: (1) amino-, (2) acethyl-, (3) pyridine, (4) chloro-, (5) bromo- and (6) ethyl-pyridine.

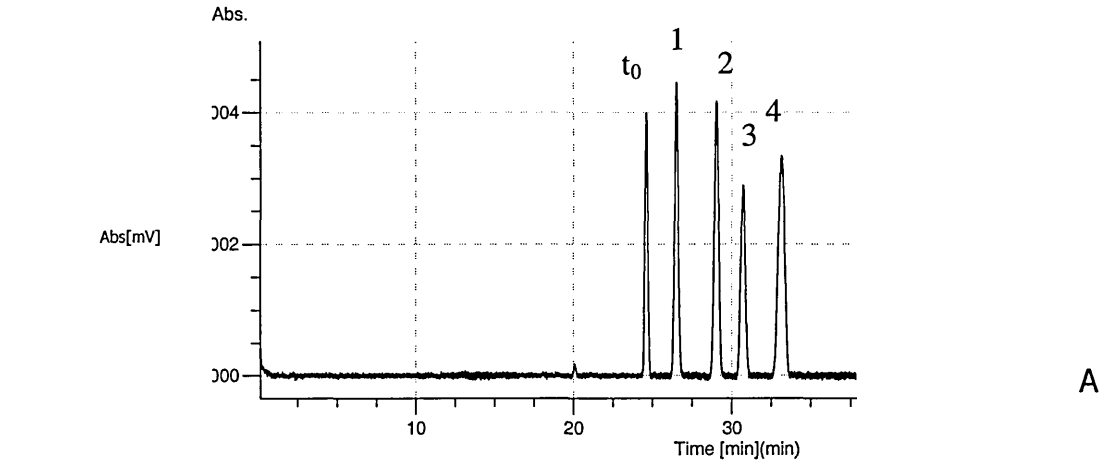

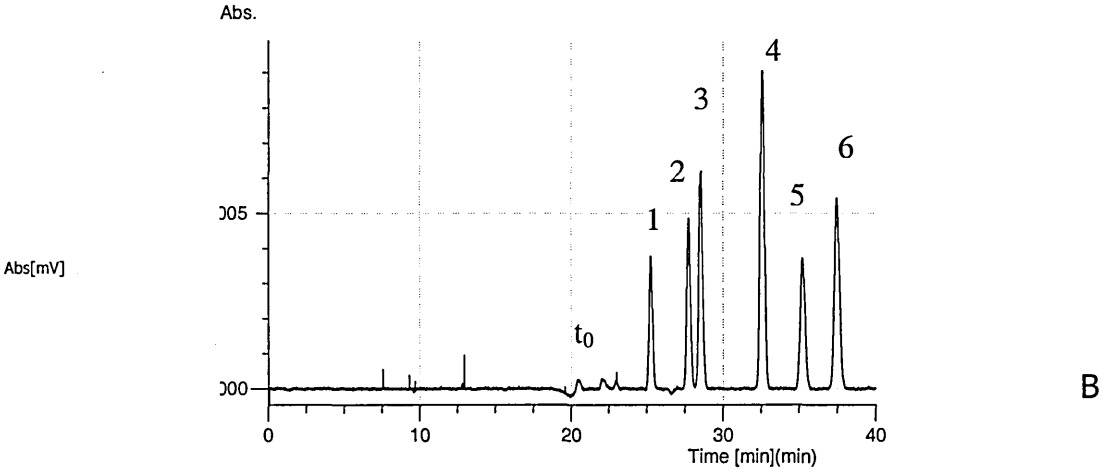

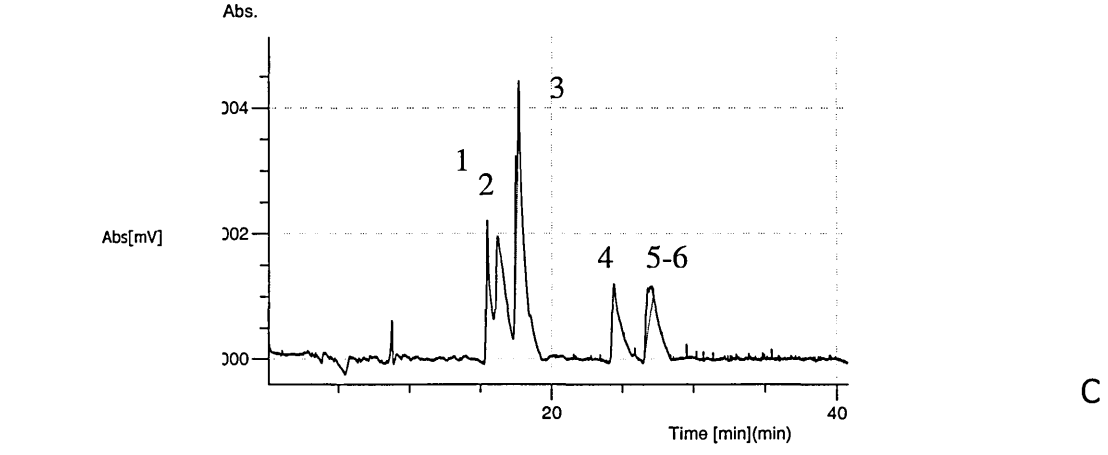

Appendix II. Figure 4. CEC separations of (A) barbital, (B) biphenyl and (C) pyridine test mixtures on **Hypersil 3 ODS** stationary phase with uracil neutral marker (t_0). For CEC conditions see section 4.4 and Table 4.7.
The peaks correspond to [A]: (1) barbital, (2) phenobarbital, (3) butethal and (4) amobarbital; [B]: (1) acethyl-, (2) methoxy-, (3) biphenyl, (4) methyl-, (5) bromo- and (6) ethyl-biphenyls; [C]: (1) amino-, (2) acethyl-, (3) pyridine, (4) chloro-, (5) bromo- and (6) ethyl-pyridine.

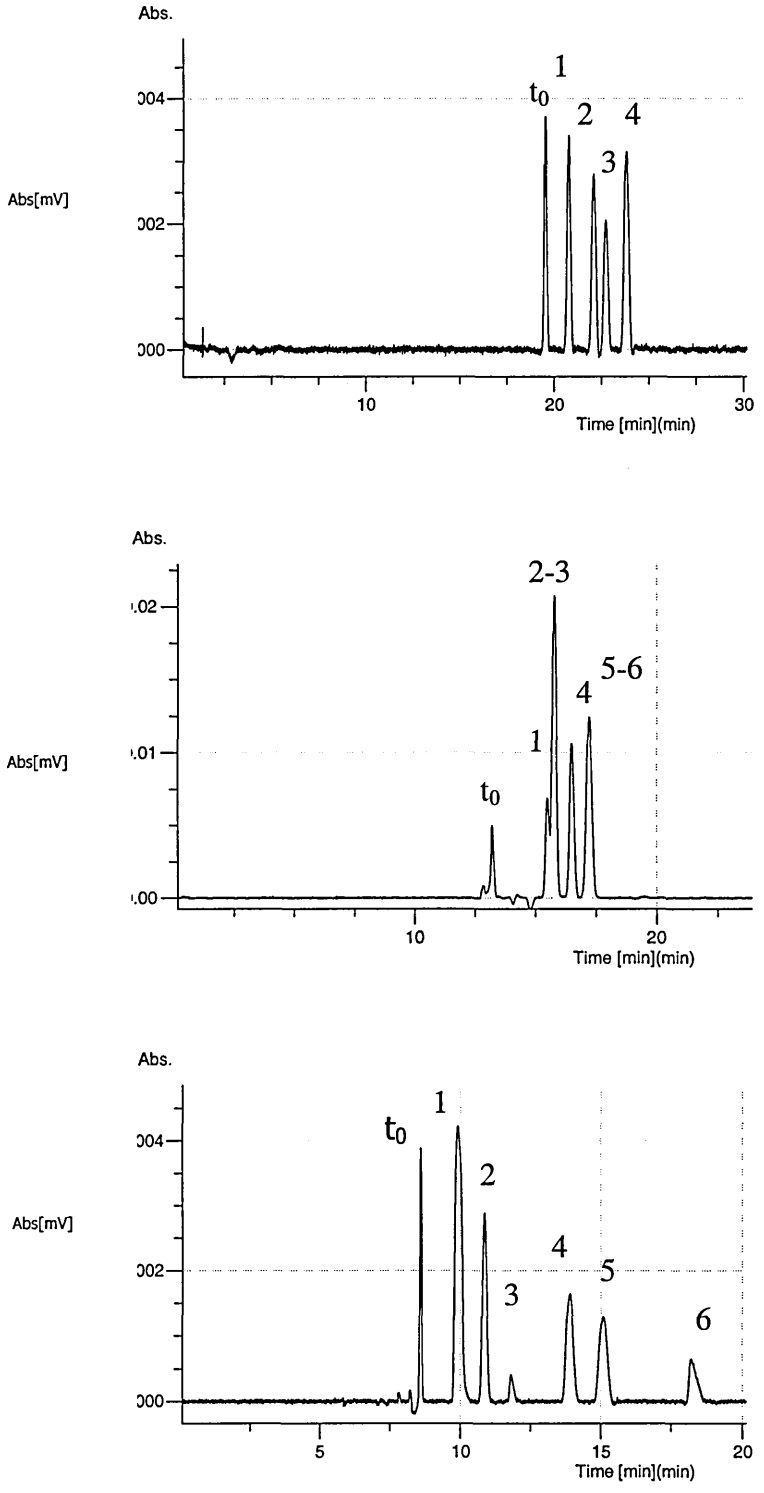

Appendix II. Figure 5. CEC separations of (A) barbital, (B) biphenyl and (C) pyridine test mixtures on **Platinum EPS** stationary phase with uracil neutral marker (t_0). For CEC conditions see section 4.4 and Table 4.7.
The peaks correspond to [A]: (1) barbital, (2) phenobarbital, (3) butethal and (4) amobarbital; [B]: (1) acethyl-, (2) methoxy-, (3) biphenyl, (4) methyl-, (5) bromo- and (6) ethyl-biphenyls; [C]: (1) amino-, (2) acethyl-, (3) pyridine, (4) chloro-, (5) bromo- and (6) ethyl-pyridine.

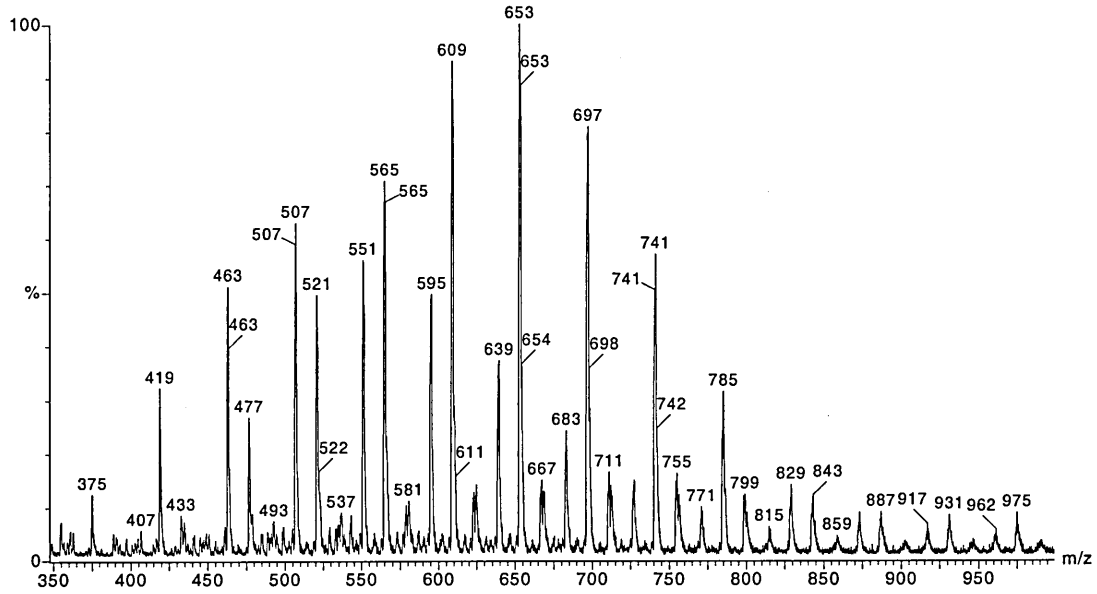

Appendix III. Figure 1. Full scan ESP+ spectra of NPEOSp surfactant (direct infusion of 1μg/ml sample solution at 1μl/min) showing the range of different ions of EO units from n = 2 (m/z = 433) to n = 17 (m/z = 859). Other operational parameters as described in Section 5.2.7.7.

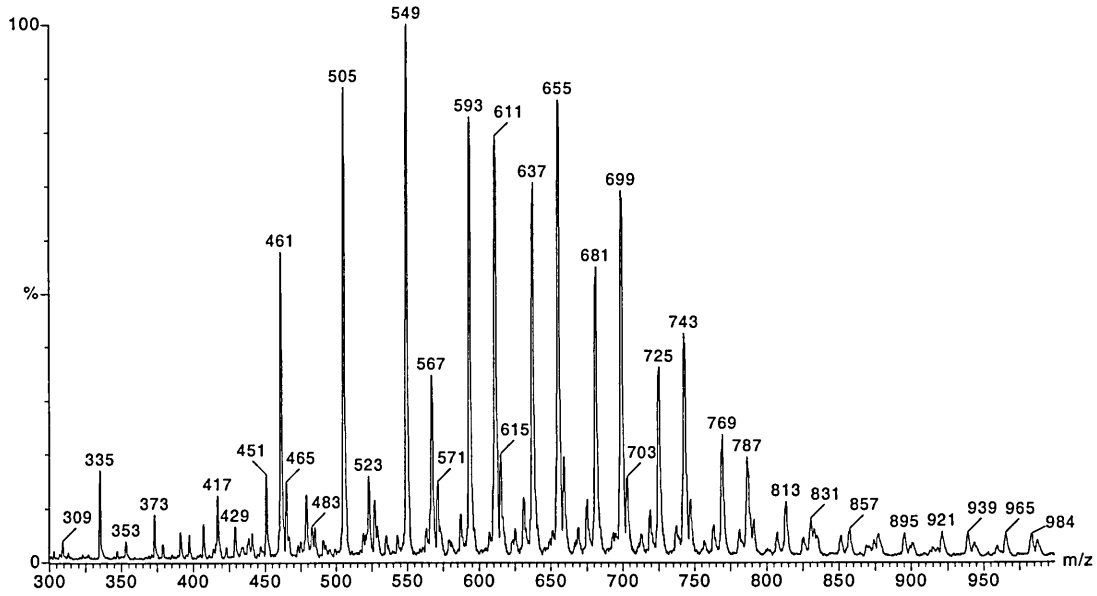

Appendix III. Figure 2. Full scan ESP+ spectra of NPEOS surfactant (direct infusion of 1μg/ml sample solution at 1μl/min) showing the range of different ions of EO units from n = 1 (m/z = 373) to n = 17 (m/z = 857). Other operational parameters as described in Section 5.2.7.7.

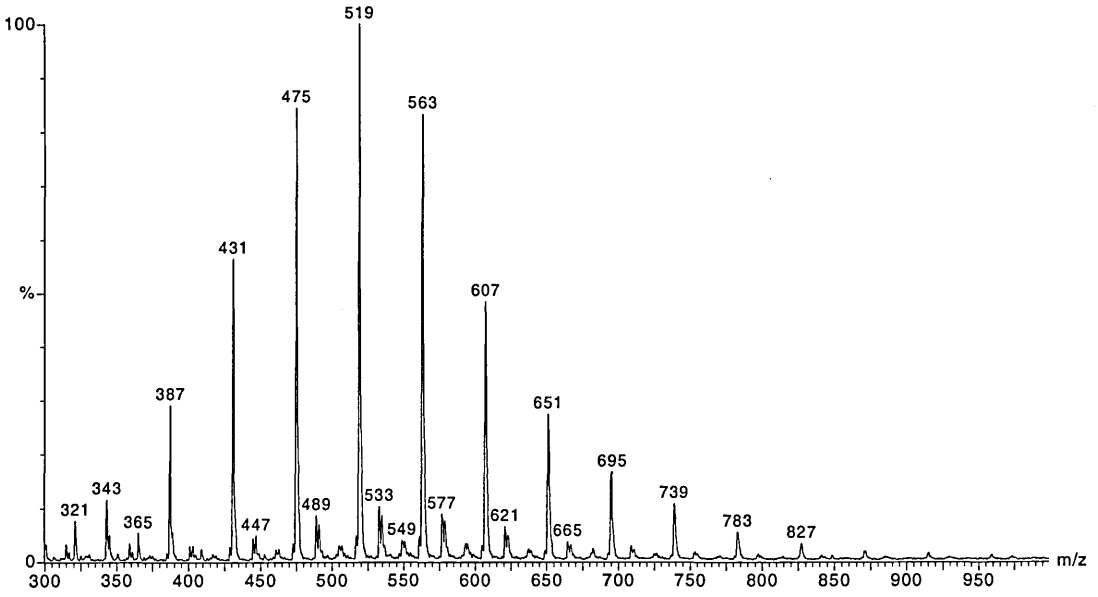

Appendix III. Figure 3. Full scan ESP- spectra of NPEOSp surfactant (direct infusion of 1μg/ml sample solution 1μl/min) showing the range different ions of EO units from n=1 (m/z = 371) to n=12 (m/z = 871). Other operational parameters as described in Section 5.2.7.7.

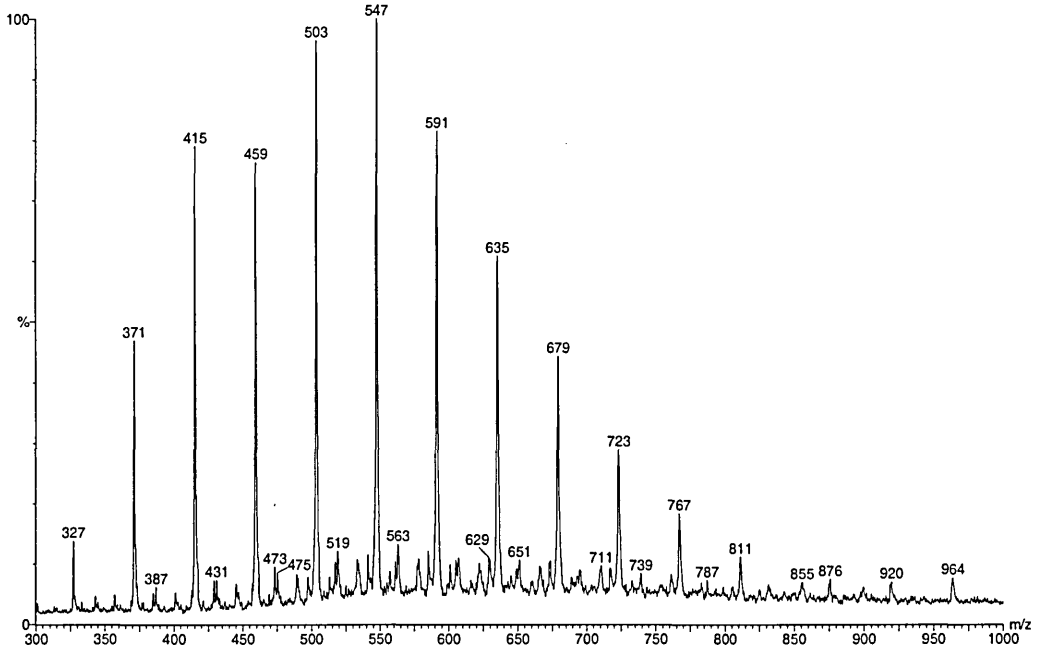

Appendix III. Figure 4. Full scan ESP- MS spectra of NPEOS surfactant (direct infusion of 1μg/ml sample solution 1μl/min) showing the range of different ions of EO units from n=1 (m/z = 371) to n=12 (m/z = 855). Other operational parameters as described in Section 5.2.7.7.